The Dissertation Committee for Tod A. Harper Jr. Certifies that this is the approved version of the following dissertation:

Novel Insights into Normal Aryl Hydrocarbon Receptor Biology Through the Regulation of Stanniocalcin 2

Committee:

Cornelis J. Elferink, Ph.D., Mentor

Istvan Boldogh, D.M&B., Ph.D.

Shawn B. Bratton, Ph.D.

Xiaodong Cheng, Ph.D.

Fernanda Laezza, M.D., Ph.D.

_____

Dean, Graduate School

Novel Insights into Normal Aryl Hydrocarbon Receptor Biology Through the Regulation of Stanniocalcin 2

by

Tod Arliss Harper Jr.

Dissertation

Presented to the Faculty of the Graduate School of

The University of Texas Medical Branch

in Partial Fulfillment

of the Requirements

for the Degree of

Doctor of Philosophy

The University of Texas Medical Branch

December, 2012

Dedication

Dedicated to my family for their continued support in all aspects of my life and my dog Sierra girl for always being there to make me smile.

Acknowledgements

I first would like to acknowledge my mentor, Dr. Kees Elferink, for his constant support, endless supply of ideas, and the opportunity to perform my dissertation research in his laboratory. I would also like to acknowledge the current and past directors of the NIEHS T32 training grant, Drs Bill Ameredes and Mary Moslen, for their guidance and support in the advancement of my career as an independent scientist. Additionally, I would like to acknowledge the current and past members of the lab – Aditya Joshi, Dwayne Carter, Li Chen, Mehnaz Mustafa, Dan Jackson, Shelly Wilson, Gengming Huang, Kristen Mitchell, and Premnath Shetty for their input and support throughout the years. I must also acknowledge my dissertation committee for their support and guidance as I progressed through the ranks as a Ph.D. student.

Novel Insights into Normal Aryl Hydrocarbon Receptor Biology Through Regulation of Stanniocalcin 2

Publication No._____

Tod Arliss Harper Jr., Ph.D.

The University of Texas Medical Branch, 2012

Supervisor: Cornelis J. Elferink

Proper hepatocyte function is vital for survival; hence unrepaired destruction of the parenchymal tissue leading to liver decompensation is devastating. Therefore, understanding the homeostatic process regulating liver regeneration is clinically important, and evidence that the Aryl hydrocarbon Receptor (AhR) can promote cell survival following intrinsic apoptotic stimuli is integral to the regenerative process. Recent evidence suggests that the AhR promotes cell survival through the PI3K-Akt/PKB axis in the absence of an exogenous ligand. However this study was performed using a cancer cell line that does not accurately represent normal liver biology. Therefore, I hypothesize that the AhR mechanistically contributes to liver homeostasis through the regulation of genes hitherto not associated with AhR functions in the absence of an exogenous ligand. To test this hypothesis the current studies utilize primary hepatocytes to identify survival mechanisms consistent with normal AhR biology. Taking advantage of the Cre-lox system to manipulate AhR status, I report here that primary hepatocyte apoptosis is preferentially suppressed in cells expressing the AhR. Studies revealed that Akt/PKB activation previously linked to AhR dependent cell survival was not involved. Likewise, expression profiling of 84 key genes involved in apoptosis failed to account for the differential apoptotic susceptibility associated with AhR status. However, a comprehensive microarray analysis designed to identify immediate and direct changes in the transcriptome concomitant with AhR loss identified Stanniocalcin 2 (Stc2) as a novel receptor target gene previously reported to have a cytoprotective role in endoplasmic reticulum stress. The Stc2 promoter contains multiple xenobiotic response elements (XRE) clustered in a 250 bp region that was shown to recruit the AhR by chromatin immunoprecipitation. Interestingly, Stc2 gene expression is refractory to classic exogenous AhR agonists, but responds to cellular stress in an AhR-dependent mechanism consistent with a process promoting cell survival. In conclusion, AhR mediated transcriptional control of Stc2 represents a novel target gene associated with normal AhR biology that contributes mechanistically to liver homeostasis.

TABLE OF CONTENTS

List of Figures

List of Abbreviations

AhR	Aryl hydrocarbon Receptor
Arnt	Ahr nuclear translocator
bHLH	basic-Helix-Loop-Helix
PAS	Period-Arnt-Single minded
HAH	Halogenated aromatic hydrocarbon
TCDD	2,3,7,8-tetrachlorodibenzo-p-dioxin
PAH	Polycyclic aromatic hydrocarbon
XRE	Xenobiotic Response Element
AhRR	Aryl hydrocarbon Receptor Repressor
Cyp1a1	Cytochrome P450 1a1
NC-XRE	non-consensus Xenobiotic Response Element
ER stress	Endoplasmic reticulum stress
FasL	Fas Ligand
HCC	hepatocellular carcinoma
PI3K	Phosphoinositide 3-kinase
NMT2	N-myristoyltransferase 2
EGFR	Epidermal Groowth Factor Receptor
qRT-PCR	quantitative Real Time Polymerase Chain Reaction
DMSO	Dimethyl Sulfoxide
CKO	Conditional Knock Out
ANOVA	Analysis of Variances
CDS	Coding Sequence

GAPDH	Glyceraldehyde 3-phophate Dehydrogenase
IPA	Ingenuity Pathways Analysis
ChIP	Chromatin Immunoprecipitation
Stc2	Stanniocalcin 2
rStc2	recombinant Stanniocalcin 2
FGR	Gardner-Rasheed feline sarcoma viral oncogene homolog
Htra2	HtrA serine peptidase 2
NFκB	Nuclear Factor kappa-light-chain-enhancer of activated B cells
SAhRM	Selective Aryl hydrocarbon Receptor Modulator
pRb	Retinoblastoma tumor suppressor protein
3-MC	3-methylcholanthrene
BNF	Beta-napthoflavone
HRP	Horseradish Peroxidase
MAT	Metal Affinity Tag
CHO	Chinese Hamster Ovary
UPR	Unfolded Protein Response
CHOP	C/EBP-homologous protein
PERK	Protein kinase RNA-like endoplasmic reticulum kinase
HDAC	Histone Deacetylase
TDO	Tryptophan 2,3-dioxygenase
shRNA	short hairpin ribonucleic acid

Chapter 1 Introduction[1]

The liver is an organ of immense complexity essential for survival since other tissues and organs are unable to compensate for its myriad functions. Liver damage is common in clinical practice due to the prevalent use of alcohol, exposure to pharmacological agents, hepatotropic pathogens, toxicity stemming from elevated free fatty acids associated with metabolic syndrome and obesity, and the pathobiology linked to immune-mediated inflammatory processes, genetic conditions and various other less frequent disease states. Since most forms of liver injury target the hepatocytes, either directly or indirectly, uncovering the hepatocyte cellular response mechanisms to injury is essential for understanding the molecular events involved in liver regeneration and for the development of therapeutic strategies designed to ameliorate liver function due to injury or disease. Integral to normal liver homeostasis is apoptosis as a means to remove damaged cells. Apoptosis of hepatocytes is rare in healthy adult livers, ranging from 1-5 apoptotic cells/10,000 hepatocytes (Schulte-Hermann et al., 1995), yet certain liver disease states including fulminant hepatitis (representing 0.1% of all deaths in the U.S.), cirrhosis and viral hepatitis induce pronounced hepatocyte apoptosis (Ashkenazi and Dixit, 1998; Feldmann, 1997; Feldmann et al., 1998; Galle and Krammer, 1998; Kondo et al., 1997; Krammer, 1996). The aryl hydrocarbon receptor (AhR) is highly expressed in hepatocytes, and implicated in physiological liver functions making the AhR an intriguing target for investigation into maintenance of liver homeostasis and proper liver function.

THE ARYL HYDROCARBON RECEPTOR

Aryl Hydrocarbon Receptor Gene Location and Protein Structure

The AhR is a member of the basic-Helix-Loop-Helix (bHLH) Per-Arnt-Sim (PAS) family of transcriptional regulators. The murine AhR gene is found on chromosome 12 and consists of 11 exons (Schmidt et al., 1993). Its protein sequence and structure is well characterized. Figure 1.1 depicts the AhR structure showing the key domains important for AhR function. As shown in Figure 1.1 the AhR contains a nuclear localization sequence (NLS) and a bHLH region for DNA binding at its N terminus (Gu et al., 2000). The NLS remains hidden until a ligand binds the AhR resulting in a conformational change exposing the NLS (Petrulis et al., 2003; Pongratz et al., 1992). The AhR contains 2 PAS domains (PAS A and PAS B) responsible for AhR:Arnt dimerization. The PAS B domain is also the site for ligand binding, and binding of the chaperonins heat shock protein 90 (Hsp90) (Coumailleau et al., 1995) and the immunophilin-like AhR-interacting protein (AIP: also known as Ara9 and XAP2) (Gu et al., 2000). Alanine 375 in the PAS B domain differentiates the highly responsive AhR B allele (AhR^b) from the less responsive AhR D allele (AhR^d) along with the variable length of the C terminus (Poland et al., 1994). The C terminus also contains a glutamine-rich transactivation domain (TAD) (Jain et al., 1994).

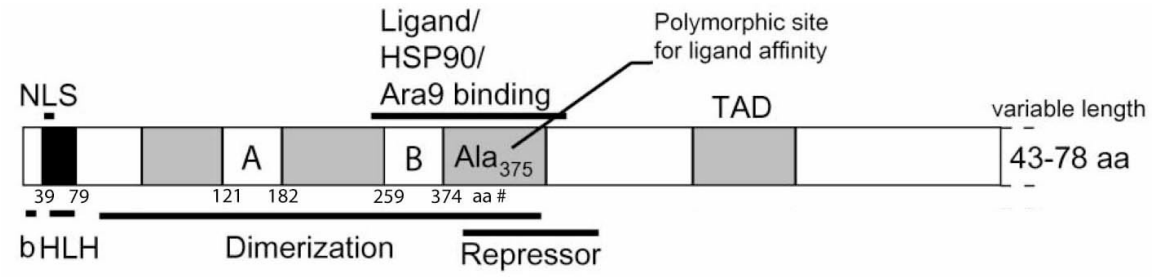

Figure 1.1. AhR structure including the established functional domains (Modified from Gu et al., 2000).

Exogenous Aryl Hydrocarbon Receptor Agonists

A large number of compounds are able to bind and activate the AhR including the planar, hydrophobic, halogenated aromatic hydrocarbons (HAHs). The HAHs possess the highest affinity for the AhR and include the halogenated dibenzo-p-dioxins, dibenzofurans, and biphenyls (Denison and Nagy, 2003). Notably, the potent and poorly metabolized AhR agonist 2,3,7,8-tetrachlorodibenzo-p-dioxin (TCDD) is included with this class of structurally related agonists. HAHs are often produced as a result of industrial accidents, or after improper waste incineration (Poland and Knutson, 1982). Unfortunately, these compounds are metabolically and environmentally stable, resulting in long half-lives and high toxicity profiles when compared to other classes of AhR agonists. Toxicities associated with HAH exposure include tumor promotion, teratogenicity, immuno- and hepatotoxicity, and alteration in endocrine homeostasis (Denison et al., 2011). In addition to being metabolically and environmentally stable, HAHs are able to activate the AhR at picomolar concentrations (Poland and Glover, 1974).

Polycyclic aromatic hydrocarbons (PAHs) make up the second class of traditional AhR agonists and are produced through combustion processes in cigarette smoke, car exhaust, and charbroiled foods. These compounds induce AhR signaling 3-4 orders of magnitude lower than TCDD, are highly metabolized, and as a consequence are far less toxic than HAHs (Poland and Glover, 1974). Nonetheless, PAHs and HAHs are both widely recognized AhR agonists responsible for the toxicities associated with AhR activation, although the exact mechanism for the toxicities still eludes investigators.

Traditional Aryl Hydrocarbon Receptor Activation

Traditional AhR activation and gene regulation involving the ligand:AhR:Arnt:XRE complex is well described and shown to regulate the expression of several genes in response to PAH and HAH ligands, such as TCDD (Okey et al., 1994; Schmidt and Bradfield, 1996). The AhR is found in the cytosol of cells as an inactive

multiprotein complex consisting of two Hsp90 molecules, AIP, and p23 (Kazlauskas et al., 1999; Perdew, 1988; Perdew, 1992). Ligand binding triggers AhR activation and nuclear translocation leading to dimerization with another PAS family member the aryl hydrocarbon receptor nuclear translocator (Arnt). The transcriptionally active AhR:Arnt dimer recognizes and binds to xenobiotic response elements (XRE) that act as enhancer elements in the promoter regions of target genes to induce gene expression through coactivator recruitment and chromatin disruption (Lees and Whitelaw, 1999) (Fig 1.2). Likewise, the AhR:Arnt complex is capable of binding the XRE and suppressing gene expression (Safe et al., 1998). AhR-mediated gene expression is terminated by nuclear export of the AhR into the cytosol where degradation occurs via ubiquitin-mediated 26S proteosome (Pollenz, 2002). Another mechanism for AhR downregulation is through the AhR Repressor (AhRR). In this negative feedback loop the AhRR is upregulated by the AhR and competes for dimerization with Arnt, thereby suppressing AhR target gene expression (Mimura et al., 1999).

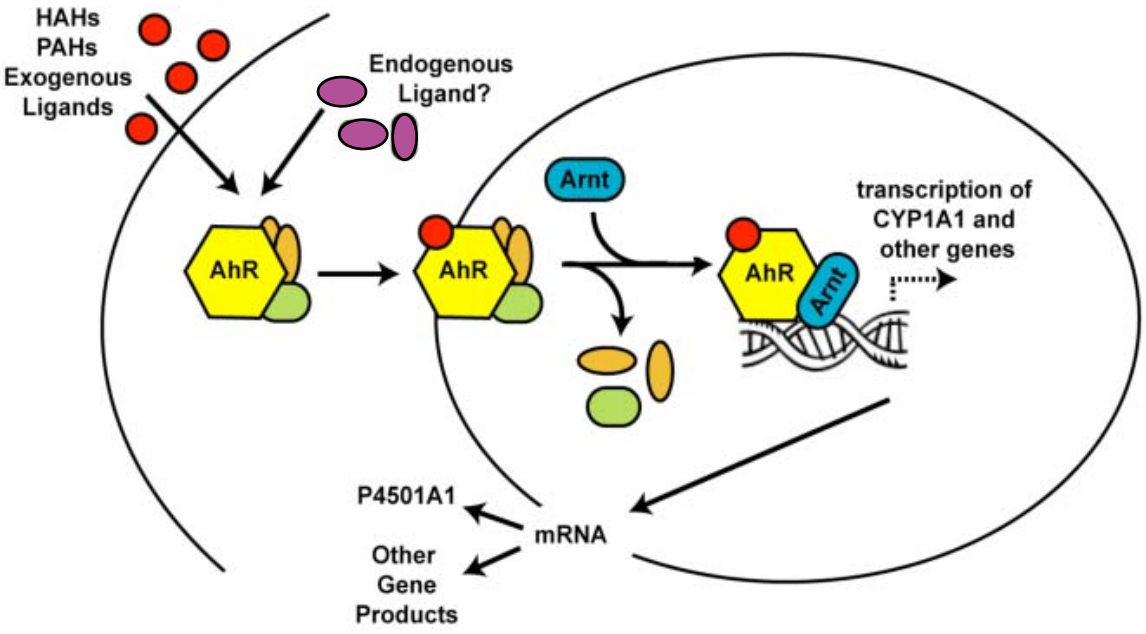

Figure 1.2. **Traditional AhR pathway.** AhR activation by an exogenous ligand results in translocation to the nucleus, heterodimerization with Arnt, and binding to canonical XREs resulting in regulation of target genes.

The AhR is associated with the adaptive metabolism of xenobiotics and the toxic responses associated with these compounds due to AhR-dependent regulation of several metabolizing proteins. Traditional AhR targets include the Cyp1a family and Phase II metabolizing enzymes including UDP-glucuronsyltransferase and glutathione S-transferase-Ya (Elferink and Whitlock, 1994; Hankinson, 1995; Probst et al., 1993). Notably, Cyp1a1 transcription is solely controlled by the AhR, making it a powerful biomarker when monitoring traditional AhR activities. In addition, it is intriguing that several AhR ligands are bioactivated by AhR target genes. For example, the PAH benzo(a)pyrene (BaP) is bioactivated by Cyp1a1 resulting in bone marrow toxicity. However, Cyp1a1 knockout mice orally administered BaP are not protected, but instead die 30 days after administration; whereas wildtype mice are protected from bone marrow toxicity due to efficient first pass metabolism by Cyp1a1 (Uno et al., 2004). As a consequence the cooperative regulation of both Phase I and Phase II enzymes provide a protective effect after AhR activation by the metabolically labile PAHs. On the other hand, the metabolically stable HAHs cause persistent AhR activation resulting in increased AhR-dependent toxicity.

Non-Traditional Aryl Hydrocarbon Receptor Activities

Traditional AhR activity is associated with the regulation of xenobiotic metabolizing genes. However, AhR activation by an exogenous ligand such as TCDD, is also able to elicit AhR-mediated transcript induction of non-xenobiotic metabolizing genes associated with normal biological processes. ChIP on chip analysis performed using liver tissue from vehicle and TCDD treated mice identified 625 differentially expressed genes as a direct result of AhR activation and binding to an XRE. Functional annotation clustering of Gene Ontology terms for genes associated with significant AhR enrichment included processes related to fatty acid and lipid metabolism in addition to xenobiotic metabolism (Dere et al., 2011b). Likewise, another study from the same group identified changes in gene expression after TCDD treatment associated with

differentiation, apoptosis, gluconeogenesis, and fatty acid uptake in a temporal and dose-dependent manner (Boverhof et al., 2005).

In addition to modulating gene expression through Arnt dimerization, the AhR also influences many biochemical and intracellular pathways following activation by an exogenous ligand. For example, the AhR is capable of binding RelA(p65), a NF-κB subunit in breast cancer cells. This AhR:RelA association results in the activation of c-myc gene transcription, leading to a possible mechanism for tumorigenesis in mammary cells (Kim et al., 2000). Our laboratory has also reported that the AhR binds directly to the retinoblastoma tumor suppressor protein (pRb) resulting in an AhR-mediated cell cycle arrest following TCDD exposure both in vivo and in vitro (Ge and Elferink, 1998). Furthermore, our laboratory has recently reported that the AhR is capable of binding a sequence termed the non-consensus XRE (NC-XRE), in the plasminogen activator inhibitor-1 (PAI-1) gene after TCDD treatment in vivo providing evidence that the transcriptional activity of the AhR is not dependent on the presence of an XRE or Arnt binding (Huang and Elferink, 2012). The previous examples of nontraditional AhR activities illustrate the complexity of AhR signaling after activation by an exogenous ligand such as TCDD. To further complicate the story, AhR activation and function has proven to be tissue, species, and ligand specific (Boutros et al., 2009; Chen et al., 1998; Flaveny et al., 2010)

Aryl Hydrocarbon Receptor Gene Regulation in the Absence of an Exogenous Ligand

Aryl Hydrocarbon Receptor Knockout Mice

In the mid-90's two laboratories independently generated an AhR knockout mouse strain using gene targeting, and demonstrating for the first time a biological need for the AhR in the absence of an exogenous ligand (Fernandez-Salguero et al., 1995; Schmidt et al., 1996). Although not identical the mice generated from the two laboratories shared similar hepatic defects including decreased liver size, hepatic portal fibrosis, and

decreased cytochrome P450 expression (Lahvis and Bradfield, 1998). In addition, both knockout strains were resistant to the toxicities associated with AhR activation after exposure to an HAH such as TCDD (Fernandez-Salguero et al., 1995; Schmidt et al., 1996). Generation of the AhR knockout mice has proven to be instrumental in the recent shift of interest in AhR activity from the traditional adaptive metabolism response to heavily focusing on identification of physiological AhR functions.

Aryl Hydrocarbon Receptor Microarray Studies

Microarray technologies have been used extensively to identify AhR target genes after activation by an exogenous ligand using a variety of models ranging from cancer cell lines to rodents including both the mouse and rat (Boverhof et al., 2005; Dere et al., 2011a; Hayes et al., 2007; Puga et al., 2000). On the other hand, AhR gene regulation in the absence of an exogenous ligand is far less described. However, recent reports are now beginning to show that the AhR is also capable of regulating gene transcription in the absence of an exogenous agonist (Boutros et al., 2009; Tijet et al., 2006; Wang et al., 2007). According to Tijet el al., AhR status alone altered the expression 392 genes in the mouse liver. Comparison of kidney and liver transcript profiles between wildtype and AhR knockout mice, concluded that basal gene expression in the absence of TCDD were similar with 379 and 471 AhR-dependent, TCDD-independent changes in transcript levels respectively (Boutros et al., 2009). The similarities in gene expression between the kidney and liver of the AhR knockout mice suggest the AhR has an important role in regulating gene expression during homeostasis. This data is consistent with the idea of physiological functions for the AhR and the regulation of basal level gene batteries.

Cell Death Via Apoptosis

Apoptosis is a fundamental process in all multi-cellular organisms that occurs during embryonic development, and is involved in maintaining tissue homeostasis through the removal of damaged or diseased cells (Kerr et al., 1972). Aberrant apoptotic signaling can result in unregulated cell growth leading to cancer or incresased cell death

resulting in disruption of physiological processes. Therefore, the decision to undergo apoptosis is tightly regulated containing many checks and balances. Once a cell has committed to apoptosis, cell suicide is carried out by one of two pathways depending on the origin of the insult and signal: the intrinsic pathway and the extrinsic pathway. Despite their differences in initiation, both pathways culminate with the activation of the effector caspases. Caspases are a family of cysteine-dependent aspartic acid-specific proteases expressed as proenzymes requiring activation through proteolysis (Nicholson and Thornberry, 1997). The initiator caspases (caspase 2, 8, 9, and 10) are responsible for the activation of the effector caspases (caspase 3, 6, and 7) (Thornberry and Lazebnik, 1998). Once active, the effector caspases are able to carry out cell death through proteolysis of anti-apoptotic proteins, disassembly of cell structure, and deregulation of proteins resulting in loss or gain of function (Enari et al., 1998; Orth et al., 1996; Rudel and Bokoch, 1997). Morphological hallmarks of apoptosis resulting from caspase activation include nuclear condensation, chromatin fragmentation, and the formation of apoptotic bodies (Kerr et al., 1972).

Intrinsic Pathway

The "intrinsic" pathway also known as the "mitochondrial" pathway is initiated from signals that originate within the cell. Damage resulting from genotoxic stress and reactive oxygen species (ROS), cell starvation, and endoplasmic reticulum stress (ER stress) are capable of initiating signaling pathways to induce apoptosis. The intrinsic pathway relies heavily on the Bcl-2 family of anti- and pro-apoptotic proteins. Anti-apoptotic members associate with the mitochondria to maintain membrane integrity during homeostatic conditions and include the members Bcl2, Bcl-xL, Bcl-w and Mcl1 (Cory and Adams, 2002). The pro-apoptotic members are divided into two groups based on their sequences: the BH3-only proteins and Bax family proteins. The BH3-only proteins possess only the BH3 motif and act as stress sensors that bind directly to the anti-apoptotic Bcl-2 family to initiate the intrinsic pathway (Huang and Strasser, 2000).

Bax family proteins on the other hand retain sequence homology with the anti-apoptotic proteins and act downstream to disrupt mitochondrial integrity through oligomerization in the mitochondrial outer membrane releasing cytochrome C, SMAC/ Diablo, and other apoptotic proteins into the cytosol (Gross et al., 1999). The formation of the apoptosome (cyctochrome C, Apaf-1, ATP) then recruits and activates procaspase-9, which subsequently activates the effector caspases leading to cell death (Fig 1.3).

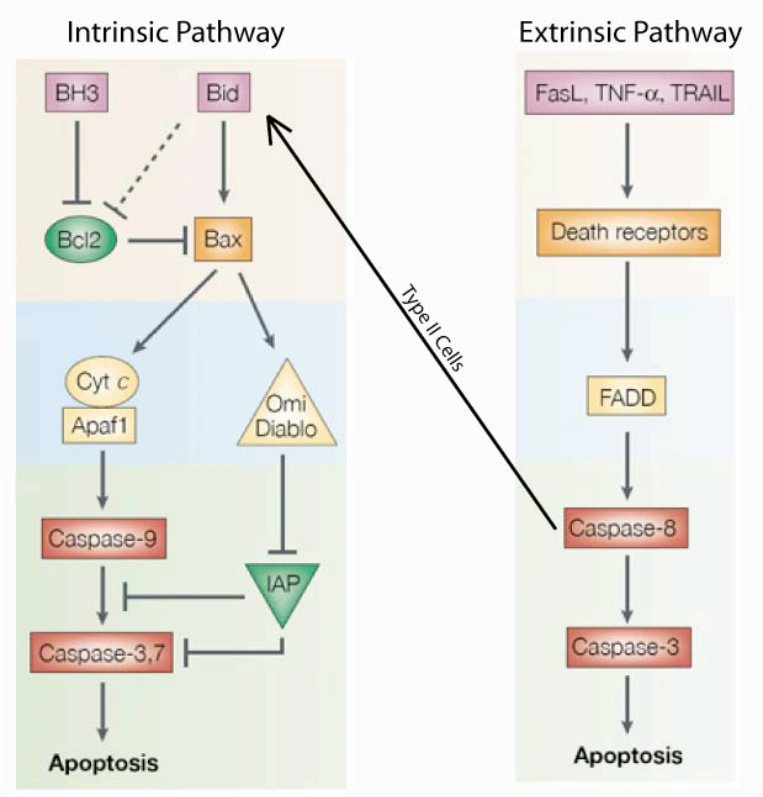

Figure 1.3. **Generalized intrinsic and extrinsic apoptosis pathways.** Type II cells lack sufficient activation of caspase 8 after an extrinsic stimulus and therefore execute apoptosis through Bid truncation and the release of mitochondria pro-apoptosis proteins (Modified from Cory and Adams, 2002)

Extrinsic Pathway

The "extrinsic" pathway also known as the "death receptor" pathway is mediated through activation of the death receptors (TNFR1, TRAILR1, Fas) by receptor specific cytokines (TNFα, TRAIL, and FasL) (Schulze-Osthoff et al., 1998). The binding of a death ligand to its respective death receptor initiates a specific, but well described pathway for each receptor. The general scheme is depicted in Figure 1.3. The death receptor Fas is highly expressed in hepatocytes and known to play a key role in the development of drug-induced hepatotoxicities, fulminant hepatitis, and viral hepatitis due to aberrant activation of the extrinsic pathway (Kiyici et al., 2003; Lapinski et al., 2004;

Taieb et al., 1998). Similarly, decreased expression of Fas has been identified in hepatocellular carcinoma (HCC) resulting in cancer that displays increased resistance to cytotoxic treatments (Schattenberg et al., 2011). The agonistic Fas antibody Jo2 triggers massive cell death in the murine liver (Ogasawara et al., 1993), suggesting a potential for monoclonal antibodies in anticancer directed therapeutics (Muntane, 2011).

Type I vs Type II Pathways of Fas-Mediated Apoptosis

Fas-mediated apoptosis proceeds along two different paths depending on the cell type, termed Type I and Type II (Scaffidi et al., 1998). Type I proceeds through activation of Fas along the traditional pathway continuing with the formation of the death-inducing signaling complex (DISC), activation of initiator caspase-8, culminating in activation of the effector caspase-3 and apoptosis (Scaffidi et al., 1998). However Type II cells, such as hepatocytes, are dependent on the mitochondrial release of apoptotic proteins to fully execute apoptosis after Fas activation (Luo et al., 1998). In Type II cells activation of caspase-8 cleaves Bid instead of activating caspase-3, resulting in mitochondria permeabilization leading to apoptosis through activation of caspase-3 by the apoptosome. The knockout of Bid in mice protects their liver from massive hepatocyte damage and eventual death normally induced by treatment with Jo2 (Yin et al., 1999). Furthermore, a recent publication indicates that primary hepatocytes in culture behave as Type I cells rather than undergoing Type II apoptosis identified in vivo (Walter et al., 2008). The reasoning for the two different pathways remains unknown, but does add a layer of complication when examining cell death in hepatocytes.

PI3K-AKT/PKB Survival Pathway

Opposing every death signal is a survival signal and depending on the strength of each dictates the fate of the cell. One of the most influential survival signals propagates from the PI3K-Akt/PKB pathway. This pathway is activated when growth factors, such as insulin-like growth factor (IGF), bind their respective receptor. Signaling then continues through a series of highly regulated phosphorylation events as depicted in

Figure 1.4, ultimately ending with phosphorylation and activation of the serine/threonine kinase protein Akt (also known as protein kinsase B (PKB)) (Franke, 2008). Once active Akt is able to alter several biological processes including cell survival, proliferation, growth, and apoptosis. The PI3K-Akt/PKB pathway is often constitutively active in solid cancers including HCC (Chen et al., 2005; Whittaker et al., 2010). Aberrant signaling in HCC has been attributed to over-expression of IGF II (Cariani et al., 1988), over-expression of epidermal growth factor (EGF) (Yeh et al., 1987), mutations and reduction of phosphatase and tensin homolog (PTEN) expression (Hu et al., 2003), and mutations in PI3K (Lee et al., 2005). Considering the majority of HCC cases arise as a complication from chronic liver diseases such as fulminant and viral hepatitis, nonalcoholic fatty liver disease, and cirrhosis, it is crucial to understand these diseases mechanistically and any influence the AhR may have on the decision between survival and death.

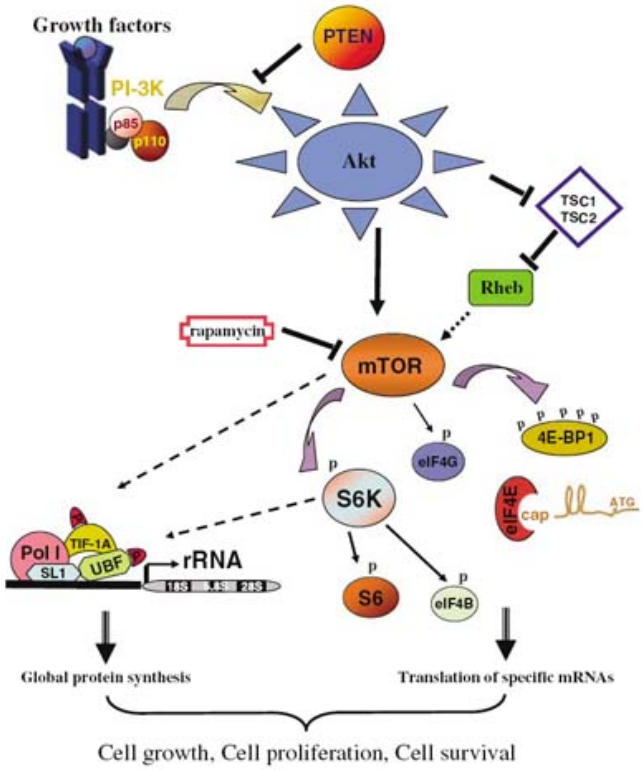

Figure 1.4 PI3K-Akt/PKB signaling pathway. Activation of Akt/PKB through phosphorylation at serine 473 and threonine 308 leads to downstream signaling resulting in cell growth, proliferation, and survival (Ruggero and Sonenberg, 2005)

ARYL HYDROCARBON RECEPTOR, APOPTOSIS, AND CELL SURVIVAL

Exogenous AhR Activation and Apoptosis

Numerous reports suggest that exogenous AhR agonists, such as TCDD can induce apoptosis. TCDD treatment killed human lutenized granulosa cells (Heimler et al., 1998), the developing vasculature of fish, and Xenopus hepatocytes during

embryogenesis (Cantrell et al., 1998; Sakamoto et al., 1995). Immunosuppresion is a toxicity associated with TCDD exposure hypothesized to be mediated by apoptosis (Dearstyne and Kerkvliet, 2002; Laiosa et al., 2003). Studies have reported induction of apoptosis after TCDD exposure in immature thymocytes both in vitro (McConkey et al., 1988) and in vivo (Kamath et al., 1998). Moreover, lpr mice deficient for the death receptor, Fas, are less sensitive to TCDD-mediated thymic atrophy than Fas-positive counterparts (Kamath et al., 1999; Rhile et al., 1996). Likewise, Fas ligand (FasL) defective gld mice are refractory to TCDD-induced thymic atrophy (Kamath et al., 1999).

TCDD is classified as a human carcinogen and causes tumor formation in several rodent tissues including the liver (IARC, 1997). Several studies have shown that pretreatment with a genotoxic agent enhances TCDD induced cancer (Knerr and Schrenk, 2006) through inhibition of apoptosis in vivo (Reyes-Hernandez et al., 2010; Stinchcombe et al., 1995). This suggests that AhR activation by an exogenous ligand suppresses apoptosis in certain cell types, thereby promoting cancer growth in an AhR dependent fashion (Ambolet-Camoit et al., 2010; Davis et al., 2003). Inhibition of apoptosis by TCDD was also shown in vitro using rat primary hepatocytes treated with UVC or 2-acetylaminofluorene, but not transforming growth factor β1 (TGF-β1) (Worner and Schrenk, 1998). On the other hand, Christensen et al. reported that TCDD treatment could not protect mouse primary hepatocytes from apoptosis induced by bleomycin and TGF-β. In addition, TCDD treatment alone caused an increase in apoptosis (Christensen et al., 1998). The previous studies indicate that although AhR activation by TCDD is required for inhibition or induction of apoptosis, the mechanism(s) remains unknown.

AhR and Apoptosis in the Absence of an Exogenous Ligand

As mentioned previously, the AhR knockout mouse exhibits multiple physiological abnormalities including decreased liver size. Gonzalez and Fernandez-Salguero reported that in addition to decreased liver size they also observed increased apoptotic rates in the knockout mouse liver compared to wild-type counterparts

(Gonzalez and Fernandez-Salguero, 1998) suggesting the AhR plays an important role in maintaining cell number during homeostasis independent of activation by an exogenous ligand. In addition, spontaneous apoptosis was increased in primary hepatocytes (Zaher et al., 1998) and mouse embryo fibroblasts (Elizondo et al., 2000) isolated from AhR knockout mice in comparison to the wild-type counterparts. These data are consistent with the AhR providing a protective role during homeostasis.

Stimulus Dictates the Aryl Hydrocarbon Receptor Response

Recently, our laboratory demonstrated that the AhR predisposes hepatocytes to FasL-induced apoptosis in the absence of an exogenous AhR agonist (Park et al., 2005), suggesting that the AhR promotes apoptosis in response to extrinsic apoptotic cues. This increase in apoptosis is thought to be due in part by AhR-dependent upregulation of N-myristoyltransferase 2 (NMT2) (Kolluri et al., 2001) resulting in increased Bid myristolation and the subsequent amplification of the apoptotic signal through the mitochondria (Zha et al., 2000). On the other hand, Wu and coworkers showed that AhR expression promoted hepatoma cell survival in response to intrinsic death signals, but enhanced cell death in response to extrinsic signals (Wu et al., 2007). Cell survival in response to intrinsic cues was attributed to activation of the PI3K-Akt/PKB pathway, and to a lesser extent the EGFR survival pathway, in a process dependent on AhR expression. More recently, AhR expression was shown to protect immortalized mouse embryo fibroblasts from E2F1-mediated apoptosis induced by oxidative stress and DNA damage (Marlowe et al., 2008). Although consensus on the role of the AhR in modulating apoptosis is coalescing, the precise mechanism responsible remains to be resolved. To this end, I embarked on studies using primary mouse hepatocytes as a physiologically normal in vitro system to validate the previous findings in either immortalized or transformed cell lines.

The Cre-lox System and AhR Floxed Mice

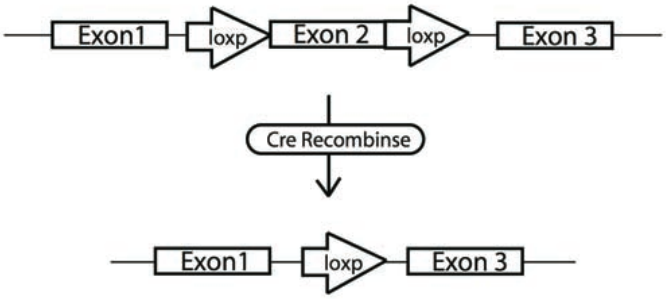

Figure 1.5. **Schematic of the Cre-lox system.** The AhR floxed mice contain loxP sites that flank exon 2 of the AhR gene. Introduction of Cre-recombinase results in a truncated transcript and loss of protein translation.

The Cre-lox system is an important molecular tool used to conditionally alter gene expression in vitro and in vivo. This system utilizes the Cre recombinase of the P1 bacteriophage capable of efficiently altering the intervening genetic element between two 34 base pair recognition sites (loxP sites) (Hamilton and Abremski, 1984). The orientation of the loxP sites dictates whether deletion, inversion, or translocation of the intervening sequence will occur (Nagy, 2000). Our laboratory has generated an adenovirus that expresses Cre recombinase (AdCreGFP) allowing me to examine the role of the AhR in apoptosis using primary hepatocytes isolated from the $AhR^{fx/fx}$ (AhR floxed) mouse (Figure 1.5) (Walisser et al., 2005). The ability to monitor changes in signaling concurrent with AhR loss, gives me an unprecedented opportunity to evaluate direct AhR processes in the absence of an exogenous agonist. However, the AhR floxed primary hepatocyte Cre-lox model first needed to be validated before experiments could be performed. Figure 1.6A demonstrates that loss of the mature mRNA in hepatocytes infected with the Cre recombinase-expressing virus was essentially complete within 24 hours. The advent of the non-functional excised transcript identified by RT-PCR reflects removal of the intervening genetic element encoding exon 2 that is flanked by the loxP sites (Walisser et al., 2005). Accordingly, I next examined loss of AhR protein expression by western blot analysis. As shown in Figure 1.6B AhR protein expression disappears over the same period indicative of a very short protein half-life in the primary hepatocytes. Finally, in order to verify that the loss of AhR is functionally relevant, uninfected hepatocytes and those infected with the control virus (AdGFP), or

virus expressing the Cre recombinase (AdCreGFP), were treated with vehicle (DMSO) or 6 nM TCDD for 6 hours and P4501A1 expression was determined immunologically (Fig. 1.6C). This result shows that loss of the AhR was sufficiently robust to completely suppress induction of the Cyp1a1 target gene.

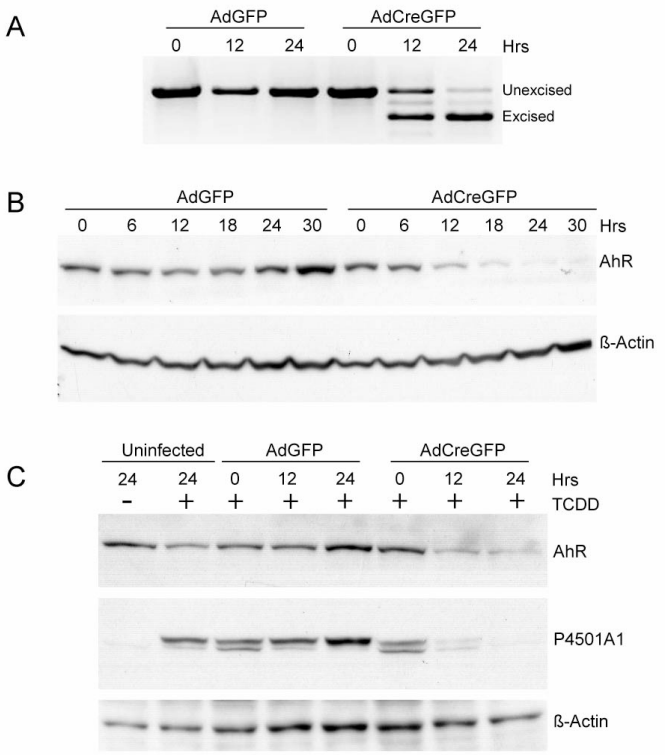

Figure 1.6. Monitoring loss of the AhR in primary hepatocytes. A. RT-PCR was performed to monitor excision of the AhR gene loxP-flanked exon 2 using total RNA isolated from $AhR^{fx/fx}$ primary hepatocytes infected with AdGFP (control) or AdCreGFP (Cre recombinase) for the indicated times. PCR primers were designed to amplify different size PCR products distinguishing the unexcised from excised transcript. **B.** Whole-cell lysate from $AhR^{fx/fx}$ primary hepatocytes infected with AdGFP or AdCreGFP were analyzed by western blotting for AhR protein. Actin was used as a loading control. **C.** $AhR^{fx/fx}$ primary hepatocytes were either uninfected (DMSO, TCDD) or infected with AdGFP or AdCreGFP for the indicated times, followed by treatment with DMSO (lane 1) or 6nM TCDD (lanes 2-8) for 6 hours. AhR and P4501A1 protein expression was monitored by western blot analysis. Actin was used as a loading control.

Loss of the Aryl Hydrocarbon Receptor Induces Caspase-3 Cleavage

Morphological observations revealed that hepatocytes infected with the AdCreGFP virus exhibited a disproportionate propensity to undergo apoptosis within two days post-infection in comparison to the AdGFP infected cells (data not shown). This coincided with a pronounced increase in the formation of a caspase-3 cleavage product indicative of caspase activation and apoptosis (Fig. 1.7), reminiscent of the increased apoptosis identified in primary hepatocytes and mouse embryo fibroblasts isolated from the AhR knockout mouse (Elizondo et al., 2000; Zaher et al., 1998).

HYPOTHESIS

Evidence supports the conclusion that the AhR has a mechanistic role regulating apoptosis and survival in the liver. However, an overwhelming majority of the evidence was found using TCDD or another exogenous ligand to activate the AhR. As such, an exogenously activated AhR was found to variously suppress and induce apoptosis in different experimental settings. In addition, these findings were complicated by the fact that TCDD was not observed to be protective in the mouse liver, unlike the rat and human, suggesting there is a species-specific role for the AhR after activation by an exogenous ligand. This is not the first time experimental models have been contradictory, as other species and tissue-specific functions of the AhR have also been reported after activation by TCDD (Boutros et al., 2009; Dere et al., 2011a). I believe the use of an exogenous ligand to study normal AhR biology risks corrupting normal physiological events and should be taken into account when hypotheses are formed and experiments are designed.

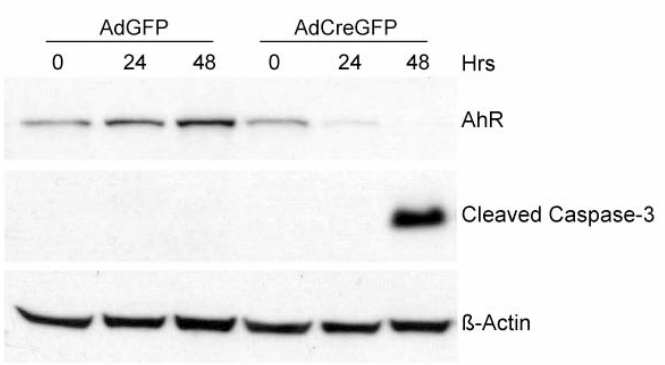

Figure 1.7. Loss of the AhR results in increased caspase-3 cleavage. Whole-cell lysate from $AhR^{fx/fx}$ primary hepatocytes infected for the indicated times with AdGFP or AdCreGFP were analyzed by western blotting for AhR and cleaved caspase-3 protein. Actin was used a loading control.

Therefore, I hypothesize that in the absence of an exogenous ligand the AhR mechanistically contributes to the balance of hepatocyte survival and death through regulation of previously unidentified target genes associated with normal AhR biology.

Chapter 2: Assessment of Aryl Hydrocarbon Receptor Activity in the Absence of an Exogenous Ligand

INTRODUCTION

The AhR is an evolutionarily conserved protein found in both vertebrates and invertebrates, suggesting the AhR is important for physiological properties beyond its traditional role in the adaptive metabolism of xenobiotics. The homologous proteins found in C. elegans (Ahr-1 and Aha-1) (Powell-Coffman et al., 1998) and Drosophila (Spineless and Tango) (Emmons et al., 1999) are constitutively active and do not require ligand binding. Evidence also exists for ligand-independent AhR signaling in mammalian cell lines, but the mechanism remains unclear (Oesch-Bartlomowicz and Oesch, 2009). On the other hand, generation of the AhR knockout mouse confirmed that the AhR is involved in regulating homeostatic processes in the absence of an exogenous ligand due to multiple developmental abnormalities found in these mice (Lahvis and Bradfield, 1998). Thanks to these mice the AhR has been implicated in several physiological activities including cell cycle regulation, cell survival, and apoptosis (Mitchell et al., 2006; Park et al., 2005; Wu et al., 2007).

The AhR's role in cell cycle regulation has been thoroughly investigated by our laboratory and others. However cell cycle regulation represents only one part necessary to maintain the balance between the removal of damaged hepatocytes and liver regeneration. The controlled removal of damaged and diseased cells occurs via apoptosis. A major protein involved in the regulation of survival and death is the tumor suppressor p53. The AhR is reported to suppress p53-mediated apoptosis through up-regulation of Mdm2 after TCDD treatment (Paajarvi et al., 2005). In addition, the AhR is thought to suppress p53 target genes due to an over-representation of p53 binding sites in down-regulated transcripts after TCDD treatment in mice (Tijet et al., 2006). Additionally, the E2F family member E2F1 is known to mediate apoptosis through p53-

dependent and independent mechanisms. Marlowe et al. (2008) reported that the AhR binds E2F1 resulting in the inhibition of apoptosis through the suppression of proapoptotic E2F1 target genes, including Apaf1 and TAp73. Further investigation of the p53, E2F1, and AhR relationship is attractive, but the previous findings were identified after TCDD treatment, which questions if these relationships are dependent on exogenous AhR activation. However, this group (Marlowe et al., 2008) also reported that the loss of the AhR increased apoptosis, reminiscent of the increased apopototic rates seen in primary hepatocytes isolated from AhR knockout mice (Zaher et al., 1998) and AhR floxed primary hepatocytes infected with the Cre-recombinase expressing adenovirus shown in Figure 1.7.

Recently, the notion that the cellular response to an apoptotic stimulus is influenced by AhR status has been reported by our laboratory and confirmed independently by other investigators (Wu et al., 2007). Our laboratory provided evidence that the AhR predisposes hepatocytes to apoptosis after treatment with Fas ligand and the anti-Fas Jo2 antibody. In these studies AhR knockout mice were protected from Fas-mediated apoptosis, whereas wildtype mice exhibited massive hepatic apoptosis and died within 8 hours (Park et al., 2005). This predisposition to extrinsic cell death was confirmed independently, however the AhR was also shown to protect mouse hepatoma cells (hepa1c1c7) after exposure to an intrinsic apoptotic stimulus such as UV irradiation (Wu et al., 2007). In these studies the hepa1 AhR-deficient derivative (LA1) was shown to have impaired Akt/PKB activation. Given the questions that still remain regarding AhRs role in cell survival and apoptosis, I was interested in identifying AhR actions in the absence of an exogenous ligand. I therefore, proposed to investigate the AhR-Akt/PKB relationship in a physiologically relevant model in the absence of an exogenous ligand after an intrinsic apoptotic stimulus.

MATERIAL AND METHODS

Materials

Antibodies were obtained from various commercial sources: AhR (Enzo Life Sciences, Farmingdale, NY); P4501A1 (Santa Cruz Biotechnology, Santa Cruz, CA); β-Actin (Millipore, Billerica, MA); Cleaved Caspase-3, Akt, and Phospho-Akt (Ser473) (Cell Signaling Technology, Danvers, MA); all HRP-conjugated secondary antibodies were purchased from Invitrogen Life Sciences (Carlsbad, CA). 2,3,7,8-tetrachlorodibenzo-p-dioxin (TCDD) was purchased from Cerilliant (Round Rock, TX). The fluorogenic caspase-3 substrate Ac-DEVD-AFC was purchased from BD Biosciences PharmingenTM (San Diego, CA).

Adenovirus Construction

Generation of AdGFP (control virus) and AdrAhRFL were described previously (Elferink et al., 2001; Park et al., 2005). To generate AdCreGFP, the Cre-recombinase expressing Ad5 vector, AdCreM2, was purchased from Microbix (Mississauga, Ontario, Canada) and amplified using human embryonic kidney 293 packaging cells. The Ad5 vector was collected and then purified by phenol/chloroform extraction. Cre-recombinase was then PCR amplified from the AdCreM2 vector using oligonucleotide primers (5'-GCGGCCGCATGCCCAAGAAGAAGAGG-3' and 5'-GCGGCCGCCTAATCGCCATCTTCCAG-3') and subsequently ligated into the pCR®4-TOPO® vector using the TOPO TA Cloning Kit as described by the manufacturer's instructions (Invitrogen, Carlsbad, CA). Successful cloning was verified by sequencing and the correct clone was designated Cre-TA. Next the Cre sequence from Cre-TA was cloned into the NotI site of the shuttle vector pAdTrack-CMV and the resulting synthesis and analysis of the recombinant adenovirus was performed as described (He et al., 1998). Viral stocks were prepared as previously described (Elferink et al., 2001).

Animals

8-10 week old $AhR^{fx/fx}$ (AhR floxed) and $AhR^{fx/fx}/Cre^{Alb}$ (AhR CKO) mice were used for hepatocyte isolation in accordance with the Institutional Animal Care and Use Committee at the University of Texas Medical Branch. The mice were maintained on a 12-hour light/dark cycle and allowed free access to water and chow. AhR floxed mice were purchased from the Jackson Laboratory (Bar Harbor, ME) and AhR CKO mice were previously described and verified (Fig. 2.1) (Mitchell et al., 2010).

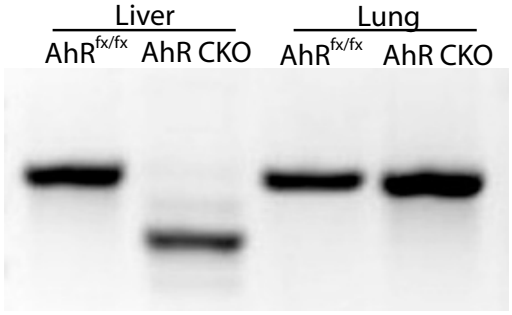

Figure 2.1. **RT-PCR showing specific excision of exon 2 from AhR mRNA**. The smaller PCR product indicative of exon 2 excision is present only in the liver.

Isolation, Culture, and Treatment of Primary Hepatocytes

AhR floxed and AhR CKO primary hepatocytes were isolated using a collagenase perfusion method as previously described (Park et al., 2005). Hepatocytes were plated at a density of $8.5x10^4$-$1.0x10^5$ cells/cm^2 in Williams E medium containing penicillin (100 U/ml), streptomycin (100 μg/ml), and 5% fetal bovine serum and replaced every 24 hours with fresh medium. Hepatocytes were infected with the appropriate adenovirus at an m.o.i. of 20-60 at the time of plating and maintained in culture for the indicated times. 100% infection was ensured via expression of green fluorescent protein using a Zeiss Axiovert 200 inverted microscope (Zeiss Microscopy, Thornwood, NY). In experiments requiring UV exposure the medium was removed and set aside, while the hepatocytes were washed with warm PBS and then UVC irradiated at 20 J/m^2 using a UV Stratalinker 1800 (Agilent Technologies, Santa Clara, CA). After irradiation the medium was immediately replaced and the hepatocytes were cultured for the indicated times. Hepatocytes treated with TCDD after infection were allowed to culture for 6 hours with 6nM TCDD after the indicated times.

RNA Isolation

Total RNA was isolated from AhR floxed and AhR CKO primary hepatocytes using the Chomezynski and Sacchi method (Chomczynski and Sacchi, 1987). Total RNA yield was assessed using a Nanodrop® ND-1000 (Thermo Scientific, Wilmington, DE) and RNA integrity was confirmed using an Agilent 2100 Bioanalyzer (Agilent Technologies, Palo Alto, CA).

RT-PCR Analysis

First –strand cDNA was generated from 1μg of total RNA using an oligo(dT) primer (New England BioLabs, Ipswich, MA) and Superscript II reverse transcriptase (Invitrogen, Carlsbad, CA). PCR using Taq polymerase (Fisher Scientific, Pittsburgh, PA) was performed using oligonucleotide primers for mouse AhR designed to produce different size PCR products depending on the presence of Exon 2 in the AhR transcript (5'-CGCAAGCCGGTGCAGAAAAAC-3' and 5'-ATGGAGGGTGGCTGAAGTGGAGTA-3'). All PCR products were analyzed by fractionation on a 0.8% (w/v) agarose gel and visualized by ethidium bromide staining.

Western Blot Analysis

Whole-cell lysates were prepared from cultured primary hepatocytes after infection or treatment by washing with PBS, then scraping directly in 2X SDS-PAGE loading buffer, and denatured for 10 minutes at 100°C. Protein was fractionated by SDS-PAGE, transferred to Amersham HybondTM-P membranes (Amersham Biosciences Inc., Piscataway, NJ) and blocked with Tris-buffered saline containing 0.1% (v/v) Tween 20 and 5% (w/v) nonfat dry milk. Membranes were incubated with primary antibodies for 3 hours at room temperature or overnight at 4°C followed by an incubation with horseradish peroxidase-conjugated secondary antibodies for 1 hour at room temperature, and the signal was visualized using enhanced chemiluminescence (Amersham Biosciences Inc., Piscataway, NJ).

Caspase-3 Activity Assays

$1X10^6$ AhR floxed primary hepatocytes were infected with the appropriate adenovirus and allowed to culture for 24 or 48 hours. When necessary the hepatocytes were UVC irradiated as described and allowed to culture for an additional 1 hour. Cultures were washed once with cold PBS and hepatocytes were harvested by scraping in cold PBS on ice. The hepatocytes were then pelleted by centrifugation at 1,000g for 5 minutes at 4°C, washed with cold PBS, and centrifuged again to pellet the hepatocytes. The pellet was then resuspended in lysis buffer (10mM Tris (pH 7.5), 10mM NaH2PO4/ Na2HPO4 (pH 7.5), 130mM NaCl, 1% (v/v) Triton X-100, 10mM NaPPi) and cellular membranes were disrupted using a dounce homogenizer. Cell lysates were then clarified by centrifugation at 10,000g for 10 minutes at 4°C and supernatants were transferred to fresh ice-cold microcentrifuge tubes. 50µl of each sample was added to 50µl assay buffer/DTT Mix (20mM PIPES, 100mM NaCl, 10mM DTT, 1mM EDTA, 0,1% (w/v) CHAPS, 10% (w/v) sucrose, pH 7.2). 5µl of 1mM fluorogenic caspase-3 substrate, Ac-DEVD-AFC, was added to each sample and allowed to incubate at 37°C for 1-3 hours. Fluorescence resulting from the cleavage of 7-amino-4-trifluoromethylcoumarin was quantified fluorometrically using a Fluoroskan Ascent fluorometer (Thermo Fisher Scientific, Waltman, MA) with a 400-nm excitation filter and 505-nm emission filter.

Apoptosis PCR Array

Total RNA was isolated from AhR floxed primary hepatocyte cultures after infection with appropriate adenovirus as described. RNA prepared from 3 independent experiments was analyzed using an ABI 7500 Real Time PCR System (Applied Biosystems, Foster City, CA) and Mouse Apoptosis RT2 ProfilerTM PCR Array (SABiosciences, Frederick, MD) according to the manufacturer's instructions by the UTMB Molecular Genomics Core Facility. Data analysis was performed online using the RT2 Profiler PCR Array Data Analysis version 3.4 (http://pcrdataanalysis.sabiosciences.com/pcr/arrayanalysis.php). Transcripts with a fold change

≥ 2 (AdCreGFP normalized expression/AdGFP normalized expression) were considered for validation. Statistical significance was calculated during online analysis using a Student's t-test where p values < 0.05 are considered significant.

Microarray Analysis

Total RNA was isolated from AhR floxed primary hepatocyte cultures after infection with appropriate adenovirus as described. Total RNA prepared from 3 independent experiments was analyzed by the UTMB Molecular Genomics Core using GeneChip Mouse Genome 430 2.0 Arrays (Affymetrix, Santa Clara, CA). Breifly, total RNA (500ng) was converted to cRNA using the Ambion MessageAmpTM Premier RNA Amplification Kit (Life Technologies Corporation, Grand Island, NY) according to manufacturer's instructions. Total fragmented cRNA (10μg) was hybridized to the Affy GeneChip array according to the manufacturer's conditions. The chips were washed and stained in a GeneChip Fluidics Station 450 and fluorescence detected with an Affymetrix-7G Gene Array scanner using the Affymetrix GeneChip Command Console software (AGCC1.1). Gene expression changes were identified using Partek Genomics Suite (Partek, St Louis, MO) following the default gene expression workflow. The resulting values were then filtered for p-values of ≤ 0.05 using a one-way analysis of variance (ANOVA). Fold change was determined by comparing AdCreGFP normalized expression to AdGFP normalized expression.

Ingenuity Pathways Analysis

The microarray data set was analyzed through the use of IPA (Ingenuity® Systems, www.ingenuity.com). The data set containing gene identifiers from all 24-hour statistically significant microarray genes and their corresponding expression values was uploaded into in the application. Each identifier was mapped to its corresponding object in the Ingenuity® Knowledge Base. All Network Eligible molecules were overlaid onto a global molecular network developed from information contained in the Ingenuity

Knowledge Base. Networks of Network Eligible Molecules were then algorithmically generated based on their connectivity.

SYBR Array Analysis

Total RNA was isolated from AhR floxed primary hepatocyte cultures and analyzed by the UTMB Molecular Genomics Core. Briefly, qRT-PCR assays were designed from the coding sequence (CDS) of the gene of interest (NCBI) and exon-exon junctions mapped via BLAT (Kent, 2002). Whenever possible, at least one of the two PCR primers was designed to encompass an exon-intron junction in order to reduce the impact of potential genomic DNA contamination in the surveyed RNA samples. Primers were synthesized (Integrated DNA Technologies, Coralville, IA) and reconstituted to a final concentration of 100mM (master stock) prior to dilution to a working stock of 2mM. Reverse transcription was performed on 1µg of total RNA with random primers, utilizing TaqMan® reverse transcription reagents (Applied Biosystems) as recommended by the manufacturer. The reverse transcription reaction was used as template for the subsequent PCR reaction, consisting of SYBR Green® PCR Master Mix, template cDNA and assay primers in a total reaction volume of 25µl. Thermal cycling was carried out with an ABI prism 7000 sequence detection system (Life Technologies, CA) under factory defaults (50^{o}C, 2 min; 95^{o}C, 10 min; and 40 cycles at 95^{o}C, 15 S; 60^{o}C, 1 min). Threshold cycle numbers (Ct) were defined as fluorescence values, generated by SYBR green binding to double stranded PCR products, exceeding baseline. Relative transcript levels were quantified as a comparison of measured Ct values for each reaction to a designated control via the $\Delta\Delta$Ct method (Livak and Schmittgen, 2001). In order to normalize for template input, GAPDH (endogenous control) transcript levels were measured for each sample and utilized in these calculations. A student's t-test was applied to GAPDH CT values to rule out any change in expression of the endogenous control due to treatment.

Statistical Analysis

Where appropriate the data are represented as mean ± SEM. GraphPad Prism 4 (GraphPad Software, San Diego, CA) was used to calculate statistical significance ($p \leq 0.05$) and is denoted using brackets to show comparison. Comparison of basal caspase-3 activity in AdGFP and AdCreGFP infected hepatocytes used a two-way ANOVA followed by a Bonferroni's post hoc test. Statistical significance in the caspase-3 activity assay 48 hours after infection, and p73 qRT-PCR validation used a one-way ANOVA followed by a Bonferroni's post hoc test.

RESULTS

Loss of the AhR Results in Increased Caspase-3 Activity After Infection with AdCreGFP

Direct measurement of caspase-3 activity revealed a significant increase in its activity after 48 hours of AdCreGFP infection (Fig. 2.2A). The differential apoptotic susceptibility coinciding with loss of the AhR is reminiscent of the observation reported by Wu et al. (2007) in cells succumbing to an intrinsic apoptotic signal. Ectopic expression of the AhR—in hepatocytes infected with AdCreGFP—using a second virus encoding a functional AhR (AdrAhRFL) (Elferink et al., 2001) successfully suppressed caspase-3 activity consistent with the receptor's protective role in apoptosis. The decreased caspase-3

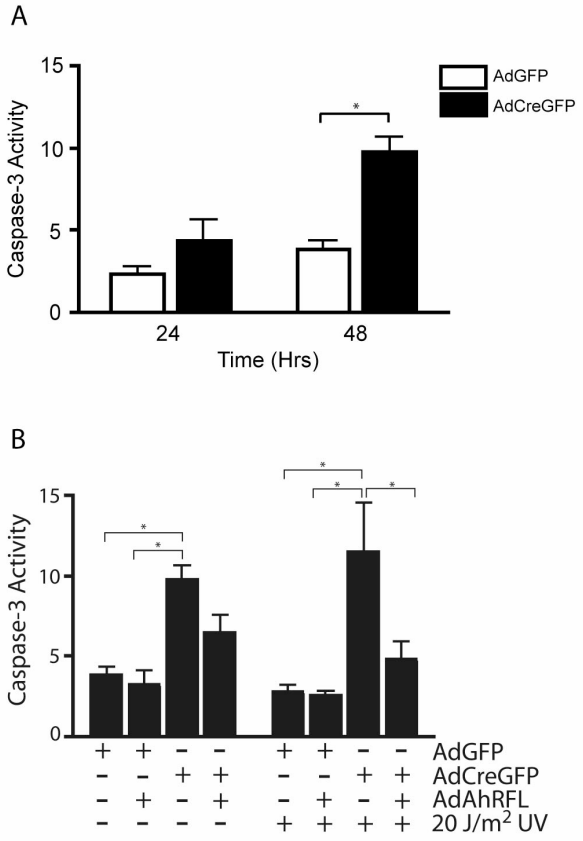

Figure 2.2. Loss of the AhR results in increased caspase-3 activity. A. $AhR^{fx/fx}$ hepatocytes were infected with AdGFP or AdCreGFP for the indicated times and caspase-3 activity assayed. B. $AhR^{fx/fx}$ primary hepatocytes were infected with either AdGFP or AdCreGFP alone, or in combination with AdrAhRFL for 48 hrs after cells were UV irradiated with 20 J/m^2 or left unirradiated. Cells were harvested 60 minutes after UV irradiation and assayed for caspase-3 activity. Asterisks indicate statistical significance ($p < 0.01$).

activity was significantly suppressed in cells subjected to UV irradiation, a trigger of intrinsic cell death (Fig. 2.2B). Accordingly, hepatocytes co-infected with the AdGFP and AdrAhRFL viruses displayed consistently low caspase-3 activity levels. These data confirm that the antiapoptotic susceptibility detected in primary heapocytes is indeed a function of the AhR status.

Apoptosis in Primary Hepatocytes is not Associated with Changes in Akt/ PKB Activity

The AhR's ability to confer cell survival in response to intrinsic cues was largely attributed to activation of the PI3K-Akt/PKB pathway (Wu et al., 2007). We sought to replicate this finding in the primary hepatocytes by examining Akt/PKB activation in UV irradiated cells (Fig. 2.3). In contrast to the reported findings using murine hepatoma cells (Wu et al., 2007), constitutive Akt/PKB activity (determined by Ser473 phosphorylation) was readily detectable in primary hepatocytes cultured for two days, but was unaltered by the AhR status or UV irradiation (Fig. 2.3A). Although

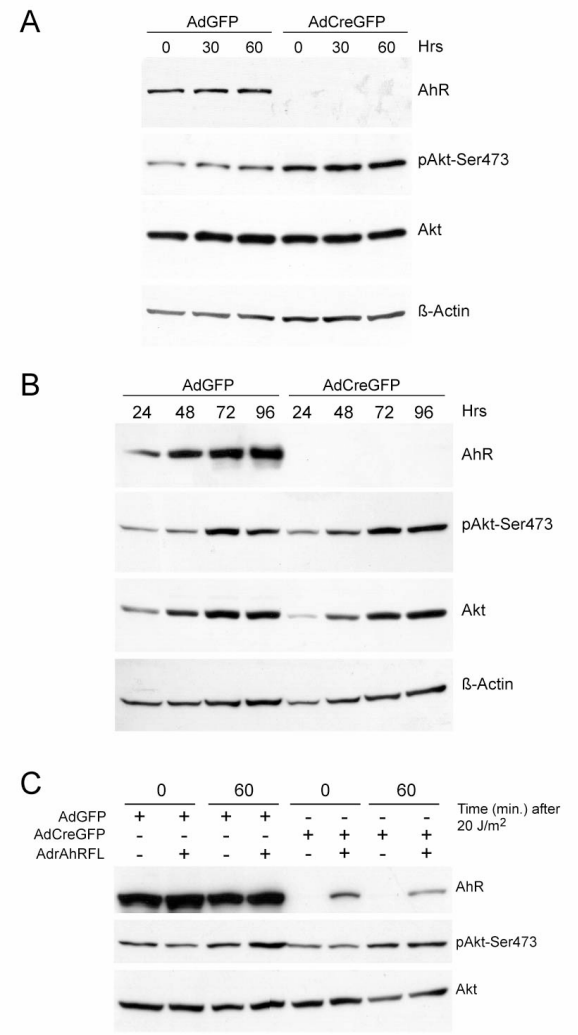

Figure 2.3. Apoptosis in primary hepatocytes is not associated with changes in Akt/PKB activity. **A.** $AhR^{fx/fx}$ primary hepatocytes were infected with AdGFP or AdCreGFP for 48 hours, UV-irradiated, and maintained in culture for the indicated times prior to preparation of whole cell lysates for analysis by western blotting for AhR, Akt phosphorylation on serine 473, and Akt. Actin was used as a loading control. **B.** $AhR^{fx/fx}$ primary hepatocytes infected with AdGFP or AdCreGFP for the indicated period, UV irradiated and whole cell lysates prepared 60 minutes later for analysis of AhR, Akt phosphorylation on serine 473, and Akt protein expression. Actin was used as a loading control. **C.** $AhR^{fx/fx}$ primary hepatocytes were infected with AdGFP or AdCreGFP alone, or in combination with AdrAhRFL for 48 hours, UV irradiated, and cell lysates prepared after 0 or 60 minutes. Western blot analysis was performed on AhR, Akt phosphorylation on serine 473, and Akt.

primary hepatocyte cultures undergo spontaneous changes with time including modest increases in Akt/PKB expression, these had no discernable effect on Akt/PKB signaling within the first 4 days (Fig. 2.3B). Lastly, ectopic expression of the AhR in the AdCreGFP infected cells lacking the endogenous AhR similarly failed to elicit a change in Akt/PKB signaling in response to UV irradiation (Fig. 2.3C), a condition shown to trigger apoptosis (Fig. 2.2). Collectively, the data indicate that the differential apoptotic susceptibility tied to AhR status is not reconciled by changes in Akt/PKB activity in normal hepatocytes.

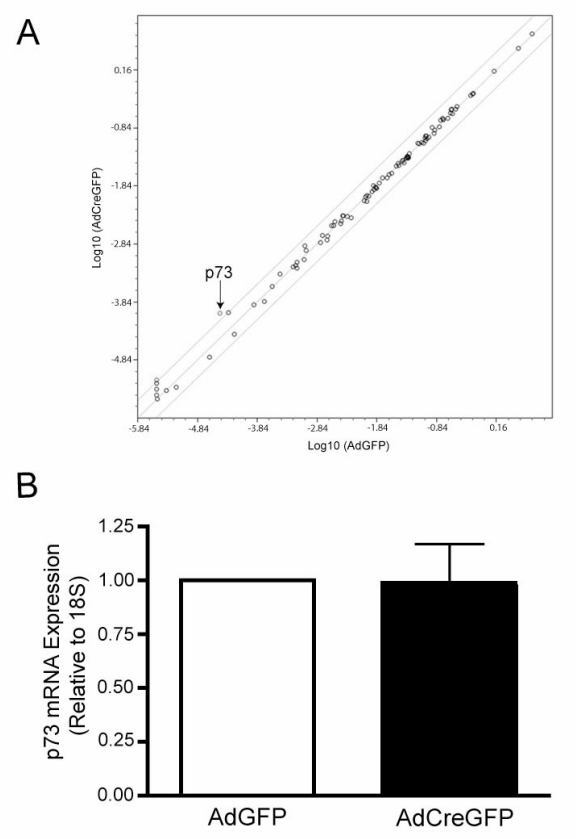

Figure 2.4 The loss of AhR protein does not alter expression of 84 well-defined apoptotic genes. **A.** $AhR^{fx/fx}$ primary hepatocytes were infected with AdGFP or AdCreGFP for 24 hours. Total RNA was prepared for use in SABiosciences Mouse Apoptosis RT^2 Profiler PCR Array as described in the Materials and Methods. Individual transcripts (open circles) in the array are plotted as a function of their expression in AdGFP and AdCreGFP infected cells. Unchanged transcripts lie along the central diagonal line. The outer lines denote 2-fold changes in expression. The array was performed in triplicate using 3 biologically independent RNA preparations. The arrow identifies p73. **B.** qRT-PCR was performed on the RNA to verify p73 expression independently. The data represents the mean ± S.E.M. of three independent experiments. p73 mRNA expression was normalized to ribosomal RNA 18S.

Loss of AhR Protein Does Not Alter Expression of Well-Defined Apoptotic Genes

In order to more broadly examine the molecular basis responsible for AhR-mediated cell survival, we performed a SABiosciences Mouse Apoptosis RT^2 Profiler PCR Array to profile 84 key genes involved in programmed cell death (see Table A.1 on page 65). The results identified a single transcript (encoding p73) whose level changed greater than 2-fold between AhR-positive (AdGFP infected) and AhR-negative (AdCreGFP infected) hepatocytes (Fig. 2.4A).

However, qRT-PCR failed to independently verify the modest increase in p73 expression associated with AhR loss detected in the array (Fig. 2.4B).

Loss of the AhR in Primary Hepatocytes Generates a Unique Microarray Data Set

Given the finding that none of the 84 established apoptotic genes included in the array underwent a reproducible change in expression in hepatocytes following AhR loss, a more comprehensive DNA microarray study was initiated. Microarray analysis was performed in triplicate using independent RNA samples isolated from primary hepatocytes at 0, 12 and 24 hours after infection with the AdGFP or AdCreGFP virus. The experiment identified 97 and 246 statistically significant ($p \leq 0.05$) changes in gene expression at 12 and 24 hours, respectively (see Table A.2 on page 68). Of the 97 changes detected at 12 hours, 88 genes increased expression and 9 decreased expression with loss of AhR expression. By 24 hours, 119 genes increased and 127 genes decreased expression. Figure 2.5 represents biological functions considered to be significantly altered in the 24 hour data set after analysis using IPA. Interestingly, there is little overlap between the sets of genes identified in this study and those identified in published microarray studies that monitored changes in expression following exposure to an exogenous AhR agonist, or changes in the steady-state transcriptome associated with prolonged AhR loss in the AhR knock out mouse (data not shown). This most likely reflects the strategy employed here designed to identify immediate changes in expression

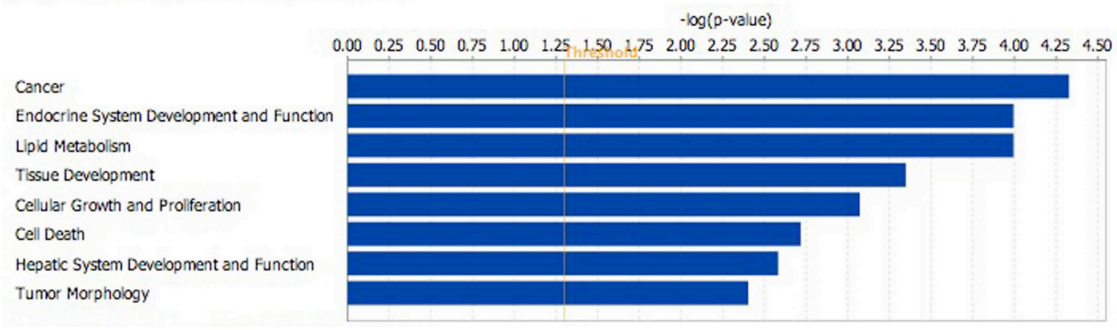

Figure 2.5. Representative graph displaying biological functions deemed to be significantly altered. Biological functions altered in the the 24-hour microarray data set after analysis with IPA. Significance was determined by IPA using a Fishers exact test.

concomitant with loss of AhR in the absence of an exogenous agonist. Custom qRT-PCR SYBR arrays were performed to validate expression of selected genes identified in the microarrays. The rationale used in choosing the validation set included focusing on well annotated genes, and those linked to relevant signaling pathways identified by IPA. Figure 2.6 depicts a network identified by IPA using the statistically significant data obtained by the 24 hour sample microarrays, indicating both decreases (green symbols) and increases (red symbols) in the AdCreGFP infected cells. A total of 31 and 145

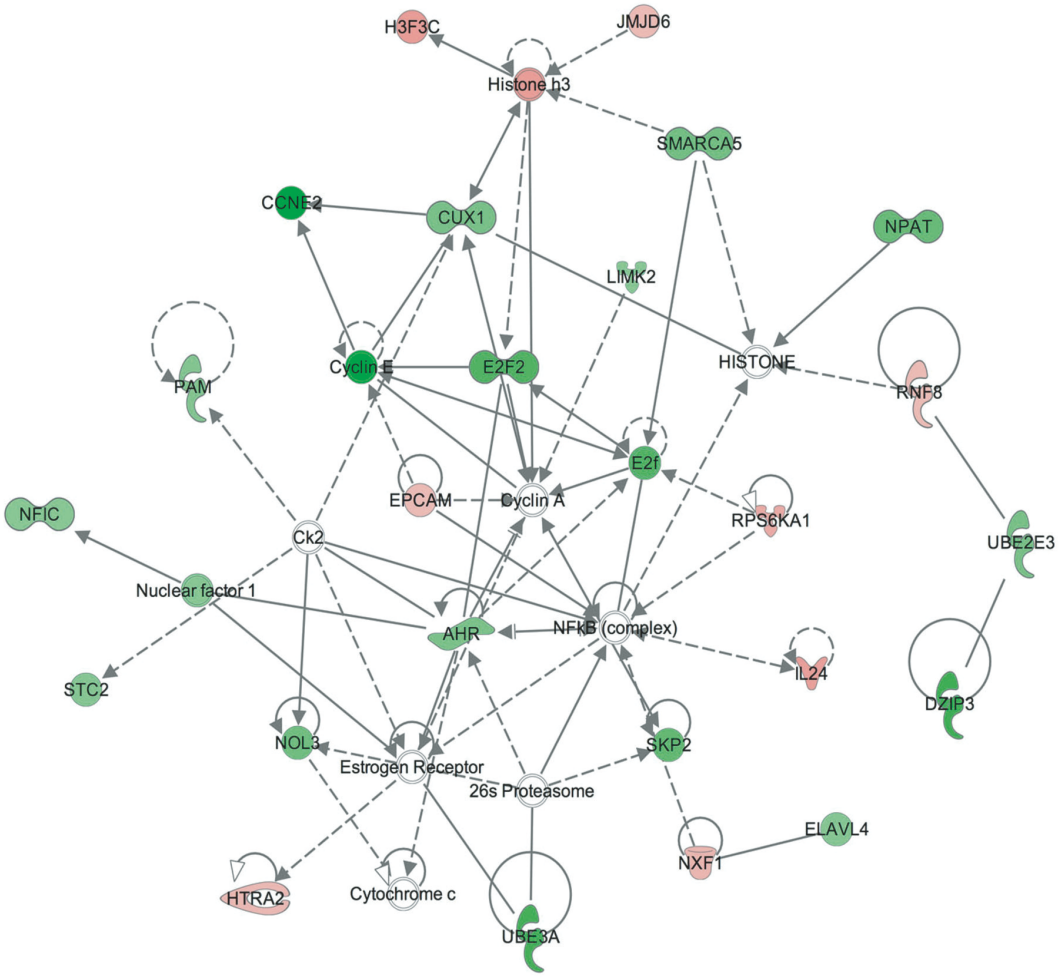

Figure 2.6. Network generated in Ingenuity Pathway Analysis (IPA) using the 24-hour microarray data comparing AdGFP and AdCreGFP infected hepatocytes. Green and red symbols denote a decrease or increase in expression, respectively, accompanying the loss of AhR. Solid lines represent a direct relationship as reported by the Ingenuity Knowledge database, whereas dashed lines represent an indirect relationship.

genes were chosen for validation at 12 hours and 24 hours post viral infection, respectively. None of the expression changes detected in the microarray at 12 hours could be verified by qRT-PCR. However, qRT-PCR identified 36 genes that reproducibly changed by 24 hours, 3 increased and 33 decreased expression following loss of the receptor (see Table A.2 on page 68). Consistent with the experimental design, AhR expression decreased. Interestingly, so did expression of Stanniocalcin 2 (Stc2), one of the genes identified by IPA and validated by qRT-PCR as consistently being altered concomitant with loss of the AhR in primary hepatocytes (Fig. 2.7A). The qRT-PCR also validated changes in FGR (Src family tyrosine kinase) and Htra2 (mitochondrial serine protease) expression, the latter also tied to AhR function based on the IPA. It is noteworthy that the decrease in Stc2 and FGR was also observed in vivo in conditional knock out mice lacking AhR expression specifically in the hepatocytes (Fig. 2.7B). These data suggest that both Stc2 and FGR are direct AhR targets, and that steady state constitutive expression is predominantly AhR dependent. In contrast, in vivo Htra2 steady state expression in hepatocytes remains unaltered in the conditional knock out mice, suggesting that the increase observed in AdCreGFP-infected primary hepatocytes may be a transient response to sudden AhR loss

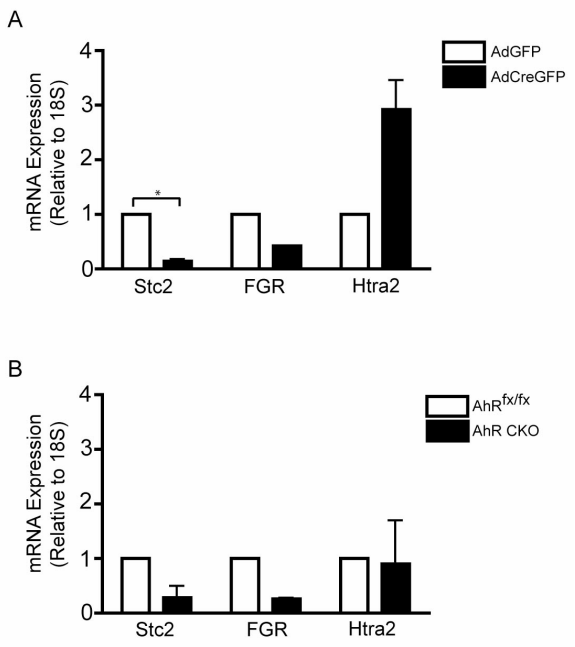

Figure 2.7. Validation of Stc2, Fgr and Htra2 expression by qRT-PCR. A. qRT-PCR was performed on total RNA isolated from $AhR^{fx/fx}$ primary hepatocytes infected with AdGFP or AdCreGFP for 24 hours. Quantitation of mRNA expression is normalized to ribosomal RNA 18S. The data presented for Stc2 represents the mean ± S.E.M. of 3 independent experiments. Asterisk indicates statistical significance ($p < 0.01$). **B.** Primary hepatocytes were isolated from an $AhR^{fx/fx}$ or AhR CKO mouse and total RNA was prepared for use in qRT-PCR assays. The data presented are the average of two independent experiments (± S.E.M.).

that is compensated for by alternative regulatory processes following prolonged loss of the AhR.

DISCUSSION

Hepatocyte damage from physical insult, pharmacological agents, and hepatotropic pathogens can result in the removal or repair of damaged cells. It is therefore no surprise that disruption of these mechanisms results in liver dysfunction leading to disease states such as steatohepatitis, fulminant hepatitis, or hepatocellular carcinoma. Many of the proteins important in apoptosis and survival have been identified and described thoroughly in the literature. However, many times these processes are first identified and characterized in immortalized or transformed cancer cell lines which may produce findings that do not faithfully capture the signaling processes in physiologically normal cells. The current study represents a case in point. I demonstrate here that in the presence of an intrinsic apoptotic stimulus, the AhR promotes hepatocyte survival (Figs. 2.2), in agreement with the observations reported by Wu and coworkers (2007). However, the underlying mechanisms differ: whereas hepatoma cell survival was attributed in large part to AhR mediated activation of Akt/PKB—a well documented survival protein often constitutively active in cancer cells (Shaw and Cantley, 2006)—survival of AhR positive primary hepatocytes was independent of Akt/PKB activity. AhR expression was also reported to protect immortalized mouse embryo fibroblasts from programmed cell death by suppressing Apaf1 and TAp73 gene expression in an E2F1-mediated manner (Marlowe et al., 2008). However, our DNA microarray studies did not detect an increase in Apaf1 or TAp73 expression following loss of the AhR (Table A.2 on page 68), and although p73 mRNA exhibited a marginal increase in the SABiosciences apoptosis array, this finding could not be verified using qRT-PCR (Fig. 2.4B). Hence, it is difficult to attribute the heightened primary hepatocyte susceptibility to apoptosis following loss of the receptor, to p73 expression. Nevertheless, the consistent observation that a positive AhR status correlates with enhanced cell survival suggests that

the AhR does indeed play a pivotal role in maintaining cell viability, irrespective of the precise mechanism responsible. Therefore, in order to examine the relationship between AhR biology and liver cell death, I considered it prudent to study the process in a physiologically normal cell model, notably primary hepatocytes.

In order to reconcile the increase in cell death with the loss of the AhR I performed a comprehensive DNA microarray designed to identify immediate and direct changes in the transcriptome concomitant with the loss of the AhR. Several independent groups have performed microarray analyses designed to link changes in the transcriptome with AhR status using knockout models, or function using exogenous AhR agonists (Boutros et al., 2009; Franc et al., 2008; Tijet et al., 2006; Wang et al., 2007). Specifically, Tijet and coworkers identified several novel AhR target genes independent of TCDD activation using AhR knockout mice generated previously (Schmidt et al., 1996). However, the transcriptome in the AhR knockout mouse liver constitutes a steady state response to prolonged receptor loss affecting myriad indirect changes. This confounds identification changes in gene expression attributable to direct AhR control. The observation that livers in the AhR knockout mice are abnormal is suggestive of robust secondary compensatory effects associated with long-term AhR loss during development. In contrast, my study differs from the previous by ones by monitoring immediate changes in the transcriptome concomitant with loss of AhR protein in order to preferentially identify transcriptional responses reflective of direct AhR target genes. Since the changes in expression occurred in the absence of any exogenous agonist, I conclude that the target genes identified are those involved in normal AhR mediated physiological processes. In this context, it is not surprising that the Cyp1a1 gene—nor several of the other AhR responsive Phase I and Phase II target genes typically associated with an exogenous agonist—went undetected in the microarrays. In fact, the finding that most of the altered transcripts are encoded by genes hitherto not associated with AhR regulation, suggests that receptor biology responding to endogenous cues differs

markedly from that following exposure to exogenous agonists and is reminiscent of AhR activation by selective AhR modulators (SAhRMs) (Safe et al., 2000). SAhRMs can be defined as receptor agonists that function through AhR-dependent activation resulting in decreased or abolished toxicities traditionally associated with AhR activation by more potent agonists such as TCDD. For example, Murray and coworkers demonstrated in an AhR dependent manner that activation by the SAhRM Way-169916 diminished the expression of inflammatory genes SAA1 and CRP, while failing to stimulate XRE-driven AhR-mediated CYP1A1 expression (Murray et al., 2010).

In keeping with the objective to reconcile the hepatic apoptotic susceptibility with loss of the AhR I examined the expression of Stc2, Fgr and Htra2 (Fig. 2.7), three proteins previously reported to affect cell viability (Ito et al., 2004; Lowell and Berton, 1998; Suzuki et al., 2001). The decrease in Stc2 and Fgr expression suggests that the AhR is required for their expression, a conclusion reinforced by the observation that their expression remained suppressed in the conditional knock out mouse liver following sustained AhR loss (Fig. 2.7B). In contrast, Htra2 expression is suppressed by the AhR, although compensatory mechanisms appear to exist that restore normal expression in vivo in circumstances of prolonged AhR loss. It is noteworthy that Stc2 and Htra2 were identified by IPA as components of a larger network encompassing several species known to be functionally linked to the AhR, including the Estrogen Receptor, NFkB, E2F, and the Cyclins A and E (Marlowe et al., 2004; Mitchell et al., 2006; Ohtake et al., 2003; Strobeck et al., 2000; Tian et al., 1999).

Further analysis of the microarray data using IPA indicated several biological functions were significantly represented in the 24-hour data set, including cancer, tissue development, cellular growth and proliferation, and cell death (Fig. 2.5). These functions are consistent with normal AhR biology and the hypothesis that the AhR promotes cell survival during homeostasis. In this study I was able to show that Akt/PKB signaling is not impaired in primary hepatocytes and none of the usual suspects associated with

apoptosis are altered with the loss of the AhR. Furthermore, I was able to identify several AhR targets not previously associated with the AhR or traditional AhR activities. Further examination of the microarray data and individual analysis of potential targets such as Stc2 is necessary to identify the mechanisms responsible for the AhR's ability to confer cell survival and to improve our understanding of normal AhR biology.

Chapter 3: Novel Insights into Normal Aryl Hydrocarbon Receptor Biology Through Regulation of Stanniocalcin 2

INTRODUCTION

The AhR is a ligand activated transcription factor traditionally recognized for its role in the adaptive metabolism of xenobiotics (Schmidt and Bradfield, 1996). Ligand binding results in AhR translocation to the nucleus where it forms a heterodimer with Arnt and binds response elements in the DNA know as xenobiotic response elements (XREs; also known as dioxin response elements (DREs) and aryl hydrocarbon response elements (AhREs)) to promote or suppress transcription of AhR target genes (Lees and Whitelaw, 1999). Recently, our laboratory reported that the AhR could also bind to a response element coined the non-consensus XRE (NC-XRE) independent of Arnt after activation by an exogenous ligand providing evidence for alternative mechanisms of AhR target gene regulation (Huang and Elferink, 2012). Additionally, the AhR has been identified in the nucleus of several cell lines without activation by an exogenous ligand (Oesch-Bartlomowicz and Oesch, 2009). This observation along with the observed phenotype of the AhR knockout mice suggest the AhR is activated by an endogenous ligand responsible for normal AhR biology including liver homeostasis.

I reported in Chapter 2 that the loss of the AhR in primary hepatocytes results in increased cell death highlighting the receptor's involvement in protecting primary hepatocyt**es** (Fig. 2.2). Previously, the AhR's ability to confer cell survival in response to intrinsic cues was largely attributed to activation of the PI3K-Akt/PKB pathway in hepa1c1c7 hepatoma cell line (Wu et al., 2007). However, I was unable to verify this finding in the primary hepatocytes (Fig. 2.3). In addition, I was unable to detect reproducible changes in the expression of 84 genes with a well-documented role in apoptosis using an apoptosis gene array (Table A.1 on page 65). However, after

performing a comprehensive microarray analysis I was able to identify a number of genes, including Stc2, that have been previously implicated in cell survival.

Stanniocalcin is a secreted glycoprotein originally identified in bony fish, where it was shown to regulate calcium levels in the gills (Wagner et al., 1986). Later Stanniocalcin 1 and 2 were identified in both mice and humans sharing 61% homology with the teleost Stc2 (Chang et al., 1996; Chang et al., 1995; Chang and Reddel, 1998; Ishibashi et al., 1998). Mammalian Stc1 and Stc2 share only 30% homolgy, but do retain a conserved glycosylation site and cysteine residues (Wagner and Dimattia, 2006). In addition, there is significant evidence suggesting mammalian Stc1 and Stc2 perform different functions and are not simply complementary or redundant (Wagner and Dimattia, 2006). Mammalian Stc2 identified in the microarray and validated using qRT-PCR is thought to confer cell survival through an unknown mechanism during cellular injury including ER stress and UPR activation (Ito et al., 2004). In addition, Stc2 is upregulated in a number of cancers (Chang et al., 2003), again supporting a pro-survival role for Stc2. Hence, the link between the AhR, Stc2 expression, and its cytoprotective function provides a potentially novel mechanism by which the AhR confers cell survival.

With the evidence that the AhR regulates Stc2 expression in the absence of an exogenous ligand I performed an in silico analysis to examine the Stc2 promoter region. As a result I identified 9 putative XREs within 1Kb of the Stc2 transcriptional start site, 8 of which were found to be clustered within a 250 bp cassette (Fig 3.1). The clustering of 8

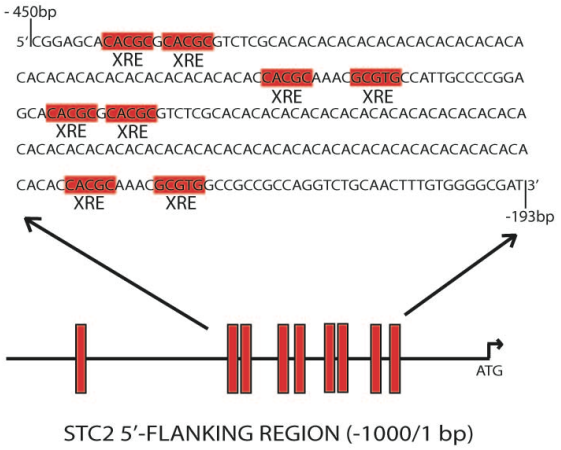

Figure 3.1. Schematic representing 9 putative XRE binding sites (5'-GCGTG-3') within 1 kb of the Stc2 transcriptional start site. The XRE cassette is located 226 base pairs upstream of the start site and spans a 218 base pair region. XRE core consensus sequences are highlighted in red.

XRE sequences in the Stc2 promoter region greatly exceeds the estimated random distribution of XRE per ~10 Kb, and connotes a functional role akin to the XRE repeats in the Cyp1a1 promoter. Intrigued with the finding that the AhR regulates Stc2 expression in the absence of an exogenous ligand despite containing a large number of XREs, I set out to further characterize the AhR-Stc2 relationship through promoter binding studies, and studies utilizing recombinant Stc2 to prove Stc2s ability to confer cell survival.

MATERIALS AND METHODS

Materials

Antibodies were obtained from various commercial sources: AhR (western) (Enzo Life Sciences, Farmingdale, NY); AhR and Histone H3 ChIP grade (Abcam, Cambridge, MA); IgG for ChIP (Cell Signaling Technology, Danvers, MA); P4501A1 and CHOP (sc-7351) (Santa Cruz Biotechnology, Santa Cruz, CA); Stc2 (Bethyl Laboratories, Montgomery, TX); FLAG M2 (Sigma-Aldrich, St. Louis, MO); β-Actin (Millipore, Billerica, MA); all HRP-conjugated secondary antibodies were purchased from Invitrogen Life Sciences (Carlsbad, CA); all fluorescent secondary antibodies were purchased from GE Healthcare (Piscataway, NJ). 2,3,7,8-tetrachlorodibenzo-p-dioxin (TCDD) was purchased from Cerilliant (Round Rock, TX). 3-methylcholanthrene (3-MC), β-napthoflavone (BNF), and thapsigargin were purchased from Sigma-Aldrich (St. Louis, MO). The fluorogenic caspase-3 substrate Ac-DEVD-AFC was purchased from BD Biosciences PharmingenTM (San Diego, CA). AdVP16 was generously provided by Dr. Marxa Figueiredo.

Animals

All animals were used as described in Chapter 2.

Isolation, Culture, and Treatment of Primary Hepatocytes or AML-12 Cells

Hepatocytes were isolated and treated as described in Chapter 2. New treatments are described as follows: Non-infected hepatocytes were allowed to attach for 3 hours

and then treated with DMSO, TCDD, 3-MC, or BNF at 0.2%, 6nM, 5μM, and 10μM respectively. Additionally selected experiments treated hepatocytes with 500nM thapsigargin to induce ER stress. The hepatocytes were then collected 24 hours after treatment. The murine immortalized AML-12 cell line was cultured as described previously (Wu et al., 1994) and infected with appropriate virus at an m.o.i of 100 due to poor infection rates as determined empirically.

Western Blot Analysis

Western blot analysis was performed as described in Chapter 2 with the following changes: HRP-conjugated antibodies were visualized using enhanced chemiluminescence (Amersham Biosciences Inc., Piscataway, NJ) and both HRP- and fluorescent secondaries were imaged using the Typhoon Trio Variable Mode Imager (GE Healthcare). Quantification of western analysis was performed using ImageQuant TL software (Version 7.0, GE Healthcare).

Taqman qRT-PCR

Taqman qRT-PCR was performed by the UTMB Molecular Genomics Core Facility using an Stc2 primer and probe set purchased from Applied Biosystems. All single qRT-PCR assays were normalized against the internal control ribosomal RNA 18S.

Chromatin Immunoprecipitation (ChIP)

Liver tissue from AhR floxed and AhR CKO female mice were extracted either 2 hours after vehicle or TCDD gavage, or alternatively 8 hours after vehicle or 1mg/kg thapsigargin treatment by intraperitoneal injection. Livers were rinsed with ice cold PBS, finely minced and cross linked with 1% formaldehyde in PBS at room temperature for 10 min. Cross linking was stopped using 0.5M glycine solution. Samples were homogenized in a Dounce homogenizer and centrifuged at 3200g for 5 min at 4°C. Pellet was resuspended in 4 ml of cell lysis buffer (150mM NaCl, 25mM Tris, 5mM EDTA, 1% Triton X, 0.1% SDS, 0.5% Na Deoxycholate, Protease inhibitors) and homogenized with a Dounce homogenizer. Samples were incubated on ice for 15 min., centrifuged at 3200g

for 5 min at 4°C and pellet was further processed using ChIP-IT Express Enzymatic Kit (Active Motif) according to the manufacturer's instructions. The sheared chromatin (input) was incubated overnight with appropriate antibodies AhR, Histone H3 as positive control or IgG as negative control. Input and immunoprecipitated DNA were PCR amplified using vetted CYP1A1 (forward 5'-CTATCTCTTAAACCCCACCCCAA-3', reverse 5'-CTAAGTATGGTGGAGGAAAGGGTG-3') primers and primers specific to the XRE's in the STC2 promoter (forward 5'-CTCAGTCCATTCGGCCATTGC-3', reverse 5'-ACTTCTACGGGAGGAAGCGGAG-3'). PCR product was ran on a 5% polyacrylamide gel, stained with SYBR Green I (Invitrogen) and imaged on Typhoon Trio.

Luciferase Plasmid Construction and Assays

The luciferase plasmids Stc2XREpGL3 and Stc2PropGL3 containing the XRE cassette (-468/-206) or 1kb promoter region (-1000/-1) respectively in the murine genome were constructed for use in luciferase reporter assays (Figure 3.2). The designated region of the Stc2 promoter was PCR cloned from genomic DNA using the following primers: Stc2XREpGL3 Forward 5'-GGTACCCCATTCGGCCATTGC-3' and Reverse 5'-AGATCTGTTGCAGACCTGGCG-3' or Stc2PropGL3 Forward 5'-GGTACCGCCGCCTGACCCAAG-3' Reverse 5'-AGATCTGCGCCGCGAGTGCCC-3'. The forward primers contained a 5' KpnI restriction site, whereas the reverse primers contained a 5' BglII restriction site for directional cloning into the pGl3 vectors. After PCR cloning the products were analyzed

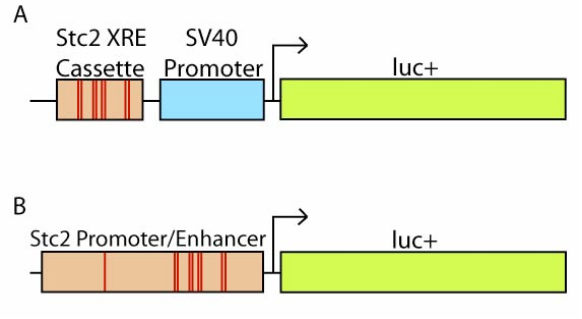

Figure 3.2. Schematic of luciferase reporter constructs. A. The XRE enhancer cassette found in the Stc2 promoter was placed in front of the SV40 promoter of the pGL3-promoter vector. **B.** The 1Kb Stc2 promoter/enhancer containing the XRE cassette was placed in the pGL3-basic vector to promoter luciferase transcription. Red lines indicate location of the XREs.

on an agarose gel, purified, and TOPO cloned into the pCR®4-TOPO vector for sequencing. After sequence verification the Stc2XRETOPO and Stc2ProTOPO vectors were digested at 37 degrees for one hour with KpnI and BglII (New England Biolabs, Ipswich, MA), purified and then ligated using the Fast-Link Ligation kit (Epicentre Biotechnologies, Madison, WI) as directed by the manufacturer and One Shot TOP10 cells were transformed to propagate the final plasmid. Plasmid purification was performed using the Qiagen Miniprep kit (Qiagen, Valencia, CA) and concentrations determined using a NanoPhotometer® (Implen, Westlake Village, CA).

Primary hepatocytes and AML-12 cells were transfected with the appropriate Stc2 luciferase plasmid (1ug/35mm well) and the pRL-SV40 vector at a ratio of 10:1 using lipofectamine 2000 (Invitrogen) as recommended by the manufacturer. After transfection the cells were either infected with AdVP16, AdGFP (data not shown), or treated with thapsigargin (data not shown) for 24 hours. After 24 hours the samples were collected and prepared using the Dual-Luciferase Reporter Assay System kit (Promega, Madison, WI). 20ul of each sample was added to an opaque 96-half well plate and 40ul of each substrate was added sequentially and analyzed using a LMAXII384 luminescence microplate reader and SoftMax Pro Software Version 4.8 (Molecular Devices, Sunnyvale, CA). All luciferase values were normalized to the corresponding renilla value.

Generation of Recombinant Stc2

Recombinant Stc2 protein was generated as follows: The Stc2 fully sequenced cDNA clone #3665803 was purchased from Open Biosystems (Lafayette, CO) to be used as a template for cloning the Stc2 precursor open reading frame containing the N terminus secretion signal. The precursor Stc2 open reading frame was PCR cloned using the primers: Forward 5'-CCCAAGCTTTGTGCGGAGCGGCTG-3' and Reverse 5'-GGAAGATCTCCTCCGGATGTCGGA-3' containing HindIII and BglII sites at the 5' terminus respectively. The cloned fragment was then purified and cloned into the TOPO TA Cloning Kit for Sequencing according to the manufacturers instructions (Invitrogen).

After sequence validation the TOPO plasmid was digested with HindIII and BglII (New England Biolabs, Ipswich, MA), gel purified and ligated into the pT7-FLAG-MAT-Tag-2 expression Vector (Sigma-Aldrich) and transformed into One Shot TOP10 cells to introduce the desired FLAG and MAT tags at the C terminus of the protein. Selected colonies were first digest mapped and then sequence verified using the T7 and C24 primers. Next the validated plasmid was PCR cloned using the following primers to introduce a kozak/ start sequence at the 5' end and a stop sequence at the 3' end to prevent translation of the V5 and His tags possessed in the pcDNA5/FRT/V5-His TOPO TA vector: Forward 5'-ACCATGTGTGCGGAGCGGCT-3' and Reverse 5'-TCAGTGTTTGTGACGGTGGTTGTG-3'. The PCR products were then purified and used in the TOPO reaction with the pcDNA5/FRT/V5-His TOPO TA vector to obtain the desired sequence with the correct tags in a vector that can be used for high expression levels in a mammalian cell line. The final precursorStc2pcDNA5 vector was passed along to Dr. Istvan Boldogh for stable transfection into the Chinese hamster ovary (CHO) cell line using the Flp-In™ system. The concentration of secreted rStc2 in the media was analyzed using different volumes of media for western analysis and comparing the density of the rStc2 band to a standard curve created using a protein of known concentration (Fig. 3.3). The enriched media was then collected and stored at -20 degrees Celsius.

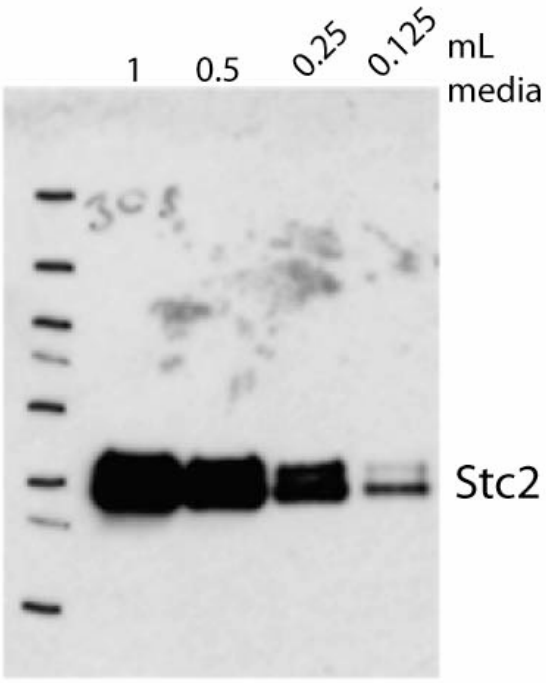

Figure 3.3. Validation of recombinant Stc2 . Expression and secretion into culture media was monitored by western blot analysis using an anti-Stc2 antibody.

Caspase-3 Activity Assays

$1X10^6$ AhR floxed primary hepatocytes were plated and allowed to attach for 3 hours. After 3 hours the hepatocytes were left untreated, treated with 300uM H2O2, 100ng/mL rStc2 (3nM) enriched media, or control media lacking rStc2 for 6 hours. Cultures were washed once with cold PBS and hepatocytes were harvested by passive lysis for 30 minutes on ice while rocking using the ice-cold lysis buffer. Cell lysates were then clarified by centrifugation at 10,000g for 10 minutes at 4°C and supernatants were transferred to fresh ice-cold microcentrifuge tubes. 50µl of each sample was added to 50µl assay buffer/DTT Mix. 5µl of 1mM fluorogenic caspase-3 substrate, Ac-DEVD-AFC, was added to each sample and allowed to incubate at 37°C for 1-3 hours. Fluorescence was quantified fluorometrically using a SpectraMax M2 with a 400-nm excitation filter and 505-nm emission filter and SoftMax Pro Software (Molecular Devices). Caspase activity values were normalized to protein concentration determined using BCA protein assay (Pierce, Rockford, IL).

rStc2 Binding/Internalization

Primary hepatocytes isolated from AhR floxed mice were allowed to attach for 3 hours. After 3 hours the media was replaced with media containing 100ng/mL (3nM) rStc2 or control media lacking rStc2 enrichment. The hepatocytes were then collected at 0, 5, 15, 30, and 60 minutes after the addition of rStc2 enriched media for analysis of binding and internalization by western blot analysis. Alternatively, primary hepatocytes isolated from AhR floxed mice were allowed to attach for 3 hours and then treated with a combination of the following: 75ng/mL (2.3nM) rStc2, 300uM H2O2, or casein kinase II (10 units). In addition 4X casein kinase II buffer (100mM Tris-HCl (pH 7.4), 40mM MgCl2, 800mM NaCl, and 0.4mM ATP) was added to the hepatocytes at the time of treatment. The cells were collected 6 hours after treatment for analysis by western blotting.

Statistical Analysis

Where appropriate the data are represented as mean ± SEM. GraphPad Prism 4 (GraphPad Software, San Diego, CA) was used to calculate statistical significance ($p \leq 0.05$). Comparison of caspase-3 activity, and comparison of CHOP protein expression used a two-way ANOVA followed by a Bonferroni's post hoc test. Statistical significance in the luciferase reporter assay used a one-way ANOVA followed by a Bonferroni's post hoc test. All qRT-PCR assays compared the fold change values calculated as a log2 ratio of the ΔΔCt averages of the biological replicates to the control sample using a Student's t-test to evaluate statistical significance.

RESULTS

Stc2 Gene Induction is Refractory to Classical AhR Agonists

After performing an in silico analysis of the murine Stc2 promoter region, where I identified 9 putative XRE consensus sequences (5'-GCGTC-3') within 1 kb of the Stc2 transcriptional start site (Fig. 3.1), I decided to examine AhRs role in Stc2 expression further. Therefore, I exposed primary hepatocytes to well-known AhR exogenous agonists to determine if Stc2 expression parallels that of the Cyp1a1 locus (Fig. 3.4). The evidence shows that Stc2 gene induction is refractory to the classical receptor agonists 2,3,7,8-tetrachlorodibenzo-p-dioxin, 3-methylcolanthrene, and ß-napthoflavone, despite efficient induction of the Cyp1a1 gene.

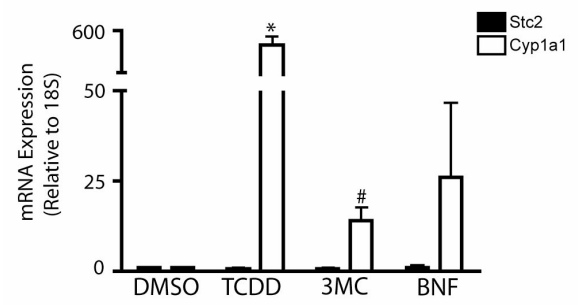

Figure 3.4. Stc2 gene induction is refractory to classical AhR agonists. qRT-PCR was performed using total RNA prepared from $AhR^{fx/fx}$ hepatocytes treated for 24 hours with the vehicle DMSO, 6 nM TCDD, 5 μM 3-methylchloranthrene (3-MC), or 10 μM ß-napthoflavone (BNF). The data presented for Stc2 represents the mean ± S.E.M. of 3 independent experiments. Asterisk or number sign indicates statistical significance of $p < 0.01$ or $p < 0.05$ respectively when compared to vehicle treated samples. Quantification of mRNA expression is relative to ribosomal RNA 18S and normalized to vehicle treated samples.

The AhR binds the XRE Cassette Located Upstream of the Stc2 Transcriptional Start Site

Chromatin immunoprecipitation (ChIP) detected direct binding of the AhR to the region encompassing the XRE cassette in the Stc2 promoter (Fig.3.5). In contrast to the TCDD-dependent AhR binding observed at the Cyp1a1 promoter, the AhR interaction with the Stc2 promoter occurs independently of TCDD treatment (Fig.3.5A). The lack of a Stc2 ChIP product in the CKO mouse liver nuclei further illustrates the specificity of the AhR ChIP product detected in wildype mice (Fig. 3.5B). The IgG and Histone H3 ChIP results serve as positive and negative controls for the ChIP assay respecitively.. The inability to induce Stc2 expression using the exogenous agonists may be reconciled with the lack of an inducible ChIP product at the Stc2 promoter. Whether the observed constitutive AhR binding reflects the action of an endogenous receptor agonist is unknown.

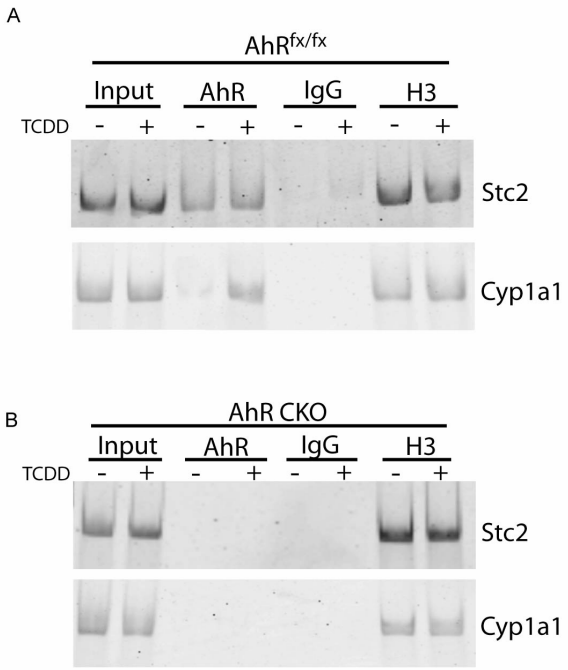

Figure 3.5. The AhR binds the putative XRE cassette located upstream of the Stc2 transcriptional start site. ChIP analysis of AhR protein binding to the Stc2 promoter region in liver tissue from $AhR^{fx/fx}$ **(A)** or AhR CKO **(B)** mice treated with vehicle (-) or 20 μg/kg TCDD (+) for 2 hours. IgG and histone H3 antibodies were used as negative and positive controls respectively. The primers used for ChIP analysis correspond to base pairs -473 to -453 (For) and -182 to -161 (Rev).

The Endoplasmic Reticulum Stress Inducer Thapsigargin Does Not Increase AhR Binding at the Stc2 Promoter nor Induce Stc2 Expression

Mammalian Stc2 expression is reported to be inducible after treatment with the ER stressor thapsigargin in the neuroblastoma cell line N2a (Ito et al., 2004). I therefore investigated whether ER stress induced by thapsigargin in vivo would increase AhR recruitment to the XRE cassette located within the Stc2 promoter (Fig. 3.6). ChIP again

shows that the AhR localizes to the Stc2 promoter in the liver of vehicle treated AhR floxed animals (Fig. 3.6A), but not that of the AhR CKO mouse (Fig. 3.6B). Furthermore, thapsigargin treatment did not increase AhR binding to the Stc2 promoter encompassing the XRE cassette (Fig. 3.6A). Additionally, constitutive levels of Stc2 transcript were again shown to be decreased in the CKO mouse compared to the AhR floxed mouse, although qRT-PCR demonstrated that Stc2 was not inducible by thapsigargin in either genotype (Fig. 3.6C). The increased expression of the ER stress marker CHOP confirms that in vivo thapsigargin treatment did indeed induce ER stress (Fig. 3.6D).

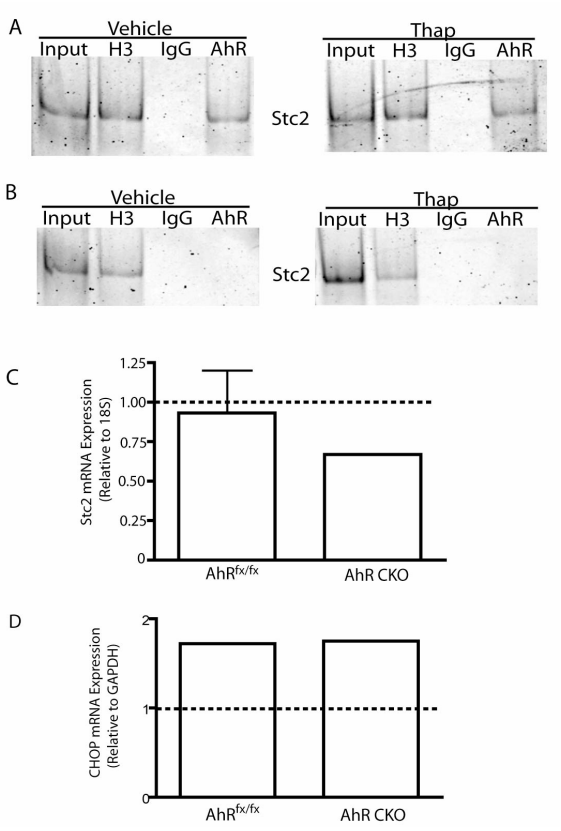

Figure 3.6. Thapsigargin treatment does not increase Stc2 expression in the liver. ChiP analysis using nuclei from the $AhR^{fx/fx}$ **(A)** and AhR CKO **(B)** mouse liveri treated with vehicle or 1mg/kg thapsigargin for 8 hours **C.** qRT-PCR analysis of Stc2 mRNA expression. **D.** RT-PCR analysis of CHOP mRNA expression.

Adenoviral Infection Induces the UPR Marker CHOP

Stc2 is a secreted glycoprotein believed to confer a protective function in the unfolded protein response (UPR) and apoptosis (Ito et al., 2004). Since numerous cellular insults result in activation of the UPR including viral infection (He, 2006), I investigated whether adenoviral infection in our primary hepatocyte model was capable of activating the UPR. Immunological monitoring of the UPR marker CHOP, suggests viral infection of both AdGFP and AdCreGFP results in activation of the UPR as indicated by a substantial increase in CHOP expression 24 hours after adenoviral infection (Fig. 3.7). Prolonged CHOP induction serves as a signal for the UPR and

subsequent endoplasmic reticulum (ER) stress, to initiate apoptosis through the intrinsic pathway ultimately resulting in caspase-3 cleavage and eventually cell death (Ma et al., 2002; McCullough et al., 2001). As revealed in Figure 3.7 infection with the adenoviruses result in persistent CHOP induction in the hepatocytes. A similar CHOP induction was also observed in the AhR-positive immortalized murine hepatocyte AML-12 cell line (Fig. 3.7C) indicating that the response to viral infection is not limited to the primary liver cells.

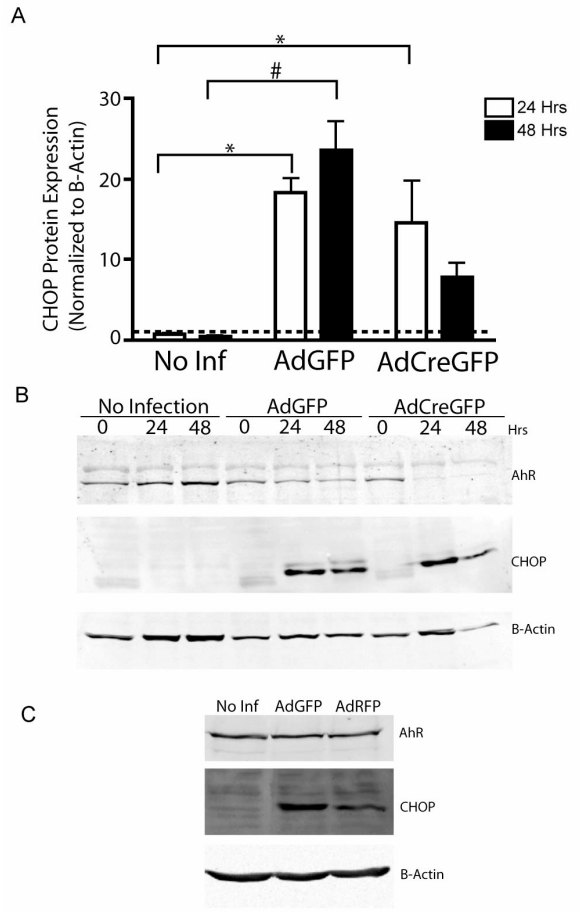

Figure 3.7. Adenoviral infection induces the UPR marker CHOP in primary hepatocytes. $AhR^{fx/fx}$ primary hepatocytes were infected with AdGFP, AdCreGFP, or allowed to remain uninfected for the indicated period after which whole cell lysates were prepared. Western blot analysis was performed on AhR and CHOP. Actin was used as a loading control. **A.** Quantification of CHOP protein expression 24 and 48 hours after adenoviral infection. The data presented for CHOP represents the mean ± S.E.M. of 3 independent experiments. Asterisk or number sign indicates statistical significance of $p < 0.01$ or $p < 0.001$ respectively when compared to uninfected samples. **B.** Representative Western blot showing loss of AhR and CHOP induction after infection with the adenovirus. **C.** Induction of CHOP in murine immortalized hepatocyte AML-12 cells after infection with AdGFP and AdRFP.

Adenovirus Infection Promotes Stc2 Expression in an AhR dependent Manner

The microarray analysis and subsequent SYBR validation demonstrated that Stc2 expression decreased in AdCreGFP infected hepatocytes concomitant with loss of the AhR, implying that the AhR is necessary for basal Stc2 expression (Table A.2). Subsequent studies however, revealed that the Stc2 transcript is nearly undetectable in uninfected cells, and is increased ~30-fold upon AdGFP infection, but not

following infection with the AdCreGFP virus (Fig. 3.8). Correspondingly, the increase in Stc2 expression is attenuated in primary hepatocytes isolated from the CKO mice lacking the AhR following AdGFP viral infection, whereas pronounced Stc2 expression is observed following infection with the AdrAhRFL to restore receptor expression (Fig. 3.8B). Collectively, these data show that Stc2 is a novel AhR target gene that has been implicated in promoting cell survival.

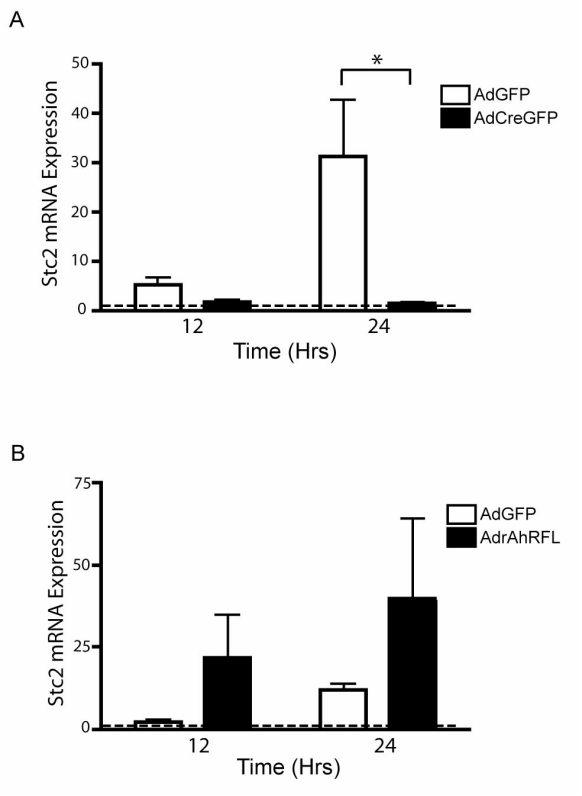

Figure 3.8. Adenoviral infection promotes Stc2 expression in an AhR dependent manner. **A.** qRT-PCR was performed on $AhR^{fx/fx}$ primary hepatocytes infected with AdGFP or AdCreGFP for the indicated times. The data presented for Stc2 represents the mean ± S.E.M. of 5 independent experiments. Asterisk indicates statistical significance ($p < 0.01$). **B.** qRT-PCR was performed on AhR CKO primary hepatocytes infected with AdGFP or AdrAhRFL for the indicated times. The data presented for Stc2 represents the mean ± S.E.M. of 3 independent experiments. Quantification of mRNA expression is relative to ribosomal RNA 18S and normalized to uninfected hepatocytes at each time point and set to a value of 1 (dashed line).

Adenovirus Infection Fails to Recapitulate Endogenous Stc2 Expression Using Transiently Transfected Luciferase Reporter Constructs

In order to show that AhR binding at the Stc2 promoter is functional, I generated two different luciferase reporter constructs containing either the Stc2 XRE cassette (Stc2XREpGl3) or a 1 Kb region of the Stc2 promoter sequence including the XRE cassette (Stc2PropGl3). Transient transfection followed by treatment with different ER stress inducers (i.e. thapsigargin) failed to induce luciferase activity using either construct (data not shown). However, considering adenovirus infection induces Stc2 expression I attempted to recreate this induction by infecting transiently transfected AML-12 cells with AdVP16 (an adenovirus lacking a fluorescent marker) (Fig. 3.9). I

chose to use the AdVP16 adenovirus instead of the AdGFP control virus to ensure the luciferase assays were not compromised by GFP fluorescense. The luciferase assays indicate that both Stc2XREpGL3 (Fig. 3.9A) and Stc2PropGL3 (Fig 3.9B) failed to induce luciferase activity when compared to uninfected cells.

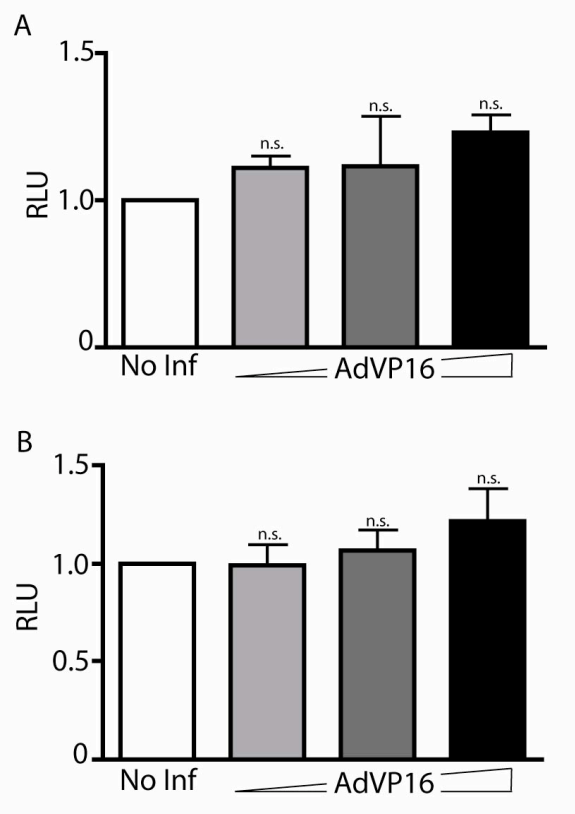

Figure 3.9. Adenovirus infection does not induce luciferase expression. Either Stc2XREpGl3 (A) or Stc2PropGl3 (B) was cotransfected with pRL-SV40 into AML-12 cells. 4 hours later the cells were infected with varying amounts of AdVP16 for 24 hours after which luciferase expression was measured using the Dual Luciferase Reporter System. N.S. = not significant ($p<0.05$) when compared to uninfected cells.

Recombinant Stc2 has No Effect on Cell Survival After Treatment with an Intrinsic Apoptotic Stimulus

I examined Stc2s cytoprotective role in primary hepatocytes using culture media enriched with a recombinant Stc2 (rStc2) protein produced in a mammalian expression system. Direct measurement of caspase-3 activity lead to an increase in activity in cells treated with H_2O_2 when compared to control treated cells as expected. However, addition of rStc2-enriched media did not have a significant effect on the H_2O_2 induced apoptosis (Fig. 3.10). The lack of significant activity in the caspase-3 assay led me to investigate whether rStc2 is able to bind the cellular membrane and/or be internalized. The inability of rStc2 to bind/internalize may explain the lack of significant change in the caspase-3 assays. Immunological monitoring of the FLAG-tagged rStc2 indicates that it is not internalized nor binds the primary hepatocytes (Fig. 3.11). Stc2 is reported to undergo post-translational modifications including phosphorylation by casein kinase II (Jellinek et al., 2000). It is possible that the rStc2 had been dephosphorylated

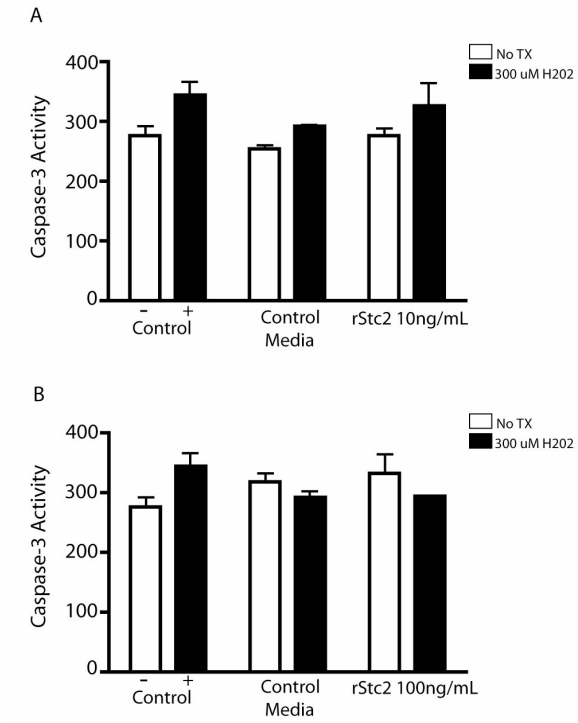

Figure 3.10. **Stc2 fails to protect hepatocytes from an apoptotic insult.** AhR$^{fx/fx}$ primary hepatocytes were allowed to attach for 3 hours after which they were treated with 10ng/mL (0.3nM) **(A)** or 100ng/mL (3nM) **(B)** rStc2 enriched media or control media lacking rStc2 in addition to treatment with 300uM H2O2 or vehicle for 6 hours. Analysis using ANOVA with a Bonferroni post hoc test found all comparisons to be not significant ($p<0.05$).

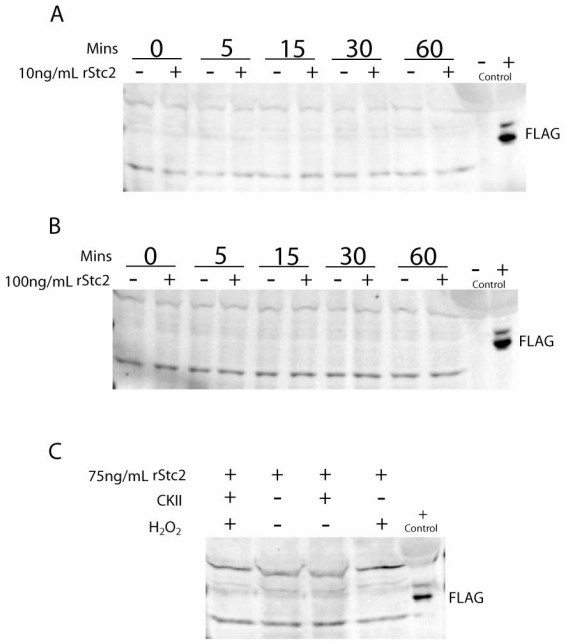

Figure 3.11. **rStc2 is not internalized by primary hepatocytes.** AhR$^{fx/fx}$ primary hepatocytes were treated with 10ng/mL (0.3nM) **(A)** or 100ng/mL (3nM) **(B)** enriched media or control media and collected at various times after to be analyzed by western blot analysis. **C.** Primary hepatocytes were treated with 75ng/mL (2.3nM) rStc2 enriched media, casein kinase II, or 300uM H_2O_2 for 6 hours and then analyzed by western blot analysis using an anti-FLAG antibody.

resulting in a loss of Stc2 activity. However, addition of casein kinase II to the rStc2 enriched media did not result in rStc2 binding or internalization (Fig. 3.11C) suggesting that other posttranslational modifications or additional components are necessary for full Stc2 activation.

DISCUSSION

The AhR has historically been a protein of interest when investigating liver injury due to its hepatotoxic mechanism(s) after activation by halogenated aromatic hydrocarbons such as TCDD. However, it was only after the generation of the AhR

knockout mouse that the field identified the importance of physiological AhR activities in the absence of an exogenous ligand. In this study we aimed to extend the understanding of normal AhR biology through characterization of the AhR-Stc2 relationship previously identified during a microarray analysis designed to identify immediate and direct changes in the transcriptome concomitant with the loss of the AhR in the absence of an exogenous ligand. It is well established that the AhR binds XREs to regulate target gene expression (Swanson et al., 1995). Considering Stc2 expression levels correlated with AhR status in the previous validation studies, I performed an in silico analysis of the Stc2 promoter region and identified 9 XREs within 1 Kb of the Stc2 transcriptional start site, 8 of which were clustered within 250 base pairs. Given the presence of the XRE cluster, I sought to characterize Stc2s responsiveness to AhR agonists in greater detail (Fig. 3.4). The evidence indicates Stc2 is completely refractory to the classical exogenous AhR agonists TCDD, 3-methylcholanthrene, and ß-naphthoflavone. This non-responsiveness may explain why previous expression studies failed to identify Stc2 as an AhR target gene. In addition, ChIP analysis identified a specific albeit constitutive AhR interaction with the Stc2 promoter encompassing the XRE cassette (Fig. 3.5). The implication is that AhR-mediated Stc2 expression may be dependent on additional regulatory events possibly involving coactivator recruitment reminiscent of the type II nuclear hormone receptors. Alternatively, higher-order chromatin rearrangements or other epigenetic modifications may contribute to Stc2 regulation. My inability to recapitulate endogenous Stc2 expression using a transiently transfected luciferase reporter system harboring either the Stc2 XRE cassette or a 1 Kb region of the Stc2 promoter sequence—including the XRE cassette—suggests that appropriate chromatin architecture may indeed be crucial for Stc2 expression (Fig. 3.9)

While few studies to date have examined Stc2 function (Chang et al., 2008; Ito et al., 2004), it is considered to be a secreted glycophosphoprotein that acts in an autocrine or paracrine manner (Wagner and Dimattia, 2006). Stc2 has been reported previously to

be inducible, as well as cytoprotective, during tunicamycin- and thapsigargin-induced ER stress using the neuroblastoma cell line N2a (Ito et al., 2004). However, I was unable to detect an increase in AhR binding to the Stc2 promoter after thapsigargin treatment, nor did I detect an increase in Stc2 transcript expression (Fig. 3.6). It should be noted that constitutive Stc2 expression was decreased in AhR CKO mice compared to AhR floxed mice consistent with my previous findings (Fig. 2.8B). The absence of Stc2 induction after thapsigargin treatment could be due to cell and tissue specificity, or an artifact of the N2a line. Recently, Fazio et al. (Fazio et al., 2011) reported that Stc2 reduced cellular injury in cerulein-induced pancreatitis involving a process associated with altered PERK signaling. It is noteworthy that PERK is activated by its release from BiP, and after auto-phosphorylation PERK phosphorylates eIF2alpha to reduce translation but targets the increase in translation of Atf4 for which CHOP is a target gene. (Gregersen and Bross, 2010). I show here that adenovirus infection induced prolonged CHOP expression (a hallmark of ER stress) in both primary hepatocytes and the AML-12 cell line regardless of AhR status (Fig. 3.7). I reported previously that the loss of AhR resulted in enhanced caspase-3 activity (Fig. 2.2) and increased apoptosis following the intrinsic trigger, consistent with previous findings that the AhR promotes cell survival (Gonzalez and Fernandez-Salguero, 1998; Wu et al., 2007). On the other hand, Stc2s mechanism of action is not fully understood. This makes analysis of the negative results in Figures 3.10 and 3.11 difficult. Stc2 is phosphorylated by casein kinase II, so dephoshorylation resulting in Stc2 inactivation may be an explanation for the lack of protection in the caspase-3 assay. This could also explain the lack of binding/ internalization, although no evidence exists that suggests Stc2 binds the cell membrane and is internalized to propagate its protective signal.

From a pathophysiological perspective, chronic viral infection by hepatitis viruses B or C results in ER stress, and can lead to many liver disease states including

hepatitis, cirrhosis, and hepatocellular carcinoma (Malhi and Kaufman, 2011). Here we report that adenovirus infection leads to cellular stress, presumably in the ER as evidenced by the induction of CHOP, and a concomitant induction of Stc2 in an AhR-dependent manner (Fig. 3.8). However, the inability to induce Stc2 expression with canonical exogenous receptor agonists and the evidence for constitutive AhR binding to the Stc2 promoter suggests that receptor control of the gene differs significantly from the well characterized mechanism regulating Cyp1a1 expression. Accordingly, our observed AhR-dependent virally-mediated induction of Stc2 represents a novel insight into normal AhR biology. These findings merit further investigation into the AhR-Stc2 relationship with focus on virally-mediated ER stress regulation during times of liver dysfunction and insult.

Chapter 4: Conclusions and Future Aims

CONCLUSIONS

The AhR is recognized historically for its role in the adaptive metabolism of xenobiotics and the toxic responses associated with these compounds. Interestingly, AhR activation by certain exogenous ligands results in greater toxicity than others. For example, AhR activation by β-napthoflavone results in minimal toxicities, because it is rapidly cleared by Cyp1a1 in a feedback mechanism. However AhR activation by TCDD also results in Cyp1a1 up-regulation, but is poorly metabolized resulting in a longer half-life and greater toxicity (Poland and Glover, 1974). Some investigators have hypothesized that the toxicities associated with AhR activation by an exogenous ligand are a result of competitively outcompeting an unknown endogenous ligand. This binding is thought to redirect AhRs priorities to the upregulation of Phase I and Phase II metabolizing enzymes to clear the body of these compounds leaving physiological AhR activities unattended resulting in the toxicities associated with exogenous AhR activation. However, evidence for this hypothesis is absent and the exact mechanisms responsible for the toxicities associated with exogenous agonists still elude investigators years after discovering the AhR is required for the observed toxicities. I believe this dearth of knowledge stems from the incomplete understanding of normal AhR biology during homeostasis. Many laboratories have explored AhR's involvement in physiological processes outside of adaptive metabolism, however they are often investigated after AhR activation by an exogenous ligand.

Generation of the AhR knockout mouse provided the first evidence for physiological AhR actions in the absence of an exogenous ligand. These mice exhibit multiple abnormalities including decreased liver size and impaired vasculature formation, proving that the AhR is necessary for proper development (Schmidt et al., 1996). In addition, one group reported that the livers of the knockout mice exhibit increased rates

of apoptosis compared to their wild-type counterparts (Gonzalez and Fernandez-Salguero, 1998). Likewise, the same group identified increased rates of apoptosis in embryonic fibroblasts isolated from the knockout mouse (Elizondo et al., 2000). The AhR has previously been implicated in apoptosis and survival, but only after activation by an exogenous ligand making it difficult to distinguish direct effects of the AhR, and secondary effects from reactive intermediates and downstream signaling. Many studies also use an apoptotic stimulus in addition to an AhR agonist further complicating data interpretation. On the other hand, our laboratory recently demonstrated that the AhR predisposes hepatocytes to apoptosis mediated by extrinsic apoptotic signals in the absence of an exogenous ligand (Park et al., 2005), whereas another group reported that the lack of the AhR results in impaired Akt/PKB activation resulting in increased cell death after an intrinsic apoptotic stimulus in the absence of an exogenous ligand (Wu et al., 2007). These complementary studies suggest that the nature of the apoptotic stimulus dictates AhR actions in the absence of an exogenous ligand. In this context I used primary hepatocytes and the Cre-lox system to examine AhRs role in cell death and survival. Additionally, since my preliminary studies resulted in increased cell death simply with the loss of the AhR, I decided to explore this observation further, in addition to examining the effect of an intrinsic apoptotic stimulus in primary hepatocytes.

The overall goal of my dissertation was to extend the understanding of normal AhR biology by providing mechanistic insights to AhR functions in the absence of an exogenous ligand, thereby allowing a better understanding of disease etiology that occurs after AhR activation by an exogenous ligand.

In Chapter 2, I examined AhR activity in the absence of an exogenous ligand, by investigating the influence of AhR status on cell survival both with and without an intrinsic apoptotic stimulus, specifically looking at Akt/PKB activation. I chose to focus specifically on this kinase since impaired Akt/PKB activation was previously reported to increase cell death in the hepa1c1c7 AhR deficient derivative LA1 cell line (Wu et al.,

2007). However, while validating the Cre-lox system I noticed an increase in the incidence of an apoptotic phenotype in hepatocytes infected with the Cre-recombinase expressing virus. Further investigation using caspase-3 activity assays proved that the loss of AhR significantly increases caspase-3 activity, consistent with other reports suggesting the AhR confers cell survival (Ambolet-Camoit et al., 2010; Davis et al., 2003). In addition, ectopic expression of the AhR using a virus that expresses the rat full length receptor reduced caspase-3 activity significantly in hepatocytes exposed to an intrinsic apoptotic stimulus. On the other hand, neither AhR status nor UV irradiation had an affect on Akt/PKB phosphorlyation at serine 473. This observation suggests that impairment of Akt/PKB activation is not responsible for the increased cell death seen after an intrinisic apoptotic stimulus or simply with the loss of the AhR in primary hepatocytes.

In order to reconcile the increase in cell death with the loss of the AhR, I performed an apoptosis PCR array to examine 84 key genes implicated in cell death and survival processes. Only one transcript resulted in a significant change of more than 2 fold (p73), but could not be validated independently by qRT-PCR. Next I expanded the search for novel AhR target genes implicated in cell survival by performing a comprehensive microarray designed to identify immediate and direct changes in the transcriptome with the loss of the AhR to reconcile the increase in hepatocyte death. The microarray analysis yielded 246 genes that were significantly altered at the 24-hour time point. Using IPA to perform a secondary analysis, I found several biological functions that were significantly represented in the 24-hour data set including cancer, cellular growth and proliferation, and cell death. In addition, 25% of the genes chosen for validation by qRT-PCR were successfully validated.

Of the validated genes, Stc2 was the most interesting and promising for several reasons. First, Stc2 was decreased 7-fold in AdCreGFP infected primary hepatocytes during qRT-PCR validation. In addition, Stc2 levels were also decreased in the livers of

CKO mice compared to floxed mice suggesting the AhR is responsible for constitutive Stc2 expression levels. Second, Stc2 is found in the same IPA network as the AhR. Third, little is known about the mammalian Stanniocalcin family and even less is known about Stc2. A handful of reports suggest that Stc2 confers cytoprotection during cellular stresses such as ER stress and UPR activation. Stc2 was recently reported to be upregulated in human HCC tissue when compared to normal adjacent tissue (Wang et al., 2012). In addition others have reported that Stc2 is upregulated in various cancers including prostate cancer (Tamura et al., 2009), ovarian cancer (Law and Wong, 2010a), and neuroblastoma (Volland et al., 2009) indicating Stc2's cytoprotective function may confer a survival benefit upon tumor cells. In summary, AhRs ability to confer survival in the absence of an exogenous ligand is not mediated through Akt/PKB activation or transcriptional control of well-defined survival/apoptotic genes, but rather through regulation of novel AhR targets.

Having highlighted AhR's role in cell survival in the absence of an exogenous ligand in Chapter 2, I decided to next characterize the Stc2-AhR relationship to further define AhRs ability to confer survival in Chapter 3. In silico analysis of the Stc2 promoter region identified an XRE cassette spanning 218 base pairs located 226 base pairs up-stream of the transcriptional start site. However, despite the concentration of XREs indicative of functional importance, expression of Stc2 was refractory to activation by traditional exogenous AhR ligands. In a complementary study, ChIP showed that AhR binding to the Stc2 promoter is constitutive, unlike that of the protypical AhR target Cyp1a1. This suggests that additional or novel mechanisms are involved during AhR-mediated upregulation of Stc2 that are not associated with the canonical pathway. Matikainen et al. have previously reported that AhR activation by the PAH 9,10-dimethylbenz[a]anthracene (DMBA) in oocytes induces transcription of the proapoptotic protein Bax culminating in oocyte death (Matikainen et al., 2001). In addition, this group also noted that Bax induction is absent after treatment with the prototypical AhR agonist,

TCDD. They demonstrated that this differential induction was due to the DNA sequence flanking the XRE core site. A base substitution rendered the Bax gene TCDD-responsive, implying that AhR DNA binding was affected by agonist-specific events altering the receptors affinity for the XRE site. This study reinforces the concept that AhR transcriptional regulation is dependent on the ligand and the XRE sequence. On the other hand, several previous reports provide evidence for Stc2 upregulation after treatment with the ER stressors thapsigargin and tunicamycin. However, the lack of mechanistic information on AhR-mediated Stc2 induction makes it difficult to interpret the negative results obtained after thapsigargin treatment. Thapsigargin failed to increase Stc2 expression in either mouse genotype, but did increase CHOP expression indicating that the thapsigargin treatment did induce an ER stress. Similar problems were encountered using a transiently transfected luciferase reporter system containing segments of the Stc2 promoter. AML-12 cells transiently transfected with the reporter plasmid and treated with thapsigargin failed to produce a signal leading me to believe that Stc2 is not inducible by ER stress resulting from thapsigargin in liver cells.

On the other hand, viral infection was shown to result in ER stress and activation of the UPR as evidenced by a sustained CHOP induction 24 hours after viral infection in both primary hepatocytes and AML-12 cells. This virally mediated ER stress resulted in the upregulation of Stc2 in an AhR-dependent manner after infection with AdGFP in AhR floxed primary hepatocytes and in CKO hepatocytes infected with the AhR (AdrAhRFL) expressing virus. The adenovirus's ability to induce ER stress resulting in Stc2 expression in an AhR-dependent manner is a novel discovery regarding normal AhR biology in the absence of an exogenous ligand. Given that both thapsigargin and viral infection are able to trigger ER stress but only viral infection induces Stc2 expression, suggests that Stc2 up-regulation is dependent on excessive protein traffic caused by viral infection rather than Ca^{2+} depletion caused by thapsigargin. The adenovirus early region protein E3/19K has been reported to induce ER stress (Pahl et al., 1996). However, my

adenoviral vector (pAdEasy-1) lacks the sequence encompassing the E3 gene sequence (He et al., 1997). This suggests an alternative adenovirus protein is responsible for the induction of ER stress in my model. Furthermore, my inability to recapitulate the endogenous induction of Stc2 after viral infection using the luciferase reporter plasmids discussed previously indicates that appropriate chromatin architecture my indeed be crucial for faithful Stc2 expression. In summary, the evidence shows that the AhR regulates Stc2 expression through constitutive binding to a newly identified XRE cassette located in the Stc2 promoter. This mechanism differs from that of traditional AhR targets such as Cyp1a1, and may require coactivator recruitment or higher-order chromatin arrangements. In addition, these actions are independent of exogenous AhR activation and dependent on ER stress and UPR activation resulting from viral infection.

In conclusion, my dissertation provides the first evidence in primary hepatocytes showing that in the absence of an exogenous ligand the AhR is necessary for proper regulation of survival and death processes through regulation of genes hitherto not associated with AhR regulation. Furthermore, an impaired Akt/PKB signaling was not responsible for hepatocyte survival both with and without exposure to an intrinsic apoptotic stimulus. These findings are consistent with physiological AhRs functions, and attributed to AhRs transcriptional control of Stc2, identified during the comprehensive microarray analysis. In silico analysis of the Stc2 promoter region revealed 9 XREs within the 1 Kb region upstream of the Stc2 transcriptional start site. Further examination of the Stc2-AhR relationship revealed that although Stc2 expression is AhR-dependent, it is refractory to induction by exogenous AhR agonist, but is induced after an ER stress resulting from viral infection in an AhR dependent manner. Thus, the evidence provides the first molecular insights into normal AhR biology associated to ER stress and activation of the UPR in a cytoprotective response. Although the mechanism for AhR activation leading to Stc2 upregulation is remains unclear, Figure 4.1 represents what I currently know about the AhR-Stc2 relationship. Moreover, these findings allow for

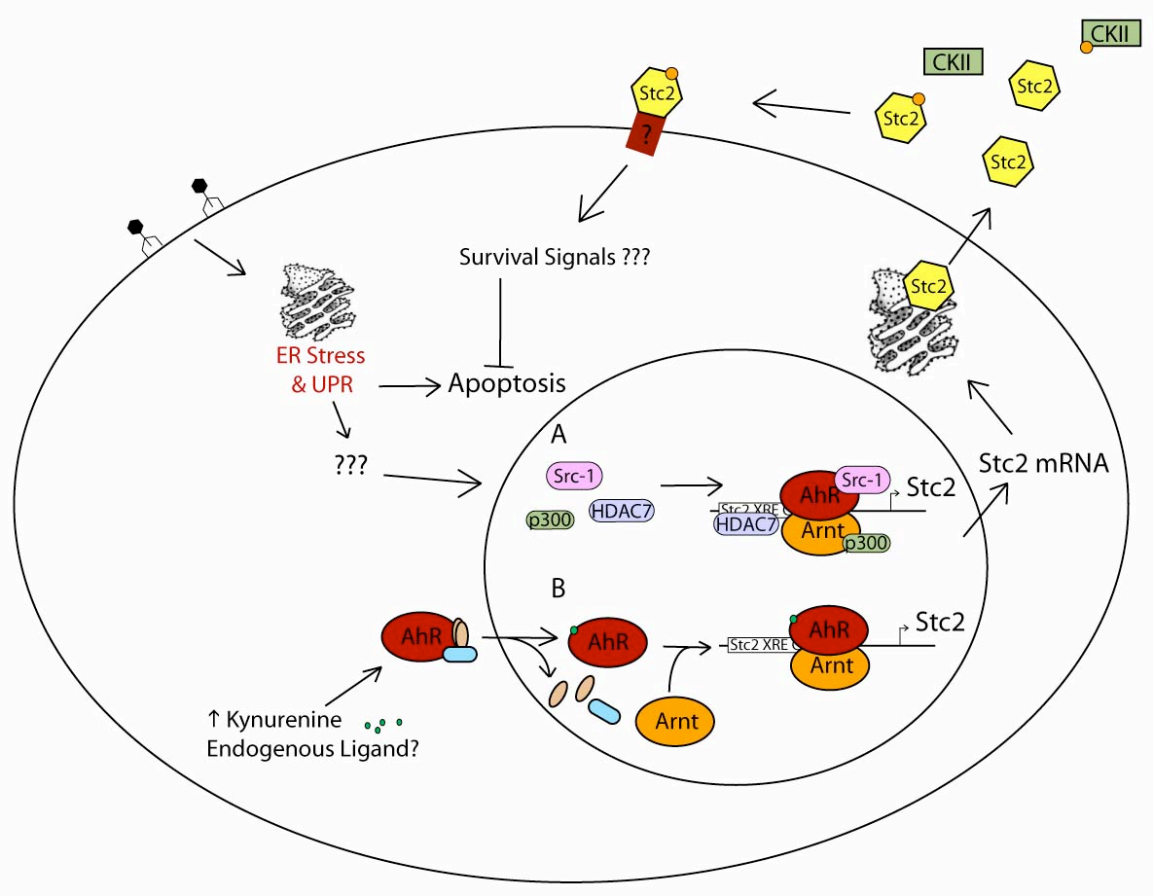

Figure 4.1. Schematic of AhR-Stc2 relationship. AhR-mediated induction of Stc2 promotes cell survival during an ER stress resulting from viral infection (A). In the absence of an ER stress the AhR occupies the Stc2 promoter regulating basal levels of Stc2 to maintain homeostasis. During a virally-mediated ER stress the AhR promotes Stc2 expression through undiscovered mechanisms promoting cell survival. Alternatively the tryptophan catabolite kynurenine, is a putative endogenous AhR agonist. Preliminary data suggests kynurenine is able to induce Stc2 in an AhR dependent manner (B). Secreted Stc2 is phosphorylated by caesin kinase II. In keeping with signaling properties identified for Stc1, I hypothesize that phosphorylated Stc2 binds an unknown surface receptor initiating a signaling cascade to inhibit apoptosis and promote survival..

further investigation into the mechanism of action for the AhR and Stc2 after an ER stress in the liver.

FUTURE DIRECTIONS

Take Advantage of the AhR$^{fx/fx}$Alb$^{+/Cre\text{-}ERT2}$ Mouse to Monitor Transcript Changes with the Loss of the AhR In Vivo

The majority of the experiments performed in my dissertation utilized the physiologically relevant primary hepatocyte model. This in vitro model coupled with the Cre-lox system enabled me to elegantly remove the AhR from hepatocytes in order to

address the AhRs activities consistent with normal AhR biology. However, being able to extrapolate these findings to an in vivo model is necessary for future translation of AhR cytoprotection in the liver. In order to reproduce these findings in vivo I need to again be able to monitor changes in signaling concurrent with AhR loss. The AhR CKO mice have many advantages over traditional total AhR knockout mice, but they do not allow for temporal monitoring of gene change similar to that of the Cre-lox system in the primary hepatocyte model. Fortunately, with permission from Dr. Pierre Chambron, I have recently obtained mice that contain an inducible Cre-recombinase under the control of the albumin promoter from Dr. Ben Stanger at the University of Pennsylvania. These mice express a Cre-recombinase and mutated estrogen receptor chimeric protein whose activity is induced by tamoxifen (Schuler et al., 2004). I am currently crossing these mice with the AhR floxed mice ($AhR^{fx/fx}Alb^{+/Cre\text{-}ERT2}$), which will result in efficient and temporally controlled removal of the AhR in vivo providing an unprecedented opportunity to evaluate direct AhR processes in the absence of an exogenous agonist (Fig. 4.2). Once these mice are available they will first need to be characterized to determine when complete loss of the AhR occurs and monitored for any pathological changes that occur in the liver with the loss of the AhR. Next RNA-seq should be performed to identify immediate and direct changes in the transcriptome concomitant with the loss of the AhR. RNA-seq should be used instead of microarray analysis because it is a newer technology that allows for examination of all

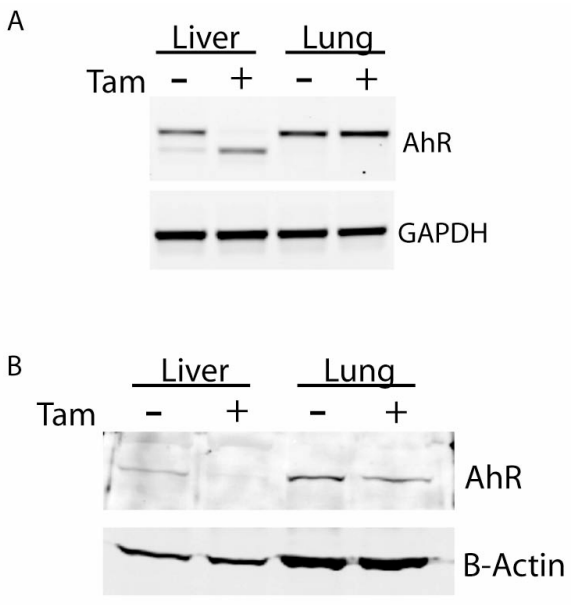

Figure 4.2. Liver specific excision of exon 2 in the $AhR^{fx/fx}Alb^{+/Cre\text{-}ERT2}$ mouse after tamoxifen treatment. $AhR^{fx/fx}Alb^{+/Cre\text{-}ERT2}$ mice were treated with tamoxifen or vehicle for 3 days and tissues were collected 4 days after the last treatment. RT-PCR (A) or western blot analysis (B) was performed to assess the specificity of exon 2 excision after tamoxifen treatment.

transcript changes, not just those that are annotated and used on the microarray chip. In addition, early RNA-seq appears to be more quantitative than microarray analysis. Identification of changes that occur both in vitro and in vivo should be carefully analyzed as they represent true targets associated with physiological AhR activities.

Further Characterize AhR Dependent Upregulation of Stc2

I have presented data demonstrating a survival role for the AhR in primary hepatocytes in the absence of an exogenous ligand through up-regulation of Stc2. However, the exact mechanism remains elusive because Stc2 expression is refractory to expression by exogenous agonist, and ChIP assays show constitutive binding of the AhR to the Stc2 promoter. In order to address the mechanism for Stc2 induction additional experiments need to be performed. First, ChIP assays need to be standardized using AhR floxed primary hepatocytes infected with either the control or Cre-recombinase expressing virus. Alternatively, primary hepatocytes can be isolated from the AhR floxed and AhR CKO mice, and infected with the control virus (AdGFP). After the ChIP assay has been standardized in primary hepatocytes immunoprecipitation should be carried out using antibodies against known AhR coactivators such as p300 (Beedanagari et al., 2010) and Src-1 (Kumar and Perdew, 1999). Positive results will include increased recruitment of these coactivators to the XRE cassette when compared to uninfected hepatocytes. However, all studies to date examining AhR coactivator recruitment have been performed after activation by an exogenous ligand (Hankinson, 2005), so it is possible that under endogenous conditions different coactivators are recruited or they are recruited in a temporal manner. ChIP assays shoud also be performed by immunoprecipitating HDAC7, as both this protein and p300 were shown to be necessary for Stc2 induction during hypoxic conditions (Law and Wong, 2010b). ChIP analysis identifying increased coactivator recruitment

to the Stc2 promoter will be used to extend future charactization of the mechanisms responsible for AhR-mediated Stc2 expression.

Characterize Stc2 Inducibility After AhR Activation Using the Putative Endogenous Agonist Kynurenine

Recent studies suggest that the tryptophan catabolite, kynurenine, is an endogenous AhR ligand (Denison and Nagy, 2003; Opitz et al., 2011). The first and rate-limiting step in the kynurenine catabolism pathway involves tryptophan 2,3-dioxygenase (TDO). TDO is highly expressed in the liver and has been reported to have antimicrobial properties. For example, overexpression of TDO in a HeLa tetracycline-on system significantly reduced viral replication of the herpes simplex virus through increased catabolism of tryptophan to kynurenine thereby preventing viral replication (Schmidt et al., 2009). One can envision that Stc2 up-regulation by the AhR after viral infection may be due to an increase in kynurenine as a result of increased tryptophan catabolism by TDO. Preliminary studies using kynurenine to induce Stc2 expression in AhR floxed and CKO primary hepatocytes show a dose-dependent induction of Stc2 in an AhR dependent fashion (Figure 4.3). Additional studies to address this mechanism need to be performed using a commercially available TDO inhibitor in combination with viral infection to investigate TDO's influence on Stc2 induction. Additionally, during these experiments all media should be protected from light to prevent tryptophan breakdown to other putative AhR agonists (Denison and Nagy, 2003). Lastly, should kynurenine reproducibly induce

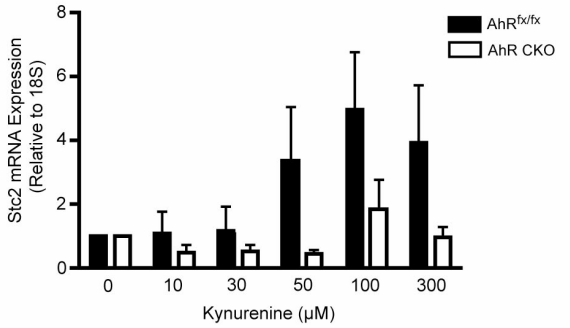

Figure 4.3. AhR dependent induction of Stc2 expression by kynurenine. qRT-PCR was performed using total RNA from AhR$^{fx/fx}$ and AhR CKO primary hepatocytes treated with kynurenine at the indicated concentrations for 24 hours. RNA expression was normalized against ribosomal RNA 18S. Two-way ANOVA identified a statistically significant difference ($p < 0.05$) in Stc2 expression between genotypes: AhR$^{fx/fx}$ and AhR CKO in kynurenine treated cells.

Stc2, it could be used as a tool similar to TCDD, in order to study the AhR-Stc2 cytoprotective properties identified during viral ER stress.

Demonsrate that Knockdown of Stc2 Results in Enhanced Viral-mediated ER Stress Induced Apoptosis

I have shown that Stc2 gene expression is refractory to classic exogenous AhR agonists, but responds to cellular stress in an AhR-dependent mechanism consistent with a process promoting cell survival. I am currently working to generate several adenovirus-encoded shRNAs to inhibit Stc2 expression. Once all the viruses are generated, they will be tested to determine which provides the greatest knockdown. Figure 4.4 demonstrates suppression of Stc2 after testing shRNA1. The shRNA providing the greatest knockdown (AdiStc2GFP) will be amplified and purified for use in primary hepatocyte cultures to directly examine Stc2s role in cell survival and apoptosis. I hypothesize that infecting primary hepatocytes with AdiStc2GFP will result in increased apoptosis compared to AdGFP infected hepatocytes similar to that after loss of the AhR using AdCreGFP. These experiments will demonstrate that suppression of endogenous Stc2 expression directly influences cell survival after an ER stress mediated by viral infection. In addition, rescue experiments will be performed through knockdown of Stc2 and then adding rStc2 to the hepatocyte cultures to rescue cell survival. However, I reported in Chapter 3 that rStc2 did not have an affect on caspase-3 assays nor was it internalized or bound by the hepatocytes. So, before the rescue experiments can be performed more characterization and troubleshooting of rStc2 needs to be performed. Once the recombinant protein is deemed

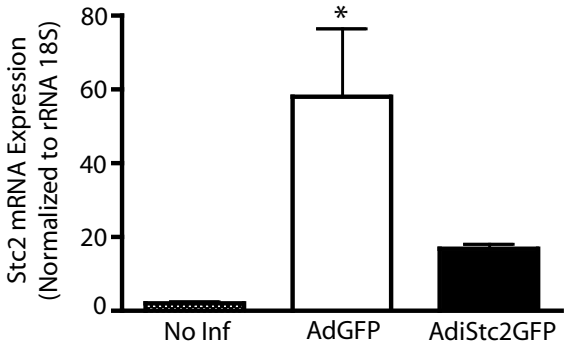

Figure 4.4. qRT-PCR analysis of Stc2 mRNA expression. Hepatocytes remained uninfected or infected with AdGFP or AdiStc2GFP for 24 hours. All values are normalized to the uninfected sample.

active additional studies involving Stc2 binding, transport, and signaling can be performed to elucidate Stc2 activities.

SUMMARY

The AhR has been implicated in cell survival both with and without activation by an exogenous ligand. However, AhRs ability to confer cell survival in the absence of an exogenous ligand is much less understood. Recent evidence suggests that the AhR promotes cell survival in the absence of an exogenous ligand through the PI3K-Akt/PKB pathway. However, I hypothesized that the AhR mechanistically contributes to cell survival and death through regulation of genes hitherto not associated with AhR functions in the absence of an exogenous ligand. The evidence shows that AhRs ability to confer survival in the absence of an exogenous ligand is not mediated through Akt/PKB activation, but rather through regulation of Stc2. Furthermore the AhR-Stc2 relationship exists independent of exogenous AhR activation through constitutive AhR binding to a newly identified XRE cassette located in the Stc2 promoter.

Appendix A

A.1 Apoptosis Array Results

Position	Accession#	Gene Symbol	Fold Change	p-value
A01	NM_009652	Akt1	-1.0494	0.575155
A02	NM_009684	Apaf1	-1.1122	0.538733
A03	NM_007466	Api5	-1.055	0.357989
A04	NM_030693	Atf5	1.179	0.430692
A05	NM_007522	Bad	1.1511	0.191158
A06	NM_009736	Bag1	1.0017	0.948147
A07	NM_013863	Bag3	-1.0637	0.776846
A08	NM_007523	Bak1	1.096	0.212927
A09	NM_007527	Bax	1.1826	0.036937
A10	NM_009740	Bcl10	1.0821	0.396296
A11	NM_009741	Bcl2	-1.1087	0.921669
A12	NM_009743	Bcl2l1	1.1501	0.083586
B01	NM_013479	Bcl2l10	-1.0122	0.862293
B02	NM_007537	Bcl2l2	1.1122	0.603846
B03	NM_007544	Bid	-1.0827	0.510183
B04	NM_008670	Naip1	1.0197	0.698234
B05	NM_010872	Naip2	1.0006	0.999082
B06	NM_007465	Birc2	-1.0376	0.994115
B07	NM_007464	Birc3	-1.073	0.458288
B08	NM_009688	Xiap	-1.1114	0.260304
B09	NM_009689	Birc5	1.2532	0.583405
B10	NM_016787	Bnip2	1.1176	0.403777
B11	NM_009760	Bnip3	1.0474	0.964045
B12	NM_009761	Bnip3l	-1.134	0.361186
C01	NM_016778	Bok	1.0342	0.935255
C02	NM_130859	Card10	-1.3176	0.341805
C03	NM_172729	Nod1	-1.1009	0.562298
C04	NM_001163138	Card6	-1.0762	0.535551
C05	NM_009807	Casp1	-1.0006	0.936319
C06	NM_009808	Casp12	-1.4719	0.814716
C07	NM_009809	Casp14	1.9474	0.047898
C08	NM_007610	Casp2	-1.1168	0.406468
C09	NM_009810	Casp3	-1.0469	0.756387
C10	NM_007609	Casp4	-1.2572	0.371658
C11	NM_009811	Casp6	1.0346	0.702864
C12	NM_007611	Casp7	-1.1103	0.223447
D01	NM_009812	Casp8	1.0936	0.745722
D02	NM_015733	Casp9	-1.0103	0.847121
D03	NM_009805	Cflar	-1.095	0.528602

Position	Accession#	Gene Symbol	Fold Change	p-value
A01	NM_009652	Akt1	-1.0494	0.575155
A02	NM_009684	Apaf1	-1.1122	0.538733
A03	NM_007466	Api5	-1.055	0.357989
A04	NM_030693	Atf5	1.179	0.430692
D04	NM_007702	Cidea	1.1702	0.545034
D05	NM_009894	Cideb	1.068	0.839597
D06	NM_009950	Cradd	-1.2767	0.141518
D07	NM_010015	Dad1	1.0257	0.787195
D08	NM_029653	Dapk1	1.4792	0.069371
D09	NM_010044	Dffa	-1.0794	0.527051
D10	NM_007859	Dffb	1.0902	0.62773
D11	NM_010286	Tsc22d3	-1.0999	0.536857
D12	NM_010175	Fadd	1.1727	0.277642
E01	NM_007987	Fas	-1.1025	0.636813
E02	NM_010177	Fasl	-1.4051	0.551408
E03	NM_008234	Hells	1.0903	0.826413
E04	NM_010548	Il10	1.0354	0.888941
E05	NM_010712	Lhx4	-1.2877	0.903227
E06	NM_010736	Ltbr	1.1344	0.318929
E07	NM_008562	Mcl1	1.0811	0.541574
E08	NM_008689	Nfkb1	-1.0614	0.503123
E09	NM_080637	Nme5	-1.2941	0.052921
E10	NM_030152	Nol3	-1.0119	0.898491
E11	NM_172858	Pak7	1.5231	0.107904
E12	NM_138606	Pim2	-1.0168	0.980845
F01	NM_011130	Polb	1.0051	0.920105
F02	NM_011563	Prdx2	1.056	0.220058
F03	NM_023258	Pycard	-1.0238	0.701389
F04	NM_009068	Ripk1	-1.041	0.60112
F05	NM_011279	Rnf7	1.0327	0.69533
F06	NM_020011	Sphk2	1.014	0.85871
F07	NM_013693	Tnf	-1.2124	0.757824
F08	NM_020275	Tnfrsf10b	-1.0169	0.72608
F09	NM_008764	Tnfrsf11b	-1.035	0.936248
F10	NM_011609	Tnfrsf1a	-1.0169	0.904077
F11	NM_011611	Cd40	-1.0044	0.816689
F12	NM_009425	Tnfsf10	1.1196	0.539142
G01	NM_011614	Tnfsf12	-1.0515	0.706286
G02	NM_011616	Cd40lg	2.1935	0.371788
G03	NM_011617	Cd70	-1.0132	0.834762
G04	NM_009421	Traf1	1.1968	0.597383
G05	NM_009422	Traf2	-1.1384	0.733029
G06	NM_011632	Traf3	1.1227	0.297877
G07	NM_011640	Trp53	1.1796	0.156061
G08	NM_173378	Trp53bp2	-1.0869	0.686425

Position	Accession#	Gene Symbol	Fold Change	p-value
A01	NM_009652	Akt1	-1.0494	0.575155
A02	NM_009684	Apaf1	-1.1122	0.538733
A03	NM_007466	Api5	-1.055	0.357989
A04	NM_030693	Atf5	1.179	0.430692
G09	NM_021897	Trp53inp1	1.0592	0.689263
G10	NM_011641	Trp63	1.9219	0.028383
G11	NM_011642	Trp73	2.7307	0.046853
G12	NM_172735	Zc3hc1	-1.1286	0.286754
H01	NM_010368	Gusb	1.0653	0.705086
H02	NM_013556	Hprt	-1.0649	0.294596
H03	NM_008302	Hsp90ab1	1.0197	0.840758
H04	NM_008084	Gapdh	1.0443	0.620793
H05	NM_007393	Actb	1.0607	0.525201
H06	SA_00106	MGDC	1.1976	0.208904
H07	SA_00104	RTC	-1.036	0.713616
H08	SA_00104	RTC	1.0009	0.999736
H09	SA_00104	RTC	-1.0178	0.856584
H10	SA_00103	PPC	-1.0438	0.64306
H11	SA_00103	PPC	-1.0339	0.730433
H12	SA_00103	PPC	-1.0167	0.849347

A.2 Microarray and qRT-PCR Validation

	ProbeSet ID	Accession#	Gene Symbol	Fold Change (Microarray)	p-value (Microarray)	Fold Change (qRT-PCR)	p-value (qRT-PCR)
12 Hour	1422565_s_at	NM_008688	Nfic	-1.46	0.0377478	-1.316	ND
	1452074_at	NM_028343	Tmem135	-1.41	0.0439033	-1.074	ND
	1455645_at	NM_175418	8030451F13Rik	-1.36	0.0197448	-1.4109	0.705204
	1452395_at	NM_025885	Med19	-1.34	0.0135541	1.337	ND
	1431722_a_at	NM_027827	Afmid	-1.31	0.00871236	1.048	ND
	1426519_at	NM_011030	P4ha1	-1.3	0.00165891	-1.09	ND
	1428865_at	NM_029410	Bcl2l12	-1.29	0.015628	-1.437	ND
	1415957_a_at	NM_010925	Rrp1	-1.28	0.0477517	30.1258	0.073179
	1440915_at	NM_001081323	Mphosph9	-1.15	0.038924	-1.181	ND
	1447675_x_at	NM_010866	Myod1	-1.12	0.0187223	-1.2997	0.735987
	1443244_at	NM_029880	Ptgr2	1.15	0.0433498	-1.2532	0.589443
	1447659_x_at	NM_133826	Atp6v1h	1.15	0.00132547	-1.7491	0.758352
	1448070_at	NM_001035226	Xpo1	1.15	0.00319851	-1.2935	0.338644
	1458441_at	NM_172271	Slc6a17	1.15	0.013995	-3.4553	0.152444
	1419526_at	NM_010208	Fgr	1.15	0.0118045	-6.8066	0.184597
	1453495_at	NM_027097	Klk12	1.15	0.0519622	-4.3943	0.456866
	1443244_at	NM_029880	Ptgr2	1.15	0.0433498	1.273	ND
	1457724_at	NM_009984	Ctsl	1.15	0.0277524	1.016	ND
	1450912_at	NM_007641	Ms4a1	1.15	0.0453903	-2.768	ND
	1416434_at	NM_013479	Bcl2l10	1.16	0.023027	2.0216	0.594844
	1442149_at	NM_172443	Tbc1d16	1.17	0.019704	-1.2495	0.614209
	1443903_at	NM_008910	Ppm1a	1.17	0.0378589	1.0119	0.727244
	1432439_at	NM_027264	Zfp715	1.18	0.0130613	-2.0477	0.478696
	1427291_at	NM_011516	Sycp1	1.18	0.0593509	-7.521	ND
	1457240_at	NM_130860	Cdk9	1.19	0.0478827	-1.045	ND
	1430936_at	NM_134078	Chmp7	1.2	0.0185533	1.0179	0.806008
	1418263_at	NM_013932	Ddx25	1.22	0.0199518	1.1761	0.922095
	1442417_at	NM_020000	Med8	1.22	0.00702729	-1.3303	0.843149
	1445861_at	NM_013918	Usp25	1.22	0.0449911	-1.3338	0.275507
	1426512_at	NM_153157	Olfm3	1.23	0.0202879	2.252	ND
	1456033_at	NM_011536	Tbx4	1.24	0.00655649	-2.353	0.258499
	1458922_at	NM_177395	Map3k9	1.24	0.018436	-2.83	ND
	1446477_at	NM_144523	Zfp622	1.25	0.00508075	-1.1233	0.693553

	ProbeSet ID	Accession#	Gene Symbol	Fold Change (Microarray)	p-value (Microarray)	Fold Change (qRT-PCR)	p-value (qRT-PCR)
12 Hour	1423824_at	NM_026582	Gpr177	1.25	0.0584336	-1.139	ND
	1445543_at	NM_144842	Zmym5	1.26	0.00119374	-1.2485	0.676999
	1446315_at	NM_134037	Acly	1.26	0.00670916	-1.1031	0.942234
	1450211_at	NM_053011	Lrp1b	1.26	0.0178174	-5.0425	0.206188
	1458111_at	NM_145413	Fam20b	1.27	0.0293357	-1.034	ND
	1446448_at	NM_019663	Pias1	1.28	0.0198857	-1.1597	0.794687
	1420402_at	NM_001036684	Atp2b2	1.28	0.0402428	-1.274	ND
	1441631_at	NM_020494	Ddx24	1.28	0.0469727	-1.466	ND
	1416618_at	NM_008911	Ppox	1.29	0.0132195	-1.0092	0.809206
	1447243_at	XM_001476619	BC040756	1.29	0.0153648	-1.3757	0.703501
	1439569_at	NM_010287	Gpr83	1.3	0.00709981	-1.0988	0.66427
	1449729_at	NM_010202	Fgf4	1.3	0.024994	-1.628	ND
	1456967_at	NM_181853	Trim66	1.3	0.0313985	-4.491	ND
	1438493_at	NM_183139	Pld6	1.32	0.015361	-1.299	ND
	1447828_x_at	NM_026189	Eepd1	1.33	0.0275309	-1.2962	0.940483
	1446750_at	NM_008378	Impact	1.33	0.0167558	1.154	ND
	1454970_at	NM_001008705	Bud31	1.35	0.0328001	-1.611	ND
	1445091_at	NM_019864	Atr	1.39	0.0372469	-1.19	ND
	1452104_at	NM_197995	Arl16	1.39	0.0172165	68.938	ND
	1427606_at	NM_019461	Usp27x	1.4	0.0018845	-1.0392	0.634207
	1445798_at	NM_007862	Dlg1	1.42	0.0439951	-1.2559	0.472463
	1431231_at	NM_013548	Hist1h3f	1.45	0.00653143	-3.6214	0.724804
	1439345_at	NM_053110	Gpnmb	1.46	0.000873131	1.2445	0.521103
	1439626_at	NM_016963	Tmod3	1.6	0.0443229	-1.496	ND
	1442426_at	NM_001004436	Wapal	1.6	0.0596994	1.088	ND
	1440764_at	NM_009703	Araf	1.6	0.0330434	1.091	ND
	1436769_at	NM_011965	Psma1	1.67	0.0364339	-1.41	ND
24 Hour	**1422535_at**	**NM_001037134**	**Ccne2**	**-2.3**	**0.00556455**	**-2.3069**	**0.04303***
	1447640_s_at	NM_016768	Pbx3	-2.22	0.019032	1.496	ND
	1437187_at	NM_178609	E2f7	-2.21	0.0149549	1.6182	0.016985
	1454878_at	**NM_001110017**	**Dzip3**	**-1.83**	**7.54E-04**	**-2.4505**	**0.008996**
	1429499_at	**NM_025995**	**Fbxo5**	**-1.82**	**0.0420618**	**-2.4155**	**0.034343**

	ProbeSet ID	Accession#	Gene Symbol	Fold Change (Microarray)	p-value (Microarray)	Fold Change (qRT-PCR)	p-value (qRT-PCR)
24 Hour	1416680_at	NM_001033962	Ube3a	-1.79	0.0499803	-1.361	ND
	1424020_at	**NM_022989**	**Arl6ip6**	**-1.78**	**0.00254829**	**-1.3932**	**0.044794**
	1454952_s_at	**NM_178113**	**Ncapd3**	**-1.78**	**0.00658319**	**-2.2623**	**0.005212**
	1456280_at	NM_175554	Clspn	-1.74	0.00693641	-3.4987	0.118735
	1428900_s_at	**NM_029790**	**Mett5d1**	**-1.69**	**0.0584134**	**-2.6575**	**0.021048**
	1417760_at	NM_007430	Nr0b1	-1.68	0.0052307	1.2014	0.275835
	1453592_at	**NM_027321**	**Lrrc39**	**-1.64**	**0.0387068**	**-2.412**	**0.026505**
	1424410_at	**NM_029553**	**Ttc8**	**-1.62**	**0.0370323**	**-2.2198**	**0.030252**
	1452654_at	**NM_178395**	**Zdhhc2**	**-1.58**	**0.0101698**	**-2.0041**	**0.001076**
	1423577_at	**NM_134071**	**Ankrd32**	**-1.58**	**0.0216935**	**-3.002**	**0.031489**
	1427566_at	NM_001100454	Wfikkn1	-1.58	0.0545651	1.4215	0.330086
	1427670_a_at	NM_011544	Tcf12	-1.57	0.00977476	-2.2461	0.114768
	1456359_at	**NM_172807**	**Ppwd1**	**-1.56**	**0.0137773**	**-1.6603**	**0.030693**
	1448379_at	**NM_133931**	**Pot1a**	**-1.56**	**0.0129491**	**-2.4448**	**0.055646**
	1421473_at	NM_010554	Il1a	-1.56	0.0311228	-5.982	ND
	1418969_at	NM_013787	Skp2	-1.55	0.0217402	-1.4395	0.180132
	1433946_at	NM_009577	Zik1	-1.55	0.00256565	2.0906	0.101837
	1433946_at	NM_009577	Zik1	-1.55	0.00256565	1.022	ND
	1455724_at	**NM_027322**	**Prrg1**	**-1.52**	**0.00618626**	**-2.3544**	**0.022508**
	1440226_at	NM_001008501	Zfp760	-1.52	4.76E-03	-1.3037	0.569754
	1434682_at	NM_175466	Zfp770	-1.52	0.0047638	1.598	ND
	1429313_at	**NM_013845**	**Ror1**	**-1.51**	**0.00499191**	**-3.3444**	**0.04543**
	1429129_at	**NM_028915**	**Lrrcc1**	**-1.5**	**0.017268**	**-3.2006**	**0.001882**
	1456485_at	**NM_001081152**	**Npat**	**-1.5**	**0.0212934**	**-2.0647**	**0.004807**
	1423990_at	**NM_027295**	**Rab28**	**-1.47**	**0.0226515**	**-2.1636**	**0.023441**
	1416492_at	NM_007633	Ccne1	-1.47	0.0157672	2.047	ND
	1421866_at	**NM_008173**	**Nr3c1**	**-1.46**	**0.0248413**	**-1.5194**	**0.00196**
	1424072_at	**NM_027251**	**2010107G23Rik**	**-1.46**	**0.00994554**	**-2.4089**	**0.012763**
	1431422_a_at	NM_019819	Dusp14	-1.46	0.0123517	1.7395	0.043968
	1453327_at	NM_029393	Krt24	-1.46	0.0214941	3.128	ND
	1428667_at	NM_173740	Maoa	-1.44	0.010504	-2.5298	0.114411
	1427031_s_at	NM_144550	Ccdc52	-1.44	0.00639036	-1.7552	0.011657
	1420527_s_at	NM_001013832	Gpr31c	-1.44	0.018871	-1.0564	0.96883

	ProbeSet ID	Accession#	Gene Symbol	Fold Change (Microarray)	p-value (Microarray)	Fold Change (qRT-PCR)	p-value (qRT-PCR)
24 Hour	1422125_at	NM_008311	Htr2b	-1.43	0.0402935	-2.0297	0.174259
	1449891_a_at	NM_028523	Dcbld2	-1.42	0.0207998	-2.9245	0.078322
	1448701_a_at	NM_030675	Krit1	-1.41	0.0125251	-1.5119	0.067973
	1452276_at	**NM_007958**	**Smarcad1**	**-1.41**	**0.0016967**	**-1.5881**	**0.038549**
	1451503_at	NM_030152	Nol3	-1.41	0.0170388	1.1021	0.741342
	1417837_at	NM_009434	Phlda2	-1.4	0.0437577	1.0085	0.934224
	1431777_a_at	NM_026122	Hmgn3	-1.39	0.0482411	1.8419	0.014224
	1436309_at	NM_001081324	Neto2	-1.39	0.0492571	2.3922	0.034079
	1448429_at	**NM_013755**	**Gyg**	**-1.39**	**0.00445538**	**-1.7075**	**0.002374**
	1452210_at	**NM_177372**	**Dna2**	**-1.39**	**0.0345378**	**-1.9635**	**0.041862**
	1423421_at	NM_019683	Ankrd49	-1.39	0.0134246	-1.0631	0.737063
	1451175_at	**NM_029701**	**Spcs3**	**-1.38**	**0.0372038**	**-1.6958**	**0.032139**
	1431921_a_at	**NM_009282**	**Stag1**	**-1.37**	**0.0216641**	**-2.5963**	**0.016583**
	1420507_a_at	**NM_026075**	**Sfrs12ip1**	**-1.35**	**0.0149634**	**-1.9565**	**0.054464**
	1428103_at	NM_007399	Adam10	-1.35	0.0145373	-1.6489	0.174337
	1448638_at	**NM_134092**	**Mtbp**	**-1.35**	**0.00715986**	**-1.5257**	**0.026033**
	1436543_at	NM_153116	Gtpbp10	-1.35	0.0013415	-1.2764	0.412355
	1427500_at	NM_026911	Spcs1	-1.34	0.00472816	-1.5759	0.021898
	1453822_at	NM_028821	Dnalc1	-1.34	0.0296625	-1.259	0.108904
	1428633_at	NM_172253	Twistnb	-1.34	0.0164858	-1.191	ND
	1452106_at	NM_001029836	Npnt	-1.34	0.0732311	1.556	ND
	1448670_at	**NM_009454**	**Ube2e3**	**-1.33**	**0.00155413**	**-1.6184**	**0.040876**
	1448828_at	**NM_025695**	**Smc6**	**-1.33**	**0.0160562**	**-1.6449**	**0.009969**
	1435390_at	NM_027698	Exod1	-1.32	0.00675148	2.0869	0.344391
	1437686_x_at	NM_009986	Cux1	-1.31	0.0051343	-1.1356	0.631894
	1425493_at	NM_009758	Bmpr1a	-1.3	0.0062146	-1.4118	0.134251
	1427971_at	NM_145991	Cdc73	-1.3	0.018011	-1.82	0.072477
	1456577_x_at	NM_145131	Pitrm1	-1.3	0.0253898	-1.095	ND
	1430500_s_at	NM_016804	Mtx2	-1.29	0.000437871	-1.4603	0.074679
	1421350_a_at	NM_028736	Grip1	-1.28	0.0120105	-1.9772	0.130463
	1419183_at	NM_133905	Papd4	-1.28	0.0530044	-1.727	0.075125
	1426272_at	NM_020295	Lmbr1	-1.28	0.0156544	-1.4361	0.139956
	1436436_at	NM_030131	Cnih4	-1.28	0.0107517	-1.101	0.722252

	ProbeSet ID	Accession#	Gene Symbol	Fold Change (Microarray)	p-value (Microarray)	Fold Change (qRT-PCR)	p-value (qRT-PCR)
	1452953_at	NM_026210	Fam18b	-1.28	0.0208046	1.797	ND
24 Hour	1423824_at	NM_026582	Gpr177	-1.27	0.0582184	-1.6654	0.201232
	1430129_a_at	NM_178599	Commd8	-1.27	0.00570525	-1.2904	0.132797
	1435242_at	NM_175310	Pds5b	-1.27	0.0235754	-3.1869	0.168024
	1440915_at	NM_001081323	Mphosph9	-1.27	0.00746927	-5.4427	0.536716
	1456133_x_at	NM_010580	Itgb5	-1.27	0.0424371	-1.1797	0.48399
	1437122_at	NM_009741	Bcl2	-1.25	0.0427953	1.3593	0.011624
	1454727_at	NM_178928	Afap1l1	-1.25	0.00789143	1.452	ND
	1417535_at	NM_025785	Fbxo25	-1.24	0.00358443	-1.6231	0.112262
	1425495_at	NM_001024846	Zfp62	-1.23	0.0450192	-1.1844	0.657075
	1443329_at	**NM_020575**	**C3HC4**	**-1.22**	**0.0459186**	**-1.5203**	**0.023587**
	1418908_at	NM_013626	Pam	-1.22	0.00184097	-1.7208	0.146979
	1437312_at	NM_007560	Bmpr1b	-1.21	0.00640859	1.3918	0.007601
	1449484_at	**NM_011491**	**Stc2**	**-1.19**	**0.0414261**	**-7.6243**	**0.00075**
	1425340_a_at	**NM_008980**	**Ptpra**	**-1.19**	**0.0286731**	**-1.7787**	**0.029988**
	1428741_at	NM_001038698	Elavl4	-1.19	0.0350276	-4.5072	0.062718
	1439896_at	**NM_001034030**	**Limk2**	**-1.17**	**0.0498148**	**-1.9517**	**0.001298**
	1434969_at	NM_176954	Brunol5	-1.13	0.0493031	1.4878	0.8925
	1426697_a_at	NM_013587	Lrpap1	1.15	0.033769	-1.4432	0.172929
	1419472_s_at	NM_010948	Nudc	1.16	0.0236997	-1.6958	0.216466
	1440674_at	NM_001037987	Edil3	1.16	0.00579451	-5.9214	0.017331
	1419053_at	NM_019781	Pex14	1.18	0.0388409	-1.4163	0.067536
	1430083_at	XM_900147	2610307P16Rik	1.19	0.00608651	-2.9275	0.00047
	1442199_at	NM_001001177	BC051142	1.19	0.0109164	-13.4028	0.001997
	1418270_at	NM_013906	Adamts8	1.2	0.0206855	1.9468	0.294962
	1421247_at	NM_011041	Pax9	1.2	0.0291777	-1.2671	0.297761
	1449624_at	NM_001033296	Sel1l2	1.2	0.012553	-5.9717	0.028063
	1440251_s_at	NM_009564	Zfp64	1.21	0.0240486	-1.3608	0.389488
	1422520_at	NM_008691	Nefm	1.21	0.00937113	1.2377	0.540318
	1422669_at	NM_019480	Ebag9	1.22	0.0479554	-1.1931	0.430425
	1425937_a_at	NM_138753	Hexim1	1.22	0.0479554	1.3285	0.280463

	ProbeSet ID	Accession#	Gene Symbol	Fold Change (Microarray)	p-value (Microarray)	Fold Change (qRT-PCR)	p-value (qRT-PCR)
24 Hour	1422141_s_at	NM_033616	Csprs	1.22	0.0382522	1.75	ND
	1417631_at	NM_021461	Mknk1	1.23	0.00727506	-1.2577	0.592406
	1421128_at	NM_009453	Zrsr2	1.23	0.0309647	-1.3009	0.297299
	1451472_at	NM_026140	Ears2	1.23	0.0552563	-2.0082	0.222458
	1449217_at	NM_001122978	Casp8ap2	1.24	0.0456902	-1.1248	0.745156
	1455448_at	NM_198114	Dagla	1.24	0.00654762	3.419	ND
	1416920_at	NM_009032	Rbm4	1.26	0.0214421	-1.1448	0.567153
	1424120_at	NM_021419	Rnf8	1.26	0.0205861	-1.2176	0.133634
	1437369_at	NM_008001	Fgd1	1.26	0.0532073	-2.2836	0.023557
	1416579_a_at	NM_008532	Tacstd1	1.27	0.00160433	-1.0041	0.902398
	1420056_s_at	NM_033398	Jmjd6	1.27	0.0264347	-1.1392	0.292894
	1426465_at	NM_001042487	Dlgap4	1.27	0.00283408	-1.1137	0.687162
	1427910_at	NM_028623	Cst6	1.27	0.015732	196.1754	0.985704
	1417549_at	NM_001044747	Zfp68	1.27	0.0255634	-1.1519	0.677596
	1446783_at	NM_183358	Gadd45gip1	1.29	0.0124439	-1.2252	0.54995
	1419340_at	NM_031260	Mov10l1	1.29	0.0231991	-1.403	0.233716
	1429176_at	NM_199302	Lrsam1	1.29	0.0135811	-1.6621	0.055289
	1429850_x_at	NM_028070	Alkbh4	1.29	0.00316928	-1.5349	0.063819
	1453412_a_at	NM_028777	Sec14l1	1.3	0.0200196	1.1105	0.571274
	1455403_at	NM_172865	Manea	1.3	0.0459865	-1.6054	0.234381
	1422243_at	NM_008008	Fgf7	1.31	0.0496746	1.2164	0.740811
	1424907_a_at	NM_025648	Farsa	1.31	0.0043294	-1.1316	0.54651
	1429140_at	NM_029932	Spns3	1.31	0.0340807	-2.2709	0.042832
	1436269_s_at	NM_019752	Htra2	1.31	0.0343619	2.4254	ND
	1454441_at	NM_001008238	Bnip2	1.31	0.0620141	-1.5772	0.000002
	1422435_at	NM_023333	2210010C04Rik	1.32	0.0278925	-1.5133	0.172405
	1416791_a_at	NM_016813	Nxf1	1.36	0.00840251	1.5489	0.259156
	1417603_at	NM_011066	Per2	1.36	0.00344548	-1.2936	0.582383
	1437212_at	XM_001481070	Zfp420	1.36	0.0315739	-1.9784	0.172254
	1428064_at	NM_001040111	Arap1	1.37	0.00602797	1.1278	0.585955
	1453184_at	NM_178618	2310040C09Rik	1.37	0.0239767	1.0533	0.831513

	ProbeSet ID	Accession#	Gene Symbol	Fold Change (Microarray)	p-value (Microarray)	Fold Change (qRT-PCR)	p-value (qRT-PCR)
24 Hour	1417811_at	NM_133221	Slc24a6	1.37	0.0598961	-1.0139	0.877839
	1453184_at	NM_178618	Fam83g	1.37	0.0239767	1.578	ND
	1428064_at	NM_001040111	Arap1	1.37	0.00602797	1.105	ND
	1438904_at	NM_173390	Nhsl1	1.38	0.0316195	-1.584	0.018374
	1460438_at	NM_028134	Lysmd1	1.38	0.00272478	1.4647	0.18356
	1426786_s_at	NM_178380	Dhx38	1.4	0.00451137	-1.1957	0.603455
	1422890_at	NM_130448	Pcdh18	1.42	0.050974	-1.8683	0.216253
	1457240_at	NM_130860	Cdk9	1.42	0.0302805	-1.7686	0.060803
	1434682_at	NM_175466	Zfp770	1.42	0.00914444	-1.4346	0.143049
	1431805_a_at	NM_027897	Rhpn2	1.43	0.00706566	-1.0788	0.76668
	1439190_at	NM_028429	Fhad1	1.43	0.00792059	1.8651	0.107604
	1431805_a_at	NM_027897	Rhpn2	1.43	0.00706566	1.075	ND
	1438167_x_at	NM_146018	Flcn	1.45	0.0162386	-1.0443	0.86232
	1449702_at	NM_133349	Zfand2a	1.45	0.0423697	1.1629	0.614355
	1440614_at	NM_021493	4933428G20Rik	1.53	0.00080682	-1.1004	0.505793
	1450816_at	NM_015810	Polg2	1.54	0.0261729	1.3182	0.313186
	1416041_at	NM_011361	Sgk1	1.55	0.0117658	1.136	0.591063
	1416896_at	NM_009097	Rps6ka1	1.57	0.00550452	1.111	0.557733
	1450364_a_at	NM_134248	Havcr1	1.59	0.0223734	1.6582	0.273444
	1420185_at	NM_138744	Ssx2ip	1.76	0.00669644	-1.6256	0.13017
	1447966_a_at	NM_177670	Tmem69	1.83	0.0313526	-1.0774	0.822957
	1430357_at	NM_008211	H3f3b	1.87	0.00427678	2.105	ND
	1447854_s_at	NM_178214	Hist2h2be	1.95	0.00999838	4.139	ND
	1417491_at	NM_007798	Ctsb	1.96	0.00888385	-1.1478	0.590946
	1417491_at	NM_007798	Ctsb	1.96	0.00888385	2.378	ND
	1454254_s_at	NM_029639	1600029D21Rik	2.01	0.0271417	-9908944.781	0.146438
	1435382_at	NM_010882	Ndn	2.06	0.0423586	-1.4904	0.000498
	1422327_s_at	NM_008062	G6pdx	2.12	0.00679112	2.4902	0.13793
	1437842_at	**NM_207279**	**Plcxd1**	**2.13**	**0.0487732**	**2.3004**	**0.010372**
	1457724_at	NM_009984	Ctsl	2.18	3.88E-04	-1.284	0.058499
	1417273_at	NM_013743	Pdk4	2.36	0.0270769	1.1888	0.452556
	1417273_at	NM_013743	Pdk4	2.36	0.0270769	4.366	ND
	1448354_at	**NM_008062**	**G6pdx**	**2.72**	**1.46E-05**	**2.6259**	**0.040872**
	1424752_x_at	XM_620861	Zfp71	2.98	0.0021718	-1.1017	0.641135

	ProbeSet ID	Accession#	Gene Symbol	Fold Change (Microarray)	p-value (Microarray)	Fold Change (qRT-PCR)	p-value (qRT-PCR)
24 Hour	**1441793_at**	**NM_001099632**	**Rnf39**	**3.44**	**0.016834**	**1.8708**	**0.034122**

References

Ambolet-Camoit, A., Bui, L. C., Pierre, S., Chevallier, A., Marchand, A., Coumoul, X., Garlatti, M., Andreau, K., Barouki, R., and Aggerbeck, M. (2010). 2,3,7,8-tetrachlorodibenzo-p-dioxin counteracts the p53 response to a genotoxicant by upregulating expression of the metastasis marker agr2 in the hepatocarcinoma cell line HepG2. Toxicol Sci *115*, 501-512.

Ashkenazi, A., and Dixit, V. M. (1998). Death receptors: signaling and modulation. Science *281*, 1305-1308.

Beedanagari, S. R., Taylor, R. T., Bui, P., Wang, F., Nickerson, D. W., and Hankinson, O. (2010). Role of epigenetic mechanisms in differential regulation of the dioxin-inducible human CYP1A1 and CYP1B1 genes. Mol Pharmacol *78*, 608-616.

Boutros, P. C., Bielefeld, K. A., Pohjanvirta, R., and Harper, P. A. (2009). Dioxin-dependent and dioxin-independent gene batteries: comparison of liver and kidney in AHR-null mice. Toxicol Sci *112*, 245-256.

Boverhof, D. R., Burgoon, L. D., Tashiro, C., Chittim, B., Harkema, J. R., Jump, D. B., and Zacharewski, T. R. (2005). Temporal and dose-dependent hepatic gene expression patterns in mice provide new insights into TCDD-Mediated hepatotoxicity. Toxicol Sci *85*, 1048-1063.

Cantrell, S. M., Joy-Schlezinger, J., Stegeman, J. J., Tillitt, D. E., and Hannink, M. (1998). Correlation of 2,3,7,8-tetrachlorodibenzo-p-dioxin-induced apoptotic cell death in the embryonic vasculature with embryotoxicity. Toxicol Appl Pharmacol *148*, 24-34.

Cariani, E., Lasserre, C., Seurin, D., Hamelin, B., Kemeny, F., Franco, D., Czech, M. P., Ullrich, A., and Brechot, C. (1988). Differential expression of insulin-like growth factor II mRNA in human primary liver cancers, benign liver tumors, and liver cirrhosis. Cancer Res *48*, 6844-6849.

Chang, A. C., Dunham, M. A., Jeffrey, K. J., and Reddel, R. R. (1996). Molecular cloning and characterization of mouse stanniocalcin cDNA. Mol Cell Endocrinol *124*, 185-187.

Chang, A. C., Hook, J., Lemckert, F. A., McDonald, M. M., Nguyen, M. A., Hardeman, E. C., Little, D. G., Gunning, P. W., and Reddel, R. R. (2008). The murine stanniocalcin 2 gene is a negative regulator of postnatal growth. Endocrinology *149*, 2403-2410.

Chang, A. C., Janosi, J., Hulsbeek, M., de Jong, D., Jeffrey, K. J., Noble, J. R., and Reddel, R. R. (1995). A novel human cDNA highly homologous to the fish hormone stanniocalcin. Mol Cell Endocrinol *112*, 241-247.

Chang, A. C., Jellinek, D. A., and Reddel, R. R. (2003). Mammalian stanniocalcins and cancer. Endocr Relat Cancer *10*, 359-373.

Chang, A. C., and Reddel, R. R. (1998). Identification of a second stanniocalcin cDNA in mouse and human: stanniocalcin 2. Mol Cell Endocrinol *141*, 95-99.

Chen, I., McDougal, A., Wang, F., and Safe, S. (1998). Aryl hydrocarbon receptor-mediated antiestrogenic and antitumorigenic activity of diindolylmethane. Carcinogenesis *19*, 1631-1639.

Chen, Y. L., Law, P. Y., and Loh, H. H. (2005). Inhibition of PI3K/Akt signaling: an emerging paradigm for targeted cancer therapy. Curr Med Chem Anticancer Agents *5*, 575-589.

Chomczynski, P., and Sacchi, N. (1987). Single-step method of RNA isolation by acid guanidinium thiocyanate-phenol-chloroform extraction. Anal Biochem *162*, 156-159.

Christensen, J. G., Gonzales, A. J., Cattley, R. C., and Goldsworthy, T. L. (1998). Regulation of apoptosis in mouse hepatocytes and alteration of apoptosis by nongenotoxic carcinogens. Cell Growth Differ *9*, 815-825.

Cory, S., and Adams, J. M. (2002). The Bcl2 family: regulators of the cellular life-or-death switch. Nat Rev Cancer *2*, 647-656.

Coumailleau, P., Poellinger, L., Gustafsson, J. A., and Whitelaw, M. L. (1995). Definition of a minimal domain of the dioxin receptor that is associated with Hsp90 and maintains wild type ligand binding affinity and specificity. J Biol Chem *270*, 25291-25300.

Davis, J. W., Jr., Burdick, A. D., Lauer, F. T., and Burchiel, S. W. (2003). The aryl hydrocarbon receptor antagonist, 3'methoxy-4'nitroflavone, attenuates 2,3,7,8-tetrachlorodibenzo-p-dioxin-dependent regulation of growth factor signaling and apoptosis in the MCF-10A cell line. Toxicol Appl Pharmacol *188*, 42-49.

Dearstyne, E. A., and Kerkvliet, N. I. (2002). Mechanism of 2,3,7,8-tetrachlorodibenzo-p-dioxin (TCDD)-induced decrease in anti-CD3-activated CD4(+) T cells: the roles of apoptosis, Fas, and TNF. Toxicology *170*, 139-151.

Denison, M. S., and Nagy, S. R. (2003). Activation of the aryl hydrocarbon receptor by structurally diverse exogenous and endogenous chemicals. Annu Rev Pharmacol Toxicol *43*, 309-334.

Denison, M. S., Soshilov, A. A., He, G., DeGroot, D. E., and Zhao, B. (2011). Exactly the same but different: promiscuity and diversity in the molecular mechanisms of action of the aryl hydrocarbon (dioxin) receptor. Toxicol Sci *124*, 1-22.

Dere, E., Lee, A. W., Burgoon, L. D., and Zacharewski, T. R. (2011a). Differences in TCDD-elicited gene expression profiles in human HepG2, mouse Hepa1c1c7 and rat H4IIE hepatoma cells. BMC Genomics *12*, 193.

Dere, E., Lo, R., Celius, T., Matthews, J., and Zacharewski, T. R. (2011b). Integration of genome-wide computation DRE search, AhR ChIP-chip and gene expression analyses of TCDD-elicited responses in the mouse liver. BMC Genomics *12*, 365.

Elferink, C. J., Ge, N. L., and Levine, A. (2001). Maximal aryl hydrocarbon receptor activity depends on an interaction with the retinoblastoma protein. Mol Pharmacol *59*, 664-673.

Elferink, C. J., and Whitlock, J. P., Jr. (1994). Dioxin-dependent, DNA sequence-specific binding of a multiprotein complex containing the Ah receptor. Receptor *4*, 157-173.

Elizondo, G., Fernandez-Salguero, P., Sheikh, M. S., Kim, G. Y., Fornace, A. J., Lee, K. S., and Gonzalez, F. J. (2000). Altered cell cycle control at the G(2)/M phases in aryl hydrocarbon receptor-null embryo fibroblast. Mol Pharmacol *57*, 1056-1063.

Emmons, R. B., Duncan, D., Estes, P. A., Kiefel, P., Mosher, J. T., Sonnenfeld, M., Ward, M. P., Duncan, I., and Crews, S. T. (1999). The spineless-aristapedia and tango bHLH-PAS proteins interact to control antennal and tarsal development in Drosophila. Development *126*, 3937-3945.

Enari, M., Sakahira, H., Yokoyama, H., Okawa, K., Iwamatsu, A., and Nagata, S. (1998). A caspase-activated DNase that degrades DNA during apoptosis, and its inhibitor ICAD. Nature *391*, 43-50.

Fazio, E. N., Dimattia, G. E., Chadi, S. A., Kernohan, K. D., and Pin, C. L. (2011). Stanniocalcin 2 alters PERK signalling and reduces cellular injury during cerulein induced pancreatitis in mice. BMC Cell Biol *12*, 17.

Feldmann, G. (1997). Liver apoptosis. J Hepatol *26 Suppl 2*, 1-11.

Feldmann, G., Lamboley, C., Moreau, A., and Bringuier, A. (1998). Fas-mediated apoptosis of hepatic cells. Biomed Pharmacother *52*, 378-385.

Fernandez-Salguero, P., Pineau, T., Hilbert, D. M., McPhail, T., Lee, S. S., Kimura, S., Nebert, D. W., Rudikoff, S., Ward, J. M., and Gonzalez, F. J. (1995). Immune system impairment and hepatic fibrosis in mice lacking the dioxin-binding Ah receptor. Science *268*, 722-726.

Flaveny, C. A., Murray, I. A., and Perdew, G. H. (2010). Differential gene regulation by the human and mouse aryl hydrocarbon receptor. Toxicol Sci *114*, 217-225.

Franc, M. A., Moffat, I. D., Boutros, P. C., Tuomisto, J. T., Tuomisto, J., Pohjanvirta, R., and Okey, A. B. (2008). Patterns of dioxin-altered mRNA expression in livers of dioxin-sensitive versus dioxin-resistant rats. Arch Toxicol *82*, 809-830.

Franke, T. F. (2008). PI3K/Akt: getting it right matters. Oncogene *27*, 6473-6488.

Galle, P. R., and Krammer, P. H. (1998). CD95-induced apoptosis in human liver disease. Semin Liver Dis *18*, 141-151.

Ge, N. L., and Elferink, C. J. (1998). A direct interaction between the aryl hydrocarbon receptor and retinoblastoma protein. Linking dioxin signaling to the cell cycle. J Biol Chem *273*, 22708-22713.

Gonzalez, F. J., and Fernandez-Salguero, P. (1998). The aryl hydrocarbon receptor: studies using the AHR-null mice. Drug Metab Dispos *26*, 1194-1198.

Gregersen, N., and Bross, P. (2010). Protein misfolding and cellular stress: an overview. Methods Mol Biol *648*, 3-23.

Gross, A., McDonnell, J. M., and Korsmeyer, S. J. (1999). BCL-2 family members and the mitochondria in apoptosis. Genes Dev *13*, 1899-1911.

Gu, Y. Z., Hogenesch, J. B., and Bradfield, C. A. (2000). The PAS superfamily: sensors of environmental and developmental signals. Annu Rev Pharmacol Toxicol *40*, 519-561.

Hamilton, D. L., and Abremski, K. (1984). Site-specific recombination by the bacteriophage P1 lox-Cre system. Cre-mediated synapsis of two lox sites. J Mol Biol *178*, 481-486.

Hankinson, O. (1995). The aryl hydrocarbon receptor complex. Annu Rev Pharmacol Toxicol *35*, 307-340.

Hankinson, O. (2005). Role of coactivators in transcriptional activation by the aryl hydrocarbon receptor. Arch Biochem Biophys *433*, 379-386.

Hayes, K. R., Zastrow, G. M., Nukaya, M., Pande, K., Glover, E., Maufort, J. P., Liss, A. L., Liu, Y., Moran, S. M., Vollrath, A. L., and Bradfield, C. A. (2007). Hepatic transcriptional networks induced by exposure to 2,3,7,8-tetrachlorodibenzo-p-dioxin. Chem Res Toxicol *20*, 1573-1581.

He, B. (2006). Viruses, endoplasmic reticulum stress, and interferon responses. Cell Death Differ *13*, 393-403.

He, T. C., Zhou, S., da Costa, L. T., Yu, J., Kinzler, K. W., and Vogelstein, B. (1998). A simplified system for generating recombinant adenoviruses. Proc Natl Acad Sci U S A *95*, 2509-2514.

Heimler, I., Rawlins, R. G., Owen, H., and Hutz, R. J. (1998). Dioxin perturbs, in a dose- and time-dependent fashion, steroid secretion, and induces apoptosis of human luteinized granulosa cells. Endocrinology *139*, 4373-4379.

Hu, T. H., Huang, C. C., Lin, P. R., Chang, H. W., Ger, L. P., Lin, Y. W., Changchien, C. S., Lee, C. M., and Tai, M. H. (2003). Expression and prognostic role of tumor suppressor gene PTEN/MMAC1/TEP1 in hepatocellular carcinoma. Cancer *97*, 1929-1940.

Huang, D. C., and Strasser, A. (2000). BH3-Only proteins-essential initiators of apoptotic cell death. Cell *103*, 839-842.

Huang, G., and Elferink, C. J. (2012). A novel nonconsensus xenobiotic response element capable of mediating aryl hydrocarbon receptor-dependent gene expression. Mol Pharmacol *81*, 338-347.

IARC (1997). Polychlorinated dibenzo-para-dioxins and polychlorinated dibenzofurans. IARC Monographs on the Evaluation of Carcinogenic Risks to Humans *69*, 631.

Ishibashi, K., Miyamoto, K., Taketani, Y., Morita, K., Takeda, E., Sasaki, S., and Imai, M. (1998). Molecular cloning of a second human stanniocalcin homologue (STC2). Biochem Biophys Res Commun *250*, 252-258.

Ito, D., Walker, J. R., Thompson, C. S., Moroz, I., Lin, W., Veselits, M. L., Hakim, A. M., Fienberg, A. A., and Thinakaran, G. (2004). Characterization of stanniocalcin 2, a novel target of the mammalian unfolded protein response with cytoprotective properties. Mol Cell Biol *24*, 9456-9469.

Jain, S., Dolwick, K. M., Schmidt, J. V., and Bradfield, C. A. (1994). Potent transactivation domains of the Ah receptor and the Ah receptor nuclear translocator map to their carboxyl termini. J Biol Chem *269*, 31518-31524.

Jellinek, D. A., Chang, A. C., Larsen, M. R., Wang, X., Robinson, P. J., and Reddel, R. R. (2000). Stanniocalcin 1 and 2 are secreted as phosphoproteins from human fibrosarcoma cells. Biochem J *350 Pt 2*, 453-461.

Kamath, A. B., Camacho, I., Nagarkatti, P. S., and Nagarkatti, M. (1999). Role of Fas-Fas ligand interactions in 2,3,7,8-tetrachlorodibenzo- p-dioxin (TCDD)-induced immunotoxicity: increased resistance of thymocytes from Fas-deficient (lpr) and Fas ligand-defective (gld) mice to TCDD-induced toxicity. Toxicol Appl Pharmacol *160*, 141-155.

Kamath, A. B., Nagarkatti, P. S., and Nagarkatti, M. (1998). Characterization of phenotypic alterations induced by 2,3,7,8-tetrachlorodibenzo-p-dioxin on thymocytes in vivo and its effect on apoptosis. Toxicol Appl Pharmacol *150*, 117-124.

Kazlauskas, A., Poellinger, L., and Pongratz, I. (1999). Evidence that the co-chaperone p23 regulates ligand responsiveness of the dioxin (Aryl hydrocarbon) receptor. J Biol Chem *274*, 13519-13524.

Kent, W. J. (2002). BLAT--the BLAST-like alignment tool. Genome Res *12*, 656-664.

Kerr, J. F., Wyllie, A. H., and Currie, A. R. (1972). Apoptosis: a basic biological phenomenon with wide-ranging implications in tissue kinetics. Br J Cancer *26*, 239-257.

Kim, D. W., Gazourian, L., Quadri, S. A., Romieu-Mourez, R., Sherr, D. H., and Sonenshein, G. E. (2000). The RelA NF-kappaB subunit and the aryl hydrocarbon receptor (AhR) cooperate to transactivate the c-myc promoter in mammary cells. Oncogene *19*, 5498-5506.

Kiyici, M., Gurel, S., Budak, F., Dolar, E., Gulten, M., Nak, S. G., and Memik, F. (2003). Fas antigen (CD95) expression and apoptosis in hepatocytes of patients with chronic viral hepatitis. Eur J Gastroenterol Hepatol *15*, 1079-1084.

Knerr, S., and Schrenk, D. (2006). Carcinogenicity of 2,3,7,8-tetrachlorodibenzo-p-dioxin in experimental models. Mol Nutr Food Res *50*, 897-907.

Kolluri, S., Balduf, C., Hofmann, M., Gottlicher, M. (2001). Novel target genes of the Ah (Dioxin) Receptor: transcriptional induction of N-myristoyltransferase 2. Cancer Res *61,* 8534-8539.

Kondo, T., Suda, T., Fukuyama, H., Adachi, M., and Nagata, S. (1997). Essential roles of the Fas ligand in the development of hepatitis. Nat Med *3*, 409-413.

Krammer, P. H. (1996). The CD95(APO-1/Fas) receptor/ligand system: death signals and diseases. Cell Death Differ *3*, 159-160.

Kumar, M. B., and Perdew, G. H. (1999). Nuclear receptor coactivator SRC-1 interacts with the Q-rich subdomain of the AhR and modulates its transactivation potential. Gene Expr *8*, 273-286.

Lahvis, G. P., and Bradfield, C. A. (1998). Ahr null alleles: distinctive or different? Biochem Pharmacol *56*, 781-787.

Laiosa, M. D., Wyman, A., Murante, F. G., Fiore, N. C., Staples, J. E., Gasiewicz, T. A., and Silverstone, A. E. (2003). Cell proliferation arrest within intrathymic lymphocyte progenitor cells causes thymic atrophy mediated by the aryl hydrocarbon receptor. J Immunol *171*, 4582-4591.

Lapinski, T. W., Kowalczuk, O., Prokopowicz, D., and Chyczewski, L. (2004). Serum concentration of sFas and sFasL in healthy HBsAg carriers, chronic viral hepatitis B and C patients. World J Gastroenterol *10*, 3650-3653.

Law, A. Y., and Wong, C. K. (2010a). Stanniocalcin-2 promotes epithelial-mesenchymal transition and invasiveness in hypoxic human ovarian cancer cells. Exp Cell Res *316*, 3425-3434.

Law, A. Y., and Wong, C. K. (2010b). Stanniocalcin-2 is a HIF-1 target gene that promotes cell proliferation in hypoxia. Exp Cell Res *316*, 466-476.

Lee, J. W., Soung, Y. H., Kim, S. Y., Lee, H. W., Park, W. S., Nam, S. W., Kim, S. H., Lee, J. Y., Yoo, N. J., and Lee, S. H. (2005). PIK3CA gene is frequently mutated in breast carcinomas and hepatocellular carcinomas. Oncogene *24*, 1477-1480.

Lees, M. J., and Whitelaw, M. L. (1999). Multiple roles of ligand in transforming the dioxin receptor to an active basic helix-loop-helix/PAS transcription factor complex with the nuclear protein Arnt. Mol Cell Biol *19*, 5811-5822.

Livak, K. J., and Schmittgen, T. D. (2001). Analysis of relative gene expression data using real-time quantitative PCR and the 2(-Delta Delta C(T)) Method. Methods *25*, 402-408.

Lowell, C. A., and Berton, G. (1998). Resistance to endotoxic shock and reduced neutrophil migration in mice deficient for the Src-family kinases Hck and Fgr. Proc Natl Acad Sci U S A *95*, 7580-7584.

Luo, X., Budihardjo, I., Zou, H., Slaughter, C., and Wang, X. (1998). Bid, a Bcl2 interacting protein, mediates cytochrome c release from mitochondria in response to activation of cell surface death receptors. Cell *94*, 481-490.

Ma, Y., Brewer, J. W., Diehl, J. A., and Hendershot, L. M. (2002). Two distinct stress signaling pathways converge upon the CHOP promoter during the mammalian unfolded protein response. J Mol Biol *318*, 1351-1365.

Malhi, H., and Kaufman, R. J. (2011). Endoplasmic reticulum stress in liver disease. J Hepatol *54*, 795-809.

Marlowe, J. L., Fan, Y., Chang, X., Peng, L., Knudsen, E. S., Xia, Y., and Puga, A. (2008). The aryl hydrocarbon receptor binds to E2F1 and inhibits E2F1-induced apoptosis. Mol Biol Cell *19*, 3263-3271.

Marlowe, J. L., Knudsen, E. S., Schwemberger, S., and Puga, A. (2004). The aryl hydrocarbon receptor displaces p300 from E2F-dependent promoters and represses S phase-specific gene expression. J Biol Chem *279*, 29013-29022.

McConkey, D. J., Hartzell, P., Duddy, S. K., Hakansson, H., and Orrenius, S. (1988). 2,3,7,8-Tetrachlorodibenzo-p-dioxin kills immature thymocytes by Ca2+-mediated endonuclease activation. Science *242*, 256-259.

McCullough, K. D., Martindale, J. L., Klotz, L. O., Aw, T. Y., and Holbrook, N. J. (2001). Gadd153 sensitizes cells to endoplasmic reticulum stress by down-regulating Bcl2 and perturbing the cellular redox state. Mol Cell Biol *21*, 1249-1259.

Mimura, J., Ema, M., Sogawa, K., and Fujii-Kuriyama, Y. (1999). Identification of a novel mechanism of regulation of Ah (dioxin) receptor function. Genes Dev *13*, 20-25.

Mitchell, K. A., Lockhart, C. A., Huang, G., and Elferink, C. J. (2006). Sustained aryl hydrocarbon receptor activity attenuates liver regeneration. Mol Pharmacol *70*, 163-170.

Mitchell, K. A., Wilson, S. R., and Elferink, C. J. (2010). The activated aryl hydrocarbon receptor synergizes mitogen-induced murine liver hyperplasia. Toxicology *276*, 103-109.

Muntane, J. (2011). Targeting cell death and survival receptors in hepatocellular carcinoma. Anticancer Agents Med Chem *11*, 576-584.

Murray, I. A., Morales, J. L., Flaveny, C. A., Dinatale, B. C., Chiaro, C., Gowdahalli, K., Amin, S., and Perdew, G. H. (2010). Evidence for ligand-mediated selective modulation of aryl hydrocarbon receptor activity. Mol Pharmacol *77*, 247-254.

Nagy, A. (2000). Cre recombinase: the universal reagent for genome tailoring. Genesis *26*, 99-109.

Nicholson, D. W., and Thornberry, N. A. (1997). Caspases: killer proteases. Trends Biochem Sci *22*, 299-306.

Oesch-Bartlomowicz, B., and Oesch, F. (2009). Role of cAMP in mediating AHR signaling. Biochem Pharmacol *77*, 627-641.

Ogasawara, J., Watanabe-Fukunaga, R., Adachi, M., Matsuzawa, A., Kasugai, T., Kitamura, Y., Itoh, N., Suda, T., and Nagata, S. (1993). Lethal effect of the anti-Fas antibody in mice. Nature *364*, 806-809.

Ohtake, F., Takeyama, K., Matsumoto, T., Kitagawa, H., Yamamoto, Y., Nohara, K., Tohyama, C., Krust, A., Mimura, J., Chambon, P*., et al.* (2003). Modulation of oestrogen receptor signalling by association with the activated dioxin receptor. Nature *423*, 545-550.

Okey, A. B., Riddick, D. S., and Harper, P. A. (1994). Molecular biology of the aromatic hydrocarbon (dioxin) receptor. Trends Pharmacol Sci *15*, 226-232.

Opitz, C. A., Litzenburger, U. M., Sahm, F., Ott, M., Tritschler, I., Trump, S., Schumacher, T., Jestaedt, L., Schrenk, D., Weller, M*., et al.* (2011). An endogenous tumour-promoting ligand of the human aryl hydrocarbon receptor. Nature *478*, 197-203.

Orth, K., Chinnaiyan, A. M., Garg, M., Froelich, C. J., and Dixit, V. M. (1996). The CED-3/ICE-like protease Mch2 is activated during apoptosis and cleaves the death substrate lamin A. J Biol Chem *271*, 16443-16446.

Paajarvi, G., Viluksela, M., Pohjanvirta, R., Stenius, U., and Hogberg, J. (2005). TCDD activates Mdm2 and attenuates the p53 response to DNA damaging agents. Carcinogenesis *26*, 201-208.

Pahl, H., Sester, M., Burgert, H., Baeuerle, P. (1996) Actication of transcription factor NF-kappaB by the adenovirus E3/19K protein requires its ER retention. J Cell Biol *132,* 511-522.

Park, K. T., Mitchell, K. A., Huang, G., and Elferink, C. J. (2005). The aryl hydrocarbon receptor predisposes hepatocytes to Fas-mediated apoptosis. Mol Pharmacol *67*, 612-622.

Perdew, G. H. (1988). Association of the Ah receptor with the 90-kDa heat shock protein. J Biol Chem *263*, 13802-13805.

Perdew, G. H. (1992). Chemical cross-linking of the cytosolic and nuclear forms of the Ah receptor in hepatoma cell line 1c1c7. Biochem Biophys Res Commun *182*, 55-62.

Petrulis, J. R., Kusnadi, A., Ramadoss, P., Hollingshead, B., and Perdew, G. H. (2003). The hsp90 Co-chaperone XAP2 alters importin beta recognition of the bipartite

nuclear localization signal of the Ah receptor and represses transcriptional activity. J Biol Chem *278*, 2677-2685.

Poland, A., and Glover, E. (1974). Comparison of 2,3,7,8-tetrachlorodibenzo-p-dioxin, a potent inducer of aryl hydrocarbon hydroxylase, with 3-methylcholanthrene. Mol Pharmacol *10*, 349-359.

Poland, A., and Knutson, J. C. (1982). 2,3,7,8-tetrachlorodibenzo-p-dioxin and related halogenated aromatic hydrocarbons: examination of the mechanism of toxicity. Annu Rev Pharmacol Toxicol *22*, 517-554.

Poland, A., Palen, D., and Glover, E. (1994). Analysis of the four alleles of the murine aryl hydrocarbon receptor. Mol Pharmacol *46*, 915-921.

Pollenz, R. S. (2002). The mechanism of AH receptor protein down-regulation (degradation) and its impact on AH receptor-mediated gene regulation. Chem Biol Interact *141*, 41-61.

Pongratz, I., Mason, G. G., and Poellinger, L. (1992). Dual roles of the 90-kDa heat shock protein hsp90 in modulating functional activities of the dioxin receptor. Evidence that the dioxin receptor functionally belongs to a subclass of nuclear receptors which require hsp90 both for ligand binding activity and repression of intrinsic DNA binding activity. J Biol Chem *267*, 13728-13734.

Powell-Coffman, J. A., Bradfield, C. A., and Wood, W. B. (1998). Caenorhabditis elegans orthologs of the aryl hydrocarbon receptor and its heterodimerization partner the aryl hydrocarbon receptor nuclear translocator. Proc Natl Acad Sci U S A *95*, 2844-2849.

Probst, M. R., Reisz-Porszasz, S., Agbunag, R. V., Ong, M. S., and Hankinson, O. (1993). Role of the aryl hydrocarbon receptor nuclear translocator protein in aryl hydrocarbon (dioxin) receptor action. Mol Pharmacol *44*, 511-518.

Puga, A., Maier, A., and Medvedovic, M. (2000). The transcriptional signature of dioxin in human hepatoma HepG2 cells. Biochem Pharmacol *60*, 1129-1142.

Reyes-Hernandez, O. D., Mejia-Garcia, A., Sanchez-Ocampo, E. M., Cabanas-Cortes, M. A., Ramirez, P., Chavez-Gonzalez, L., Gonzalez, F. J., and Elizondo, G. (2010). Ube2l3 gene expression is modulated by activation of the aryl hydrocarbon receptor: implications for p53 ubiquitination. Biochem Pharmacol *80*, 932-940.

Rhile, M. J., Nagarkatti, M., and Nagarkatti, P. S. (1996). Role of Fas apoptosis and MHC genes in 2,3,7,8-tetrachlorodibenzo-p-dioxin (TCDD)-induced immunotoxicity of T cells. Toxicology *110*, 153-167.

Rudel, T., and Bokoch, G. M. (1997). Membrane and morphological changes in apoptotic cells regulated by caspase-mediated activation of PAK2. Science *276*, 1571-1574.

Safe, S., Wang, F., Porter, W., Duan, R., and McDougal, A. (1998). Ah receptor agonists as endocrine disruptors: antiestrogenic activity and mechanisms. Toxicol Lett *102-103*, 343-347.

Safe, S., Wormke, M., and Samudio, I. (2000). Mechanisms of inhibitory aryl hydrocarbon receptor-estrogen receptor crosstalk in human breast cancer cells. J Mammary Gland Biol Neoplasia *5*, 295-306.

Sakamoto, M. K., Mima, S., and Tanimura, T. (1995). A morphological study of liver lesions in Xenopus larvae exposed to 2,3,7,8-tetrachlorodibenzo-p-dioxin (TCDD) with special reference to apoptosis of hepatocytes. J Environ Pathol Toxicol Oncol *14*, 69-82.

Scaffidi, C., Fulda, S., Srinivasan, A., Friesen, C., Li, F., Tomaselli, K. J., Debatin, K. M., Krammer, P. H., and Peter, M. E. (1998). Two CD95 (APO-1/Fas) signaling pathways. EMBO J *17*, 1675-1687.

Schattenberg, J. M., Schuchmann, M., and Galle, P. R. (2011). Cell death and hepatocarcinogenesis: Dysregulation of apoptosis signaling pathways. J Gastroenterol Hepatol *26 Suppl 1*, 213-219.

Schmidt, J. V., and Bradfield, C. A. (1996). Ah receptor signaling pathways. Annu Rev Cell Dev Biol *12*, 55-89.

Schmidt, J. V., Carver, L. A., and Bradfield, C. A. (1993). Molecular characterization of the murine Ahr gene. Organization, promoter analysis, and chromosomal assignment. J Biol Chem *268*, 22203-22209.

Schmidt, J. V., Su, G. H., Reddy, J. K., Simon, M. C., and Bradfield, C. A. (1996). Characterization of a murine Ahr null allele: involvement of the Ah receptor in hepatic growth and development. Proc Natl Acad Sci U S A *93*, 6731-6736.

Schmidt, S. K., Muller, A., Heseler, K., Woite, C., Spekker, K., MacKenzie, C. R., and Daubener, W. (2009). Antimicrobial and immunoregulatory properties of human tryptophan 2,3-dioxygenase. Eur J Immunol *39*, 2755-2764.

Schuler, M., Dierich, A., Chambon, P., and Metzger, D. (2004). Efficient temporally controlled targeted somatic mutagenesis in hepatocytes of the mouse. Genesis *39*, 167-172.

Schulte-Hermann, R., Bursch, W., and Grasl-Kraupp, B. (1995). Active cell death (apoptosis) in liver biology and disease. Prog Liver Dis *13*, 1-35.

Schulze-Osthoff, K., Ferrari, D., Los, M., Wesselborg, S., and Peter, M. E. (1998). Apoptosis signaling by death receptors. Eur J Biochem *254*, 439-459.

Shaw, R. J., and Cantley, L. C. (2006). Ras, PI(3)K and mTOR signalling controls tumour cell growth. Nature *441*, 424-430.

Stinchcombe, S., Buchmann, A., Bock, K. W., and Schwarz, M. (1995). Inhibition of apoptosis during 2,3,7,8-tetrachlorodibenzo-p-dioxin-mediated tumour promotion in rat liver. Carcinogenesis *16*, 1271-1275.

Strobeck, M. W., Fribourg, A. F., Puga, A., and Knudsen, E. S. (2000). Restoration of retinoblastoma mediated signaling to Cdk2 results in cell cycle arrest. Oncogene *19*, 1857-1867.

Suzuki, Y., Imai, Y., Nakayama, H., Takahashi, K., Takio, K., and Takahashi, R. (2001). A serine protease, HtrA2, is released from the mitochondria and interacts with XIAP, inducing cell death. Mol Cell *8*, 613-621.

Swanson, H. I., Chan, W. K., and Bradfield, C. A. (1995). DNA binding specificities and pairing rules of the Ah receptor, ARNT, and SIM proteins. J Biol Chem *270*, 26292-26302.

Taieb, J., Mathurin, P., Poynard, T., Gougerot-Pocidalo, M. A., and Chollet-Martin, S. (1998). Raised plasma soluble Fas and Fas-ligand in alcoholic liver disease. Lancet *351*, 1930-1931.

Tamura, K., Furihata, M., Chung S. Y., Uemura, M., Yoshioka, H., Liyama, Y., Ashida, S., Nasu, Y., Fujioka, T., Shuin, T., Nakamura, Y., Nakagawa, H. (2009) Stanniocalcin 2 overexpression in castration-resistant prostate cancer and aggressive prostate cancer. Cancer Sci *100*, 914-919.

Thornberry, N. A., and Lazebnik, Y. (1998). Caspases: enemies within. Science *281*, 1312-1316.

Tian, Y., Ke, S., Denison, M. S., Rabson, A. B., and Gallo, M. A. (1999). Ah receptor and NF-kappaB interactions, a potential mechanism for dioxin toxicity. J Biol Chem *274*, 510-515.

Tijet, N., Boutros, P. C., Moffat, I. D., Okey, A. B., Tuomisto, J., and Pohjanvirta, R. (2006). Aryl hydrocarbon receptor regulates distinct dioxin-dependent and dioxin-independent gene batteries. Mol Pharmacol *69*, 140-153.

Uno, S., Dalton, T. P., Derkenne, S., Curran, C. P., Miller, M. L., Shertzer, H. G., and Nebert, D. W. (2004). Oral exposure to benzo[a]pyrene in the mouse: detoxication by inducible cytochrome P450 is more important than metabolic activation. Mol Pharmacol *65*, 1225-1237.

Volland, S., Kugler, W., Schweigerer, L., Wilting, J., and Becker, J. (2009). Stanniocalcin 2 promotes invasion and is associated with metastatic stages in neuroblastoma. Int J Cancer *125*, 2049-2057.

Wagner, G. F., and Dimattia, G. E. (2006). The stanniocalcin family of proteins. J Exp Zool A Comp Exp Biol *305*, 769-780.

Wagner, G. F., Hampong, M., Park, C. M., and Copp, D. H. (1986). Purification, characterization, and bioassay of teleocalcin, a glycoprotein from salmon corpuscles of Stannius. Gen Comp Endocrinol *63*, 481-491.

Walisser, J. A., Glover, E., Pande, K., Liss, A. L., and Bradfield, C. A. (2005). Aryl hydrocarbon receptor-dependent liver development and hepatotoxicity are mediated by different cell types. Proc Natl Acad Sci U S A *102*, 17858-17863.

Walter, D., Schmich, K., Vogel, S., Pick, R., Kaufmann, T., Hochmuth, F. C., Haber, A., Neubert, K., McNelly, S., von Weizsacker, F*., et al.* (2008). Switch from type II to I Fas/CD95 death signaling on in vitro culturing of primary hepatocytes. Hepatology *48*, 1942-1953.

Wang, F., Zhang, R., Shi, S., and Hankinson, O. (2007). The effect of aromatic hydrocarbon receptor on the phenotype of the Hepa 1c1c7 murine hepatoma cells in the absence of dioxin. Gene Regul Syst Bio *1*, 49-56.

Wang, H., Wu, K., Sun, Y., Li, Y., Wu, M., Qiao, Qain., Wei, Y., Han, Z., Cai, Bing. (2012). STC2 is upregulated in hepatocellular carcinoma and promotes cell proliferation and migration in vitro. BMB Rep *11*, 629-634.

Whittaker, S., Marais, R., and Zhu, A. X. (2010). The role of signaling pathways in the development and treatment of hepatocellular carcinoma. Oncogene *29*, 4989-5005.

Worner, W., and Schrenk, D. (1998). 2,3,7,8-Tetrachlorodibenzo-p-dioxin suppresses apoptosis and leads to hyperphosphorylation of p53 in rat hepatocytes. Environ Toxicol Pharmacol *6*, 239-247.

Wu, J. C., Merlino, G., and Fausto, N. (1994). Establishment and characterization of differentiated, nontransformed hepatocyte cell lines derived from mice transgenic for transforming growth factor alpha. Proc Natl Acad Sci U S A *91*, 674-678.

Wu, R., Zhang, L., Hoagland, M. S., and Swanson, H. I. (2007). Lack of the aryl hydrocarbon receptor leads to impaired activation of AKT/protein kinase B and enhanced sensitivity to apoptosis induced via the intrinsic pathway. J Pharmacol Exp Ther *320*, 448-457.

Yeh, Y. C., Tsai, J. F., Chuang, L. Y., Yeh, H. W., Tsai, J. H., Florine, D. L., and Tam, J. P. (1987). Elevation of transforming growth factor alpha and its relationship to the epidermal growth factor and alpha-fetoprotein levels in patients with hepatocellular carcinoma. Cancer Res *47*, 896-901.

Yin, X. M., Wang, K., Gross, A., Zhao, Y., Zinkel, S., Klocke, B., Roth, K. A., and Korsmeyer, S. J. (1999). Bid-deficient mice are resistant to Fas-induced hepatocellular apoptosis. Nature *400*, 886-891.

Zaher, H., Fernandez-Salguero, P. M., Letterio, J., Sheikh, M. S., Fornace, A. J., Jr., Roberts, A. B., and Gonzalez, F. J. (1998). The involvement of aryl hydrocarbon

receptor in the activation of transforming growth factor-beta and apoptosis. Mol Pharmacol *54*, 313-321.

Zha, J., Weiler, S., Oh, K., Wei, M., Korsmeyer, S. (200) Posttranslational N-myristoylation of BID as a molecular switch for targeting mitochondria and apoptosis. Science *290*, 1761-1765.

Vita

Tod Arliss Harper Jr. was born October 13, 1982 in Beech Grove, Indiana to Tod Arliss Harper and Victoria May Harper. He has five sisters and one brother named Jennifer, Melissa, Andrea, Samantha, Shayla, and Traver, respectively. His early childhood consisted of moving from various cities including San Diego, California, Chicago, Illinois, and Virginia Beach, Virginia. He finally settled down in Beech Grove, IN at the age of 9. Tod attended Beech Grove Public Schools and graduated from Beech Grove High School in 2001. He then matriculated at Texas A&M University @ Galveston in Galveston, Texas where he earned a Bachelors of Science in Marine Biology and graduated Cum Laude. While at TAMUG, Tod worked in a laboratory located at the University of Texas Medical Branch – Galveston inspiring his love of research. After graduation, Tod was accepted into a Master's degree program through the Department of Pharmacology & Toxicology and joined Dr. Cornelis (Kees) Elferink's laboratory. Excelling in both class and laboratory work, he soon switched to the Ph.D. program in Pharmacology and Toxicology staying with Dr. Elferink. During his time at UTMB, Tod mentored several summer students, and team-taught an introductory toxicology course at his alma mater. Tod has one first author paper, with additional coauthor papers expected. While at UTMB, Tod was instrumental in organizing the Pharmacology & Toxicology Student Organization.

Permanent address: 1409 Post Office St, Galveston, TX 77550

This dissertation was typed by Tod A. Harper Jr.